On Loudspeaker Implementation for Feedback Control, Open-Air, Active Noise Reduction Headsets

by

Andrew D. White

Thesis submitted to the Faculty of the

Virginia Polytechnic Institute and State University

in partial fulfillment of the requirements for the degree of

MASTER OF SCIENCE
IN
MECHANICAL ENGINEERING

William R. Saunders, Chair

Roberto Burdisso

Donald J. Leo

November 19, 1999

Blacksburg, Virginia

Keywords: ANR, ANC, supra aural, loudspeaker model

On Loudspeaker Implementation for Feedback Control, Open-Air, Active Noise Reduction Headsets

by
Andrew D. White

Dr. William R. Saunders, Chair
Department of Mechanical Engineering

(Abstract)

The loudspeakers used in active noise reduction (ANR) headsets are generally identical to loudspeakers used in commercial headphones. Unfortunately, the frequency response characteristics of these loudspeakers are not particularly well suited for open-air active noise control (ANC). Open-air headsets float outside the ear with no contact between the system and the user and allow for regular conversation with others in the environment. This study has identified three limitations on the closed-loop performance of open-air headsets: the distribution of gain and phase in the loudspeaker's open-loop frequency response function, manufacturing variations in loudspeakers that can deviate from design specifications by up to 40%, and the variations in acoustic impedance coupling (ear-to-speaker) among users. This thesis explores the mechanisms that underlie these limitations with the goal of designing open-air headsets that are robust to manufacturing and user variations. Methods are introduced on ways to minimize the effects of manufacturing and user variations and are proven by experiment. With these variations minimized, the controller's design is only limited by the frequency response of the loudspeaker. A comprehensive examination of techniques to model moving-coil loudspeakers is presented followed by detailed studies on how each parameter affects the system's frequency response. A review of frequency domain control system design is then included to help the reader understand loop-shaping techniques. Finally, a compensator is designed for an open-air ANR headset using loop-shaping techniques and the robustness of the closed-loop performance is verified experimentally.

Acknowledgements

	"thank you"
mom and dad	for 23 years of encouragement and support and for those subtle reminders about how all of this builds character….
phil	for telling me stories about craptacular things that made me laugh, and sending me absolutely evil stuff
will saunders	for allowing me to work at my own pace without pressure (well maybe a little at the end) and for giving me the opportunity to explore new and frustrating things with ATI
mike vaudrey	for lifting weights, going to concerts, enjoying tv, picking me up from the airport (wait, that was mandy…), employment, and oh yeah, some help of this thesis as well
tv	for just being tv.

Table of Contents

List of Figures

List of Tables

Chapter 1: Introduction: Goals For Feedback Control Headsets

1.1 Introduction and Objectives

The active noise reduction (ANR) headset was one of the first successful implementations of active noise control (ANC) technology. The close proximity to the users ear allows for significant noise reduction over a large bandwidth. At this time, there are many companies that offer circumaural active noise reduction headsets for commercial sale. These headsets are designed with the speaker and microphone inside an ear cup that is sealed to the users head. The ear cup not only provides passive noise control, but also serves two more important purposes for active control. First, it acts as an enclosure for the loudspeaker, thereby shaping the frequency response, and secondly, it decouples the headset from the dynamics of the user's ear. It is the presence of the ear cup that allows successful active noise control at very low frequencies.

This thesis explores a different type of headset, termed supra aural. The supra aural headset does not have an ear cup and is not sealed to the users head. Supra aural can be then divided into two categories. The first use a foam cushion that rests on the user's ear that places the loudspeaker and microphone in close proximity. These designs are created as alternatives to circumaural headsets and can be used in moderate noise fields with greater comfort provided to the user. This thesis will focus on a second type of supra aural headset, termed open-air. Open-air headsets float outside the ear with no contact between the system and the user and allow for regular conversation with others in the environment. Without an ear cup to shape the response of the speaker, special design considerations must be understood in order to develop a loudspeaker system that is suitable, or even optimal, for active noise control applications.

There are several specific objectives that this thesis will try to address:

- Demonstrate how loudspeaker design objectives for active noise control differ from traditional consumer audio.
- Become familiar with the techniques for modeling loudspeakers and enclosures, and how the models affect control system design.
- Understand the causes and remedies of manufacturing and user variability for open-air ANR headsets.
- Investigate the effectiveness of frequency domain "loop shaping" control methods for open-air controller design.

The loudspeakers that are used today in the commercially available headsets are similar to speakers used in convention audio headphones. For designers of circumaural headsets, this is acceptable because they can shape the pressure response to meet the needs of ANC. For the supra aural designer, with no enclosure to augment the pressure response, it would appear that one must rely on the controller design alone to properly shape the response. This thesis examines whether there are innovations, aside form the controller, which might provide improved open-air ANR performance.

Since the design and manufacturing of loudspeakers is a very expensive proposition, this thesis does not focus on designing new loudspeakers. Rather, it focuses on understanding the design of headphone-sized loudspeakers that are available on the commercial market and how to use them successfully in an open-air ANR headset design.

1.2 ANR Headset System Description and Goals

Active noise control headsets have four major components, the electro-acoustic transducer (i.e. loudspeaker), a microphone, the enclosure the loudspeaker is mounted into and the electronics that define the compensator. Each of these components is considered to be equally significant in the design process. The system "flow" can be described as follows. The microphone measures an external disturnbance. This signal is sent to the compensator that shapes the incoming noise before passing it along to the

speaker system. The speaker system creates an anti-noise that is transmitted to the microphone. At the microphone, the disturbance and anti-noise are summed to create an error signal, which then becomes the input to the compensator, and the loop continues. Figure 1.1 shows the major components of the ANR headset system.

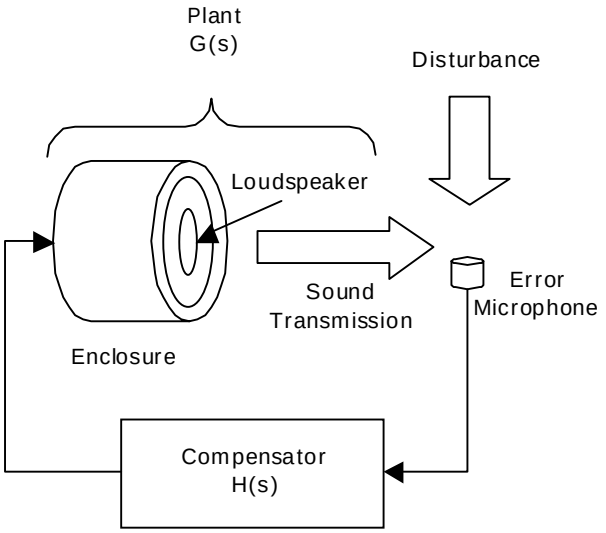

Figure 1.1 Components of an open-air ANR headset system

The first step for the control engineer is to determine how each component affects the system in terms of the open-loop frequency response. The microphone has a relatively flat frequency response over the bandwidth of interest. That is approximately 20 to 20,000 Hz, the bandwidth of human hearing perception. So, if the microphone does not saturate due to excess sound pressure levels, it will not contribute to the dynamics of the system. The engineer designs the compensator, so its dynamics can be set to whatever is desired. That leaves the loudspeaker system. The first question for the engineer is what should the pressure response of the loudspeaker optimally be, based on the objectives for closed-loop performance, and the second question is what is the uncompensated loudspeaker response currently?

The first question can be answered by considering time domain addition of two signals in the frequency domain. Imagine that the microphone measures a purely random signal of some magnitude, M. A random noise signal is the most complex noise field the headset

system could encounter. In the frequency domain, a random signal can be modeled as a constant magnitude over all frequencies with zero degrees of phase. This means that the incoming acoustic signal spans all frequencies with the same sound pressure. So in order to cancel the incoming signal, the loudspeaker system's frequency response should be exactly the same magnitude, M, and have the phase shifted by 180° when it reaches the same microphone and is summed. This is illustrated in Figure 1.2. Thus the resulting signal at the microphone has zero magnitude, no sound. If the loudspeaker could have a perfectly flat frequency response without any phase lag, it would be possible to have control over all frequencies.

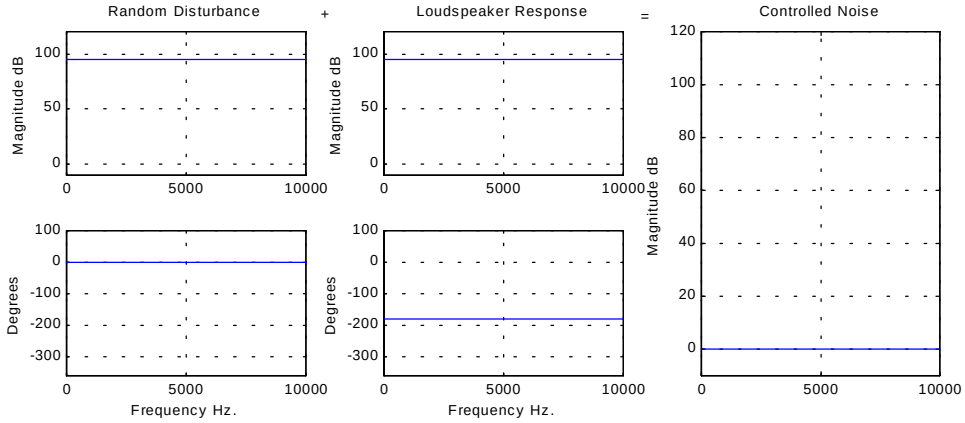

Figure 1.2 Optimal ANR headset feedback control solution

Unfortunately, the frequency response of a typical loudspeaker is far from having constant magnitude and phase. The loudspeaker presents a modally dense frequency response function that makes the control problem challenging. The third question is then, what should the loudspeaker's frequency response shape look like to be beneficial for control, and be physically possible? A typical frequency response for a loudspeaker that is used in a commercial set of headphones is shown in Figure 1.3.

Now designers must decide what approach they are going to take. They could attempt to reach the optimal design by building a compensator that contains the exact opposite dynamics of the loudspeaker, termed "inverting the plant". Or, they could choose a sub optimal design that offers less performance. If the optimal design is chosen as the goal, the designer must determine if the loudspeaker system is a minimum phase plant. This

means that all of the poles and zeros of the frequency response function are contained in the left half of the s-plane. If it is found to be non-minimum phase, they must choose a different strategy, because non-minimum phase systems are not invertible. If the system is minimum phase and a compensator can be realized, the designer must then determine if the system's frequency response changes when a loudspeaker of the same design specification is exchanged for the current loudspeaker. Due to variation in the manufacturing process, often loudspeakers of the same type experience differences in their frequency response. Next they must determine if the frequency response changes when different users wear the headset. Each person has a unique head related transfer function (HRTF) that describes the acoustics of their ear. With most ANR headset systems, small changes in the frequency response from user or manufacturing variations could cause the system to become unstable. If all of these criteria are met, the designer has achieved the optimal answer. Unfortunately, the system will usually suffer from all of the above conditions.

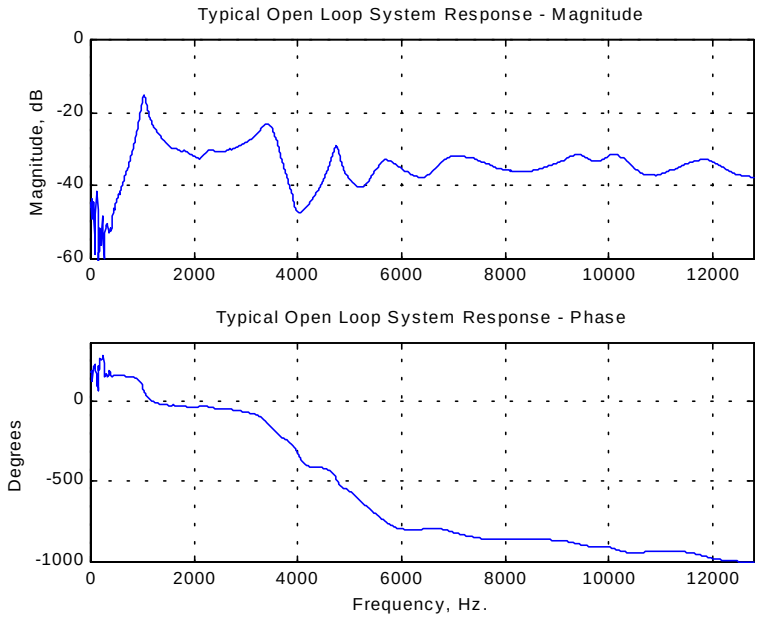

Figure 1.3 Open loop frequency response for a 1-inch headphone loudspeaker

Considering the variations mentioned above, a sub optimal open-loop frequency response goal must be developed. This goal should contain similarities with the current loudspeaker frequency response shape such that only minimum compensation will be

necessary. One goal that could be proposed is a complex set of poles. For this system, when the loop is closed, a bandwidth centered on the natural frequency of the poles is reduced in magnitude. So depending on the damping of the poles, the bandwidth of control is changed. Figure 1.4 demonstrates this type of response. Using the frequencies surrounding the first resonance of the loudspeaker as the control bandwidth and suppressing the dynamics past this point can realize this type of response. This approach has many advantages in terms of stability that will be discussed in Chapter 6.

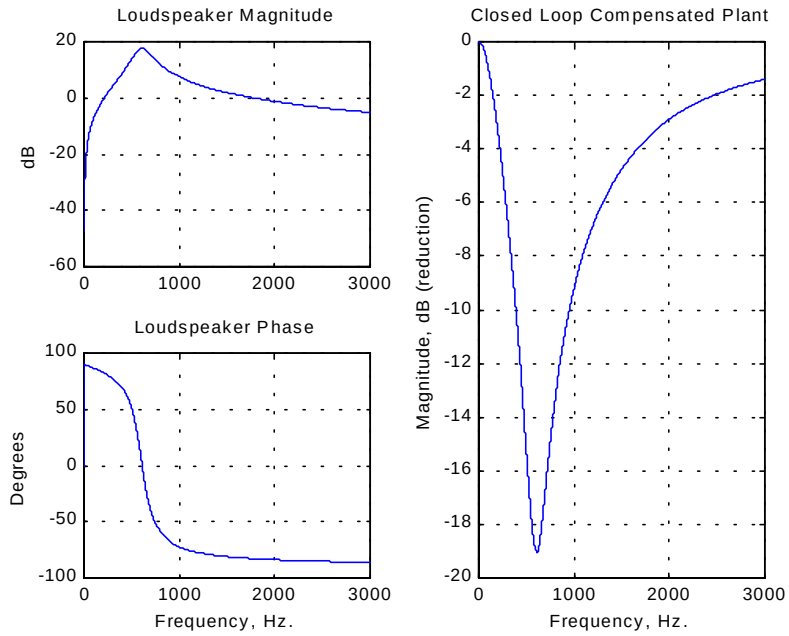

Figure 1.4 Sub-optimal closed loop performance

For the engineer, the last task is now to select, or design, a speaker that comes as close to the specified goal as possible. This will minimize the controller's order and will allow the designer to spend more effort on minimizing the variations from manufacturing and user interaction.

1.3 Presentation of Thesis

This thesis is presented in seven chapters that contain discussions on topics including: loudspeaker modeling, the open-air ANR headset design process, and corresponding robustness and control considerations. Chapter 2 will briefly discuss some of the previous literature pertaining to loudspeaker design, the ear's acoustic characterization

and the relationship between speaker design objectives for consumer audio and ANC purposes.

Chapter 3 is a detailed overview of loudspeaker modeling techniques. An introduction to the moving coil loudspeaker and its components will be presented. Next, a low frequency modeling method that utilizes impedance relations will be developed and tested. Each of the loudspeaker parameters will be evaluated to determine their effect on the overall pressure response. Due to the limitations of the impedance model, high frequency modeling will be discussed separately and several techniques will be reviewed, including finite element analysis. Finally, a simplified low frequency modeling technique will be presented that is very useful for measurement and low frequency design.

The design process for open-air headsets is examined in Chapter 4. A set of design metrics is proposed that take into account all facets of the design process. Particular attention is placed on manufacturing and user variability and on user safety. The discussions include topics such as head related transfer functions (HRTF's), power consumption, and ergonomics.

Chapter 5 contains a series of experiments that investigate the performance and robustness characteristics of the headset. The first three sections investigate methods for improving performance by modifying the loudspeaker system in each of its three domains, acoustical, mechanical, and electrical. The next two sections look at improving the manufacturing variability and user variability; therefore a robust plant can be realized. The final section is a brief look at synthesizing an "improved" loudspeaker for control application, which is completed purely as a theoretical exercise.

The results from the three previous chapters are then combined to facilitate a prototype design of an open-air ANR headset. Chapter 6 begins by presenting a short look at the theory necessary to implement the loop shaping technique. The theory presents detailed stability criteria and frequency domain compensator design techniques. Explanation of

the multi-step process to design a compensator for an open-air headset is then presented using experimental data. The end-result is a single channel prototype open-air headset. The closed-loop performance results are measured and show that an open-air headset can be realized.

The final chapter is a summary of the work done in this thesis and offers some suggestions for future work that could be undertaken to design a more suitable loudspeaker for control applications. Some of these suggestions include: an in depth study of finite element methods and understanding precisely how the material properties of a loudspeaker contribute to the pressure response would allow the engineer to prototype a speaker tailored for control applications. Other improvements could deal with improving the robustness of the overall ANR headset system.

Chapter 2: Literature Review

For a greater part of this last century, people have attempting to model moving coil loudspeakers. These attempts have all been made to further audio reproduction with the goal of creating a loudspeaker with low distortion and a uniform frequency response. During the period from 1950 to 1975 many low frequency modeling techniques were introduced. These techniques formed a generalized modeling methodology that focused on the first mode of the loudspeaker and use a minimum number of parameters to describe the model.

Since 1975, with the advancement in computer processing speed, many engineers have turned to finite element analysis (FEA) to try to develop a full range loudspeaker model. These techniques require very detailed descriptions of the properties of the loudspeaker and are very computationally expensive. The results are promising and with the ever-increasing speed of computers, the methods are becoming more accessible to designers.

Enter active noise control headsets. If the control engineer wishes to create a theoretical model for the system they must be able to describe the frequency response of the loudspeaker over the entire bandwidth of interest. This then requires a full range loudspeaker model. Realizing that the loudspeaker has more than a single mode of vibration, they must abandon the generalized methods and look to more complicated analysis techniques, like FEA. This process requires the control engineer to take on a second role, that of an audio engineer.

2.1 Low Frequency Models

The first generalized loudspeaker models were developed by electrical engineers. They related the parameters of the loudspeaker to electrical network theory. With the use of ideal transformers they were able to combine the mechanical, electrical and acoustical properties into a single lumped parameter model. In 1954 Beranak, in his book *Acoustics* [1], presents a very comprehensive acoustical circuit derivation. In this work the diaphragm velocity, sound pressure and efficiency for the low frequency response of the

loudspeaker is developed. Component level design is also discussed with emphasis on acoustic power output and efficiency.

While the electrical circuit approach was very accurate for simple loudspeaker systems, complex acoustical loading was difficult to include. By creating analogous acoustical circuits, complex-loading conditions could be easily modeled (Howard, 1972, [16]). This was accomplished by converting the acoustical properties into equivalent mechanical mass and compliance units. Also included in this work is a presentation of what the author terms “decoupled cone” response. An early attempt to create a high frequency model, this approach includes a mass and stiffness value for the dome portion (dust cap) of the loudspeaker that is attached to the rigid diaphragm by a compliant joint.

The acoustical circuit methods allowed for very accurate modeling, but did not easily facilitate design. Engineers would have to become very well studied in each of the parameters in order to specify a response. In a series of papers Richard Small [28-31] defined methods to model the low frequency response in both sealed and vented enclosures. This method relates the speaker parameters (mass, resistance, compliance, etc) to high pass filter models. He found that the systems mechanical natural frequency and the system damping dominate the frequency response at low frequencies for large woofers. With this assumption, he disregarded the electrical impedance due to its minimal contribution to the low frequency response. By converting the speaker parameters to analogous acoustical circuits, these parameters can be combined in a manner such that they form “quality factors”. These quality factors are then combined to form the total system damping. What makes this method so successful is that the engineer needs to perform only a small number of tests to evaluate the quality factors and natural frequency. Today, all commercial manufacturers specify their drivers using these quality factors.

For the control engineer these models are not sufficient for headset designs, but can be insightful when modifications are designed into the loudspeaker system.

2.2 High Frequency Models

High frequency loudspeaker modeling can be accomplished with two different methods. First, a continuous mechanical model can be realized by solving the boundary value problem. In this method, by specifying the boundary conditions and the material properties a Bessel function can be determined. Unfortunately, the material properties are rarely known in the detail necessary and the boundary conditions are seldom uniform. Even for simplified cases, the solution is extremely mathematically challenging.

The second method is a multiple lumped parameter model. By making the assumption that the diaphragm behavior acts axisymmetrically, and that the material properties are uniform over the diaphragm, the mechanical properties can be broken apart into multiple lumped systems (Murphy, 1993, [23]). By combining these multiple systems into a unified model, a multi mode representation can be realized. Having only finite mass and stiffness values for each of the systems determines the resonant frequencies, so only a rough approximation can be determined.

The finite element method has spread rapidly throughout many areas of design. The audio community has not fully embraced this method, not because the technique is not applicable, but because it is not sufficiently powerful. That is, the design tool capability is not yet fully developed. The process of converting sound to an electrical signal then to a mechanical vibration and finally back to sound involves many processes and cannot be modeled simply. There are a multitude of papers dealing with various components of the loudspeaker that FEA work has been applied, but a unified modeling technique has yet to surface.

Most analysis has focused on modeling the velocity of the diaphragm, where thin shell elements are used to simulate axisymmetric rings. This type of analysis limits the results to circumfrential modes and thus a less accurate model. Binks et al. (1991, [2]) use this assumption to model the diaphragm but explain that detailed information regarding Poisson ratio, Young's Modulus and all other mechanical properties is necessary to match experimental results. There have been attempts at a unified FE model, Y. Kagawa

et al. [17] present a finite element code that takes into account not only the diaphragm, but also a sealed enclosure. While they claim that the data is repeatable and consistent with other work being done today, they admit that they have not tested it against experimental results.

Due to the inability to exactly describe the mechanical properties for the FE code, many researchers have turned to optimization techniques to determine the pressure response from their FE models. Optimization may be considered the opposite of the modeling process where the response is known and the parameters to achieve that response are sought iteratively. Geaves, 1996, [13], presents a optimization technique for midrange diaphragm profiles utilizing Bezier curves that allow six design variables for each axisymmertic section. These design variables are iterated upon until the desired response shape is realized.

In the future, the control engineer may be able to incorporate a finite element model into their control scheme. Until then, there is not unified full bandwidth modeling procedure with the robustness necessary for open-air headset control system design.

2.3 Head Related Transfer Functions

A major problem for open-air headsets is the variability between users. This is due to a coupling between the acoustical impedance of the headset system with the impedance of the human ear. This coupling can modify the open loop pressure response of the loudspeaker system and cause the system to become unstable. On a circumaural headset, the enclosure modifies the acoustic impedance such that the headset system dominates the coupling. Without an enclosure to modify the acoustic impedance of the headset, the acoustic impedance for the open-air headset is the free air impedance. So the ear impedance influences the coupling.

Many scientists have studied the acoustic impedance of the human ear in an attempt to develop a generalized model. Since every person has unique ear impedance, these

models are driven by measurements. Gardner and Hawley, 1973, [12], developed an electrical network consisting of analogous acoustic parameters that utilizes a series of parallel acoustic circuits to model the inner ear impedance. By using 16 parallel LCR circuits, the authors were able to achieve agreement in the acoustic impedance to 16kHz.

For the headset problem, a more general model is necessary. What is desired is a model of the sound transmission path between the source (loudspeaker) and the receiver (eardrum). This is the basis of binaural recording. Møller et al., 1995, [21-22] performed a detailed study into the transfer function characteristics of headphones. Their goal was to characterize the impedance coupling between the headphone system and the ear so that they could evaluate what type of headphone was best suited for binaural sound reproduction. The goal for the headphone system is to maximize the impedance of the headphone system such that the pressure generated at the face of the loudspeaker is the same as the pressure received at the eardrum. The ANR headset is similar, except that the goal is to have the pressure at the error microphone be equal to the pressure at the eardrum. This clearly defines one of the goals for the open-air headset, to control the acoustic impedance such that the impedance of the ear does not modify the pressure response from the loudspeaker.

2.4 Consumer Audio and Active Noise Control

The loudspeakers that are used in ANR headsets are identical to those used in consumer audio headphones. Due to the lack of widespread interest in quality audio reproduction, the speakers that are available are of poor quality. This is because the general populous is not willing to spend significant extra money on a set of headphones that offers only slightly better performance [15]. The loudspeakers that are available have very poor quality control; the frequency response variations from manufacturing are quite significant. For example, since music is dynamic, most users are not going to notice if the gain is not matched on the left to the right loudspeaker, however in ANC small differences in frequency response between speakers can cause a fixed gain controller to become unstable.

Like in many industries, there is a “High-End” in audio reproduction. The loudspeakers that are produced by the high-end companies are significantly better in terms of manufacturing quality than their consumer audio counterparts. These loudspeakers are optimized to have very flat frequency response and good power handling. These speakers are not usually available for ANR headset designers due to design confidentiality, but while they exhibit vast improvements in manufacturing variability, they are not designed with the same goals as presented in Chapter 1.

Assuming that the ANR engineer does not work for a large company with the ability to prototype loudspeakers, they can decide to contract one of the high-end companies to manufacture a loudspeaker for ANC. This is entirely possible, but the investment is substantial. The tooling required to manufacture loudspeakers is extensive. Most large speaker manufacturers will not prototype speakers unless a minimum number are going to be purchased (usually around 20,000, courtesy Addax Sound). If all of the speakers met the manufacturing tolerances, that would yield 10,000 headsets which is a significant number of units to sell. So, unless the headset is truly revolutionary and can sell large volumes, the ANR engineer is left with the commercial audio speakers and must design the necessary robustness into their system.

Chapter 3: Loudspeaker Modeling

3.1Introduction

To be able to model the frequency response of a direct radiator loudspeaker will allow the control engineer to make conclusions about the potential of different loudspeakers for open-air feedback control applications. A full bandwidth model reduces the need for costly and time-consuming prototypes since multiple parameter sets can be simulated in a short time using a computer analysis package. As discussed in Chapter 1, manufacturing and user variability are challenges that have significance equal to control in the design of an open-air headset. By understanding the parameters that govern the frequency response of the loudspeaker system, insights can be made into solving these problems. A full bandwidth model will also allow the engineer to design new loudspeakers that are tailored for control applications. The block diagram for the open-air headset system is shown in Figure 3.1.

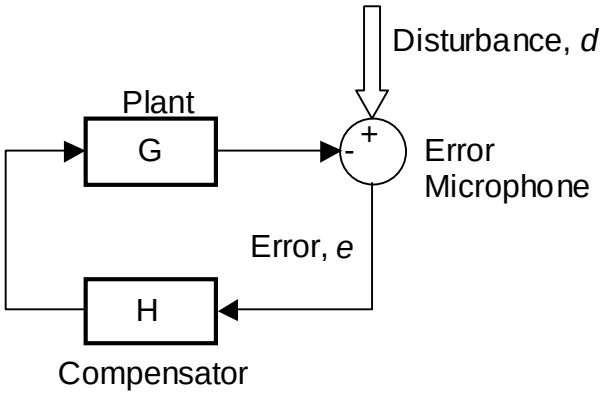

Figure 3.1 Open-air headset block diagram

3.2 Types of Transducers

There are many types of actuators that could be used for ANR headsets. Due to the zone of silence limitations the optimal realizable bandwidths for control are less than 2000 Hz, with the most effective control achieved at less than 500 Hz [24]. So any transducer chosen must have adequate bandwidth. Some examples of actuators include the moving coil loudspeaker, ribbon transducers, electrostatic transducers, Heil coil transducers, piezo-electric transducers, and bending wave panels (NXT). Several of these are not

particularly well suited for used in headsets. For example, an electrostatic transducer has a very flat frequency response, but requires two polarized metal plates with a potential exceeding 10,000 volts to create adequate sound pressures. If the diaphragm is overdriven, the system will arc and is potentially very dangerous. Ribbon and Heil coil transducers provide excellent high frequency extension for audio applications but are very fragile and cannot generate high sound pressures at low frequencies. Piezo-electric transducers can provide adequate bandwidth, but are not capable of producing the sound pressures necessary at low frequencies for open-air applications [4]. The most common actuator used is the moving coil (antireciprical) loudspeaker. It has the best combination of low frequency sound pressure and robust construction.

Figure 3.2 depicts a typical moving coil loudspeaker. The following sections will describe each component of the loudspeaker and how they contribute to the pressure-to-voltage transfer function. From this point on, the moving coil loudspeaker will be referred to as only the "loudspeaker".

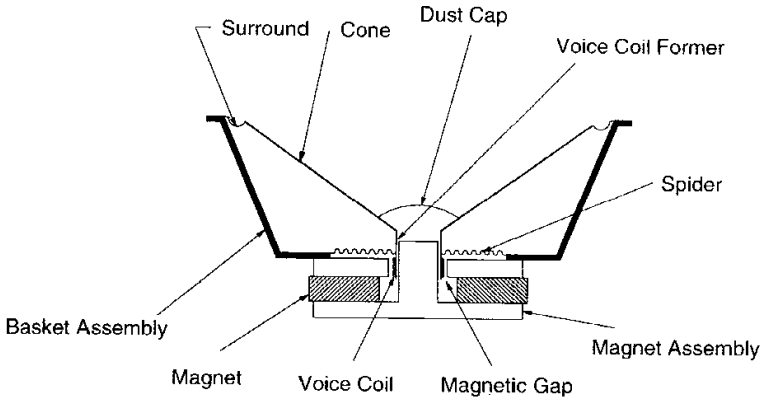

Figure 3.2 Loudspeaker component drawing

3.3 Loudspeaker Components

The loudspeaker is an electro-mechanical-acoustical device. It converts electrical signals into mechanical motion, which creates an acoustic pressure. The construction of loudspeakers is a complicated manufacturing process requiring significant tooling. Each component of the loudspeaker contributes to the frequency response so understanding of their role is critical for the control engineer.

3.3.1 The Magnet and Voice Coil

The voice coil is a lightweight tube usually made of cardboard or a plastic that is wrapped tightly with a specified length of magnet wire. Magnet wire has large gauge conductors with a baked enamel coating to allow very small center-to-center spacing. The voice coil is suspended inside the magnet. When a current is applied to the voice coil, Maxwell's equations for electromagnetics state that a force will be created that is proportional to the strength of the permanent magnet, B measured in teslas, T, and the length of the wire used on the voice coil, l, in meters. The voice coil is attached to the speaker diaphragm at one end and this force results in mechanical motion of the diaphragm.

The magnet wire is either copper or silver in composition. The material and the length of coil determine the DC impedance of the speaker. The gage of the wire and the length of the former, the tube the voice coil is wrapped around, partially controls what the maximum excursion of the speaker will be. This excursion, dubbed x_{max}, ultimately controls the overall sound pressure level, since sound pressure is linearly related to velocity. Once x_{max} is exceeded the magnetic field becomes nonlinear and harmonic distortion results. The magnet and voice coil introduce all of the electrical properties discussed in Section 3.4; coil inductance, coil resistance and the force factor, Bl.

3.3.2 The Diaphragm and Surround

The diaphragm, or cone, is an extension of the voice coil to improve acoustic efficiency. The cone is usually made of a lightweight rigid material. Some examples of cone material include: paper, plastic, aluminum, magnesium, titanium and Kevlar. All of these materials have very different mechanical resonance properties, and each has a unique "sound". The cone introduces mass, stiffness and mechanical damping terms into the pressure-to-voltage transfer function presented in Section 3.4.

The surround connects the diaphragm to the frame, or basket, of the loudspeaker. It is a compliant material, usually rubber or foam, which allows the cone to move a specified displacement. The surround adds additional mechanical damping to the cone. Its mass and stiffness, although usually significant, are normally neglected due to the small

displacements they undergo compared to the diaphragm. Also, at the extremes of displacement, many surround materials display nonlinear behavior that is very difficult to model.

3.3.3 The Spider and Basket

The spider is a compliant damping material connected to the diaphragm just above the voice coil. Its purpose is to add additional stiffness and damping to the diaphragm. Many of the speakers used in headsets do not contain a spider due to size limitations.

The basket is the frame, usually constructed from metal, which holds the diaphragm onto the magnet. It can be either cast or stamped. The design objective is to keep the mechanical resonance of the basket outside the bandwidth the speaker drives.

3.3.4 The Dust Cap and Air Vent

The dust cap is the inverted dome placed over the voice coil to keep the environment out of the magnet chamber. As of late, many designers are using cone-shaped dust caps, termed "phase plugs" that are designed to help sound dispersion at high frequencies.

The air vent is found on the bottom of the magnet. It allows airflow in and out of the magnet chamber to cool the voice coil. Not speakers used in headset applications will contain a dust cap or air vent.

3.4 Modeling

Two modeling approaches will be developed that can be summarized as being with and without the effects of the voice coil and acoustical impedances. The first is using impedance analogies to develop transfer functions between the acoustic pressure and the input voltage. This approach will incorporate the electrical inductance and is an accurate and scalable model. Due to the sheer complexities of building a multi-mode model, this thesis will only develop a single mode model. However, Section 3.4.3 delves into what is required to build a multi-mode model using an extension of the lumped parameter

method. The second approach is a simplified modeling scheme that only produces a single mode model. It was developed by Small and Thiele [28] and uses “quality” factors to simplify the analysis. These quality factors relate the speaker design process to that of electrical filter theory and have been adopted by commercial speaker manufacturers to represent their products. Although this approach neglects the electrical inductance, it is very beneficial for design of enclosures. The drawback is that this analysis does not accurately represent high inductance drivers as found in many commercial headphones.

3.4.1 Impedance Model

The first modeling scheme includes the electrical inductance, which is significant for miniature loudspeakers used in ANR headsets. The electro-mechanical-acoustical model for an antireciprocal transmitter mounted on an infinite baffle is shown in Figure 3.3. The moving coil loudspeaker is deemed "antireciprocal" because there is an inverse relation between the mechanical force and the electrical current with the transduction coefficient, *Bl.*

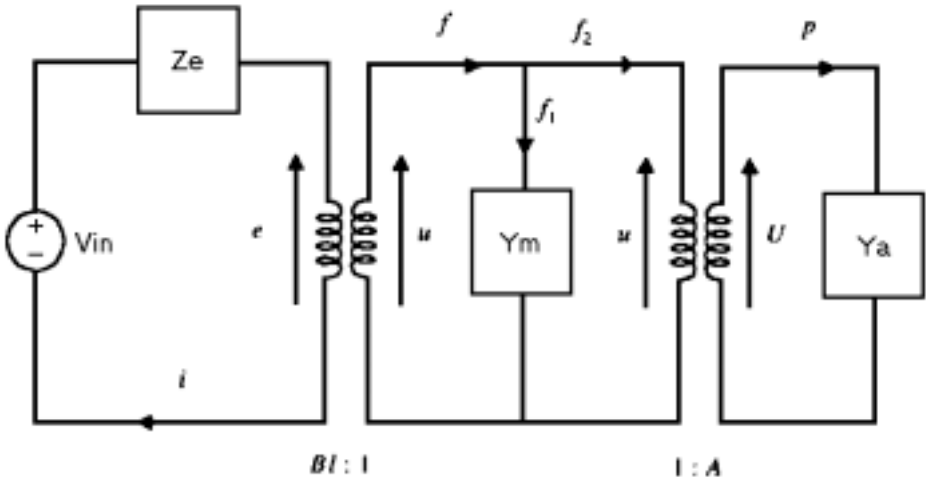

Figure 3.3 Electro-Mechanical-Acoustical impedance model

Loop Relations	Transformer Relations
$V_{in} + Z_e i - e = 0$ (3.1)	$Bli = f$ (3.4)
$u + Y_m f_1 = 0$ (3.2)	$e = Blu$ (3.5)
$U + Y_a p = 0$ (3.3)	$Au = U$ (3.6)
	$f_2 = pA$ (3.7)

Where:

Parameter	Symbol	Units
Input Voltage	V_{in}	V
Speaker Current	I	a
Mechanical Forces	f, f_1, f_2	N
Speaker Velocity	u	m/s
Volume Velocity	U	m^3/s
Acoustic Pressure	p	pa (N/m^2)
Speaker Cone Area	A	m^2
Voice Coil Force Factor	Bl	Wb/m
Speaker Back emf	e	V
Electrical Resistance	R_o	Ω
Inductance of Voice Coil	L_o	H
Speaker Moving Mass	M	g
Mechanical Damping	R_{ms}	N-s/m
Mechanical Stiffness	K	N/m
Mechanical Admittance	Y_m	m/N-s
Acoustical Admittance	Y_a	m^5/N-s
Mechanical Impedance	Z_m	N-s/m
Acoustical Impedance	Z_a	N-s/m^5
Electrical Impedance	Z_e	Ω

Table 3.1 Impedance analogy parameter list

Since the acoustic pressure and the input voltage are the parameters measured for control, we would like to form a transfer function in terms of those variables. Following the transformer and loop relations this is a fairly straightforward process.

There are many methods at arriving at the desired transfer function; the following method is helpful because it incorporates the electrical impedance transfer function, Ze_{sys}. The first step is to find a transfer function relating the diaphragm velocity and the current. Before this can be accomplished a few preliminary relationships must be determined. Using (3.3), (3.6) and (3.7):

$$p = -\frac{U}{Y_a} = -\frac{Au}{Y_a} \quad (3.8) \qquad f_2 = -A^2 \frac{u}{Y_a} \quad (3.9)$$

From the diagram:

$$f_1 = f - f_2 = Bli + A^2 \frac{u}{Y_a} \quad (3.10)$$

By inserting these quantities into (3.2):

$$u + Y_m (Bli + A^2 \frac{u}{Y_a}) = (\frac{1}{Y_m} + A^2 \frac{1}{Y_a})u + Bli = 0 \quad (3.11)$$

Since $Z_m = \frac{1}{Y_m} and\ Z_a = \frac{1}{Y_a}$ we can simplify the above expression to:

$$\frac{u}{i} = \frac{-Bl}{Z_m + A^2 Z_a} \quad (3.12)$$

Secondly, a relationship between the input voltage and the current must be found. This is the dynamic electrical impedance, Ze_{sys}.

Using expressions (3.1) and (3.5) and inserting our result for $\frac{u}{i}$ (3.12):

$$V_{in} + (Z_e + \frac{(Bl)^2}{Z_m + A^2 Z_a})i = 0 \quad 3.13a$$

$$\frac{V_{in}}{i} = -(Z_e + \frac{(Bl)^2}{Z_m + A^2 Z_a}) \quad 3.13b$$

Note that the dynamic electrical system impedance contains all three original impedance terms. This solidifies our notion of having "system" properties.

Third, a transfer function between the acoustic pressure and the current can be developed. By examining the circuit diagram, $f_1 = Bli - pA$, and inserting this into (3.2) and multiplying by Z_m yields:

$$Z_m u + Bli = pA \quad (3.14)$$

Dividing through by A and I and inserting our result for $\frac{u}{i}$ (3.12):

$$\frac{p}{i} = -\frac{1}{A}(Z_m (\frac{Bl}{Z_m + A^2 Z_a}) + Bl) \quad (3.15)$$

Finally, the transfer function from pressure to input voltage is:

$$\frac{p}{V_{in}} = \frac{p}{i}\frac{i}{V_{in}} \quad (3.16)$$

In order to evaluate the above expressions, assumptions must be made for the mechanical, electrical and acoustical impedances. At this point it has been chosen that a single mode model will be developed. This is due to the complexities of the mechanical model that will be discussed in 3.4.3.

In order to develop the model for the electrical impedance, knowledge of motor systems is helpful. As current is applied to the voice coil, a force proportional to the magnetic field multiplied by the length of the voice coil is applied to the diaphragm (Maxwell's equations) (3.4). Conversely, if the diaphragm is set into motion, it will generate a voltage in the coil (3.5). If the diaphragm is held in place, (*blocked*) the electrical impedance (as represented in the Laplace domain) can be represented the series combination of the resistance and inductance of the voice coil.

$$Z_e = L_o s + R_o \quad (3.17)$$

The electrical impedance is the relation between input voltage and current.

To vastly simplify the mechanical impedance, several assumptions are made. It is assumed that the diaphragm remains rigid over the entire bandwidth. The diaphragm is also considered a lumped mass. The stiffness and damping are assumed to be constant, and the mass, stiffness and damping of the surround, spider, basket, dust cap, and voice coil are assumed to be negligible. Thus a single mode model is created at the primary natural frequency of the diaphragm. It can be modeled in the Laplace Domain as:

$$Z_m = \frac{Ms^2 + R_{ms}s + K}{s} \quad (3.18)$$

This is a velocity relationship for the system; the impedance represents a force to velocity relation. It should be noted that the mechanical impedance is not a proper transfer function; it has more zeros than poles. Normally when modeling a mass-spring-damper system it is the mechanical admittance that is considered.

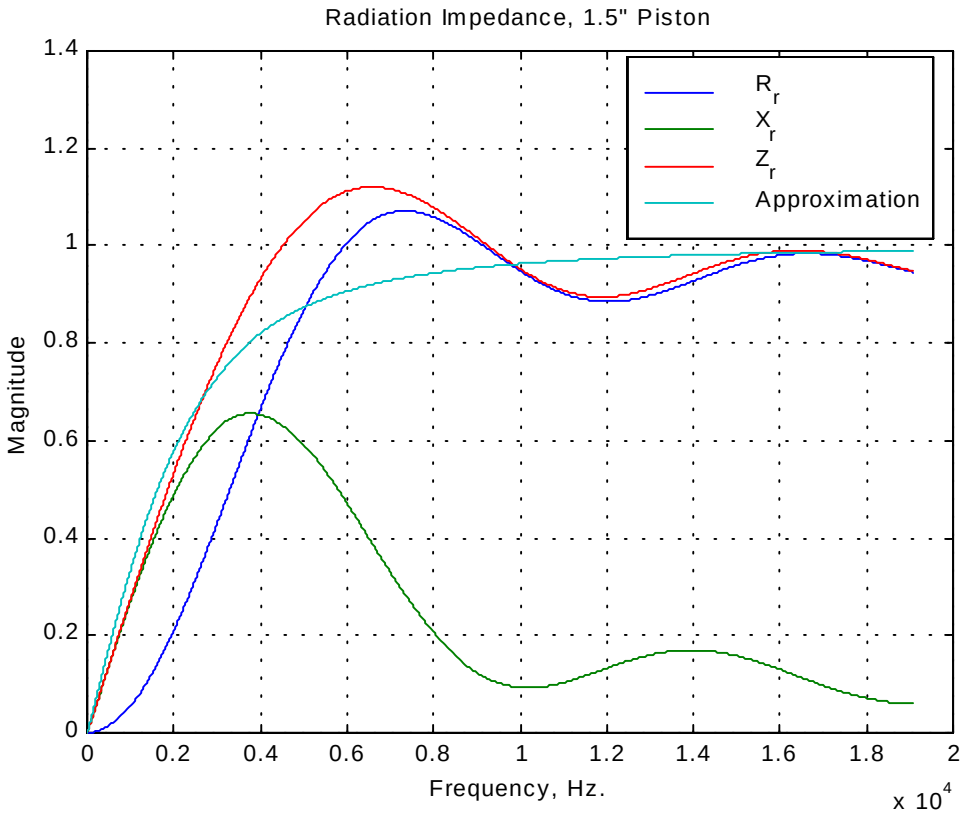

Figure 3.4 Acoustic impedance, actual and approximate

Although the surface of the diaphragm is concave and textured, it will be assumed that the geometry will be that of a flat piston. The acoustical impedance for a circular piston in an infinite baffle is defined using Bessel functions. Their derivation can be found in any acoustic text [8]. These functions require numerous terms to appreciate, so we will estimate the impedance as a high pass filter that can be seen in Figure 3.4. For a piston with a diameter of 1.5", the corner frequency, 'b', is approximately 2,800 Hz.

$$Z_a = C(r)\frac{s}{s+(2\pi b)} \quad (3.19)$$

$$C(r) = \frac{\rho c}{r}(\textit{Microphone dynamics})$$

Where 'r' is the distance from the microphone to the speaker. The microphone dynamics are also included in this expression. Most real microphones have a sufficiently flat magnitude response over the bandwidth of interest, so they can usually be disregarded.

Now inserting the above expressions into the impedance relations yields:
Velocity to current:

$$u(s) = \frac{-Bls^2 - Blbs}{Ms^3 + (Mb + R_{ms} + A^2C)s^2 + (R_{ms}b + K + A^2Ca)s + Kb} \quad (3.20)$$

Due to the sheer length of the expression, the numerator has been split into sections so it can be displayed on this page.
Input Voltage to current:

$$D = L_o(Mb + R_{ms} + A^2C) + R_oM \quad (3.21a)$$

$$E = L_o(R_{ms}b + K + A^2Ca) + R_o(Mb + R_{ms} + A^2C) + (Bl)^2 \quad (3.21b)$$

$$F = L_oKb + R_o(R_{ms}b + K + A^2Ca) \quad (3.21c)$$

$$V(s) = \frac{-L_oMs^4 - Ds^3 - Es^2 - Fs - R_oKb}{Ms^3 + (Mb + R_{ms} + A^2C)s^2 + (R_{ms}b + K + A^2Ca)s + Kb} \quad (3.21d)$$

It should be noted that V(s) is an improper transfer function; it contains more zeros than poles. This is caused by the choice for the mechanical impedance.

Acoustic pressure to current:

$$p(s) = \frac{ACs^3 + ACas^2}{Ms^4 + (Mb + R_{ms} + A^2C)s^3 + (R_{ms}b + K + A^2Ca)s^2 + Kbs} \quad (3.22)$$

Acoustic pressure to input voltage:

$$\frac{p}{V_{in}} = P(s)V(s)^{-1}$$

$$\frac{p}{V_{in}} = \frac{-(Bl)ACs^2 - (Bl)ACs}{L_oMs^4 + Ds^3 + Es^2 + Fs + R_oKb} \quad (3.23)$$

The end result is a fourth order transfer function in terms of s. The following sections will evaluate how each variable contributes the overall response of the system.

3.4.2 An Example

The model's validity was checked against a number of different loudspeakers. Figure 3.5 is speaker used in a commercial set of headphones. The speaker has a 1.5-inch diameter, with a plastic diaphragm. Figure 3.6 shows the electrical impedance of the speaker. The electrical impedance is the voltage to current transfer function determined above.

Figure 3.5 shows clearly how well the model estimates the primary mode of the speaker. After 1500 Hz. the model for this particular driver is no longer valid. The actual speaker obviously contains more than one mode over this bandwidth so the assumptions made to create the model above must be changed. The second peak in the pressure response is called the first breakup mode. At this frequency the diaphragm no longer acts as a rigid piston.

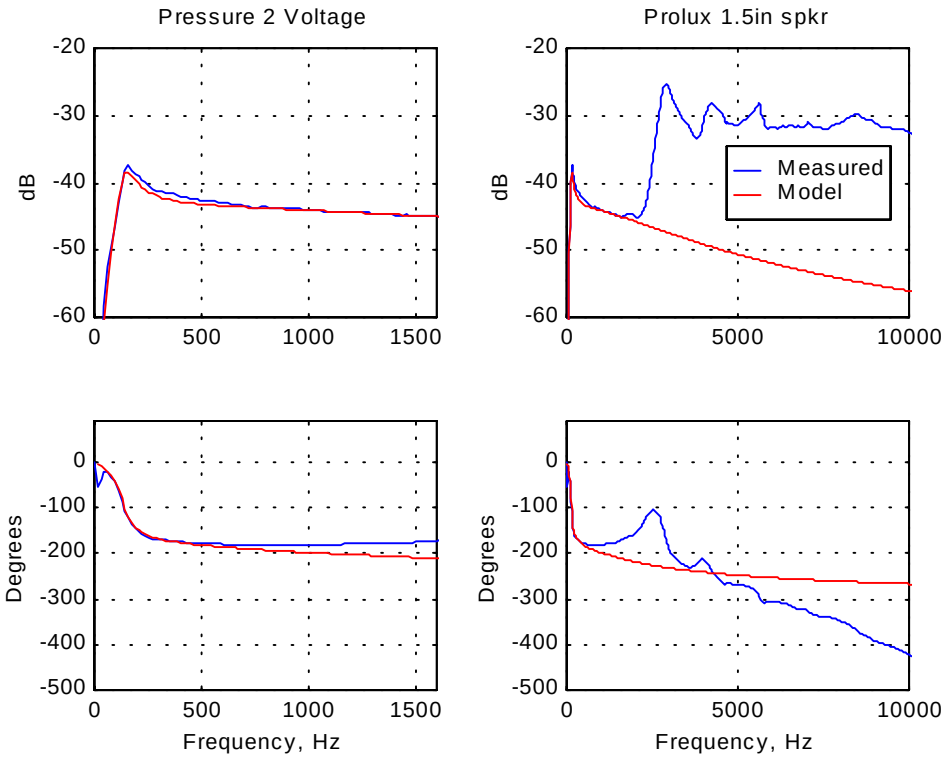

Figure 3.5 Impedance model verification

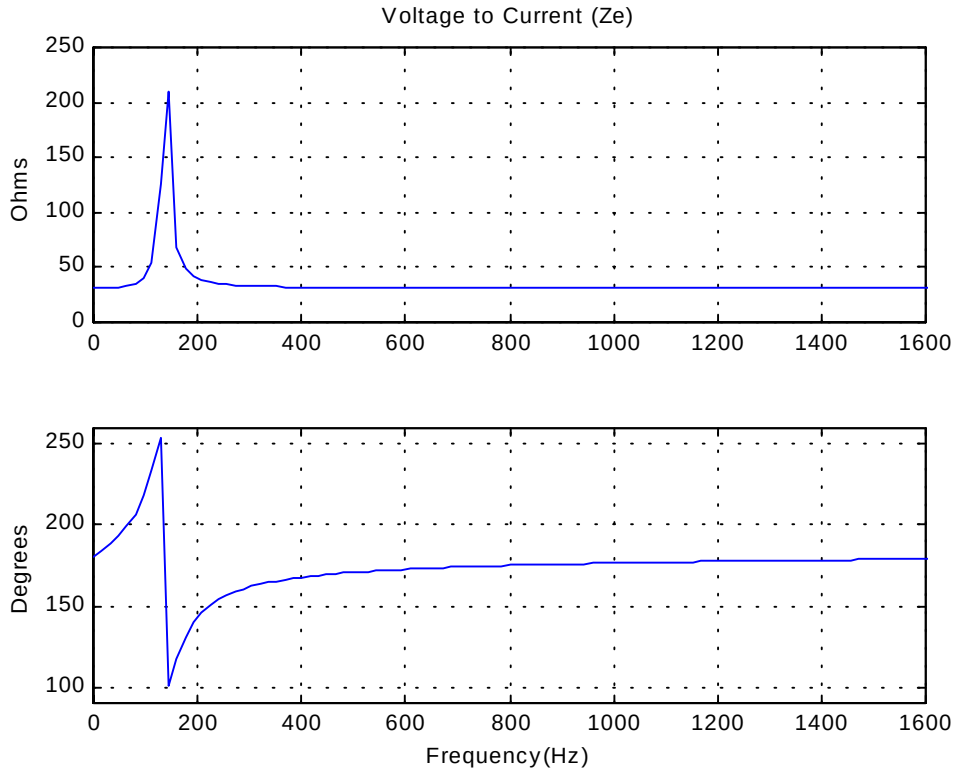

Figure 3.6 Electrical impedance model

Symbol	Value
M	4.4e-4 Kg
R_{ms}	0.001 N-m/s
K	300 N-m
L_o	0.0001 H
R_o	31.3 Ω
Bl	2.5
A	0.0011 m^2
b	15707.96 rad/s

Table 3.2 Parameters used for the Proluxe speaker model

Table 3.2 shows the parameters used for the model. Unfortunately the manufacturer did not provide the parameters for this driver, so the parameters had to be found by experimental methods. Colloms, [7] presents methods for determining loudspeaker parameters experimentally. Now with the assurance that the pressure-to-voltage (p2v) transfer function can be used effectively to model the first mode for real data, it would be beneficial to be able to characterize the effects of each parameter in the transfer function. The most benefit for a control study would be how each parameter affects the individual poles and zeros of the transfer function. With this information, the designer could synthesize a response function that could approach the goals set in Chapter 1. The first step is to factor the fourth order denominator of the pressure to voltage transfer function into its roots. Mathematica software was used in an attempt to factor the p2v transfer function. Although Mathematica did converge on an answer, the results were not friendly for analysis. Each of the four denominator terms, or poles, needed approximately 2 pages of 10 pt. text to display the answer. This is not entirely unexpected, for finding the roots of a fourth order symbolic is not usually possible by hand and any computer code will require specific optimization for the best results.

The next possibility is to graphically represent the changes in the parameters. In the following sections each of the parameters used in the pressure to voltage transfer function will be varied one at a time so that it is possible to determine how changes in that parameter will effect the transfer function. In order to make a realistic comparison, the parameters will be grouped into four categories, electrical, mechanical, magnetic and

acoustical. The goal is to be able to identify loudspeaker that have properties that could be beneficial for control.

3.4.3 Mechanical Modifications

The mass, stiffness and damping of the diaphragm are all interrelated. If one quantity is specified, the material properties set the other two as a function of the first. Thus, the choices of properties are all dependant on the material selection. In the audio world, designers have designed diaphragm cones using paper, carbon fiber, Kevlar and magnesium. These choices are driven by a need for greater bandwidth and less distortion. The goals for control are much different, a high magnitude, low frequency resonance and minimum high frequency contribution with minimum phase lag. The choice of materials that can yield those goals for control is not straightforward.

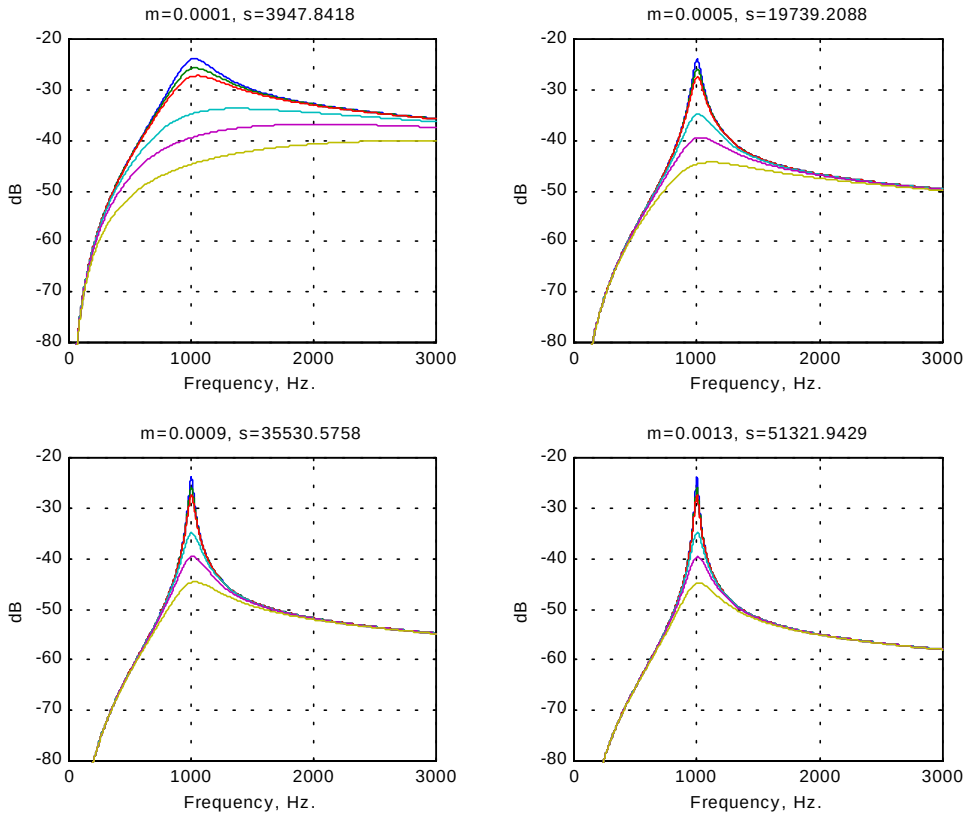

Figure 3.7 Pressure response with mechanical parameter variations

Figures 3.7 shows the system used in Section 3.4.2 modified with variation in the mass, stiffness and damping, respectively. In each trace the system has a natural frequency of 1000 Hz. and six different damping levels. As the mass and corresponding stiffness is increased, the overall damping of the system is decreased. This can be illustrated by examining the impulse response as shown in Figure 3.8. With the increased mass and stiffness, but without increasing the force factor of the motor, the system cannot control the momentum of the diaphragm and the system's time response shows a ringing phenomena. As the damping is increased, the magnitude of the resonant peak is decreased, as should be expected.

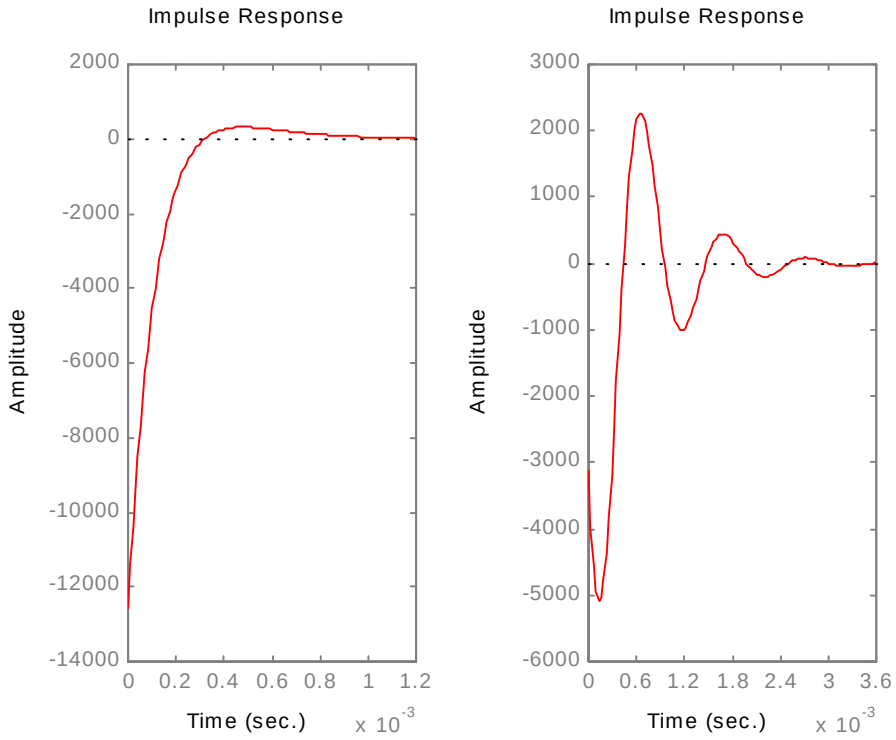

Figure 3.8 Mass and stiffness effects on the impulse response

3.4.4 Magnetic Modifications (Force Factor)

The force factor, Bl, is the product of the permanent magnet and the length of the wire wrapped in the voice coil. Bl appears in both the numerator and denominator of equation 3.23. It can be factored out of the numerator of equation 3.23 and can be thought of as gain into the system. The force factor can be modified in several ways. By using a permanent magnet with a stronger gauss field will directly increase the magnetic field, B.

This can be accomplished by using rare earth magnets made out of germanium or related metals. These metals are significantly more expensive than regular magnet materials and the designer must weigh the performance to cost ratio for whether it is appropriate for the system. Another method for augmenting the force factor is to add windings to the voice coil. This will not only increase the force factor, but will also increase the inductance and resistance of the system. A third method is to build a speaker with two voice coils. The two voice coils are cylindrical inside of one another and each have a characteristic impedance. When both the coils are run in parallel, the nominal resistance is halved, the inductance is increased and the voice coil length is effectively doubled. When the coils are run in series, the nominal resistance is doubled, the inductance is doubled and the voice coil length is still doubled. Still another method is to run only one coil for a different characteristic impedance. This makes for a very adaptable design.

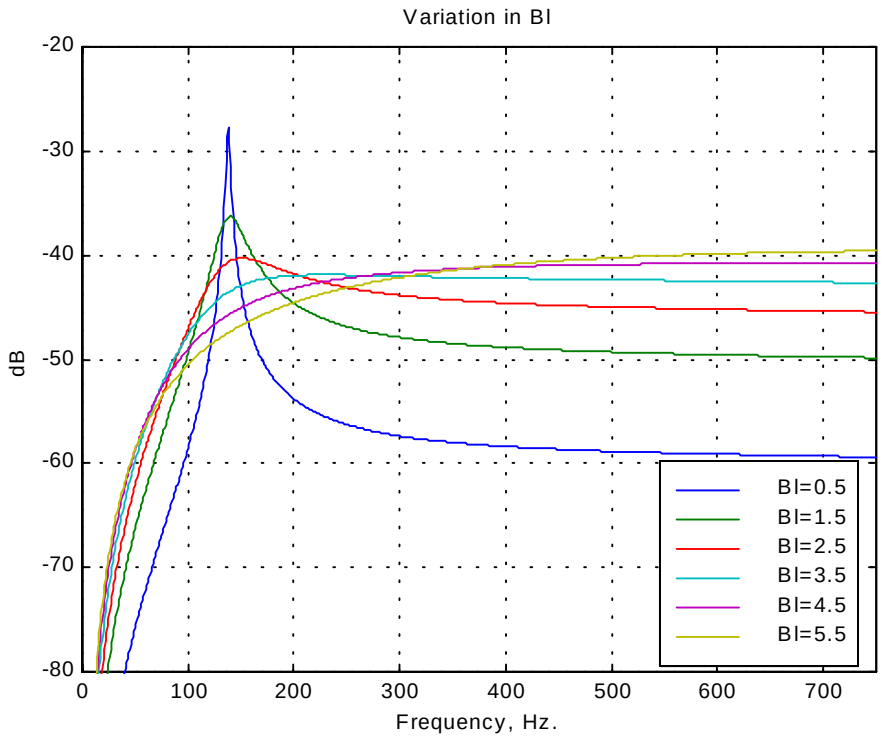

Figure 3.9 Pressure response with variation in Bl

Figure 3.9 shows the system used in the previous example with different values of Bl. In this figure there are only one set of mass and stiffness parameters. The results are the opposite of the last case where increasing the mass and stiffness with a constant force

factor led to lower damping. Now with the set mass and stiffness, the increase in force factor increases the damping. The force factor also acts a gain on the system. For about a ten times increase in force factor, the magnitude was increased 20 dB in the pass band.

3.4.5 Electrical Modifications

The electrical parameters, the resistance and inductance, are properties of the wire wound on the former of the voice coil. Differing the type and gage of wire used creates variations in the inductance and resistance. Most speakers designed for audio are 4, 6 or 8 ohms nominal impedance. This is because solid-state amplifiers make more power driving smaller loads. Many speakers for headphones are 16 or 32 ohms because the ear is at a very small distance from the driver and only very moderate amplifier power is required to create very high sound pressure levels. Also, some amplifiers that are used with headphones are powered by single semiconductors that require high output impedances to function correctly. The inductance is often disregarded when large speakers are being analyzed. This is because the mass of the speaker plays a similar role in a system perspective. When the mass or inductance of a large speaker is transformed into the corresponding domain, mechanical or electrical, the analog for the mass will have a much greater value than the inductance and will dominate the response. For small headphone speakers the inductance plays a significant role. The resistance and inductance are found in every term of the denominator of equation 3.23.

The plots in Figure 3.10 were simulated to show an inductance value for various resistance values. The parameter values were taken from a 4-inch Focal loudspeaker. These parameters were chosen because the Focal came supplied with a very complete data sheet, and these parameters were verified correct by the author. In both figures various resistance values are plotted for a given inductance. The systems overall resistance controls its overall gain, where lower resistance yields higher gain. The total inductance controls the primary resonance's damping (Q) and the frequency. As the total inductance increases, the variation in Q and frequency diminishes with changes in resistance.

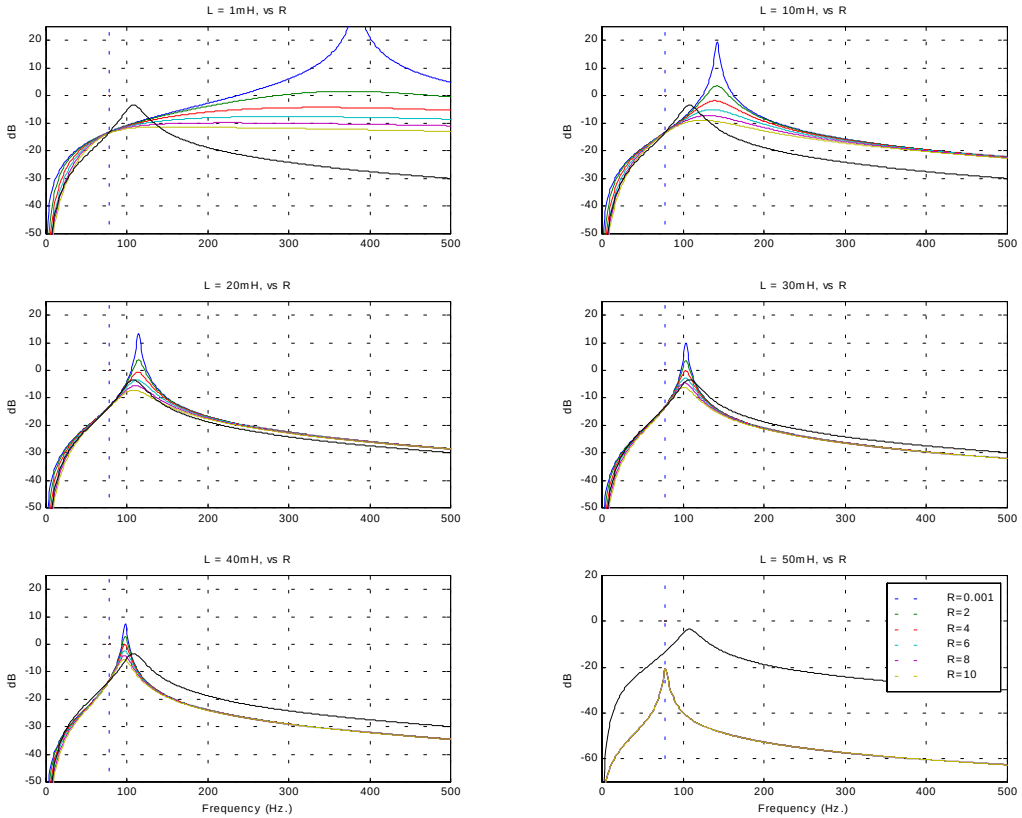

Figure 3.10 Pressure response with electrical resistance and inductance variations

In Figure 3.10 the blue vertical line represents the mechanical natural frequency. When the inductance is very small there is not any frequency shifting. The exception is when the system has nearly zero resistance, which is normally avoided because amplifiers cannot drive purely imaginary loads. As the inductance becomes larger, it shifts the primary frequency higher until it hits a limiting point, and then it decreases and becomes asymptotic with the mechanical natural frequency. It should be noted that the value of inductance is to reach the final asymptote approaches 1 Henry. This is not a reasonable possibility for the headset due to the sheer size of a 1 Henry inductor and the amount of power it would store. For a reference, the black line was added and represents the driver with its nominal inductance value.

3.4.6 Acoustic Impedance Modifications

The acoustic impedance for the system is a function of the geometry of the diaphragm and controls the acoustic radiation. As shown earlier, the acoustic impedance acts as a high pass filter. This limits is the sound pressure from the mechanical velocity at low frequencies. To investigate how much magnitude is lost from the low frequency resonance due to the acoustic impedance, a multi-mode mechanical system was created for a 1.5" speaker. This system was then modeled with the acoustic impedance for a piston on an infinite baffle, which was shown to be a high pass filter with a corner frequency of 2800 Hz., and if the acoustic impedance was modified such that the corner frequency was below the first resonance of the system.

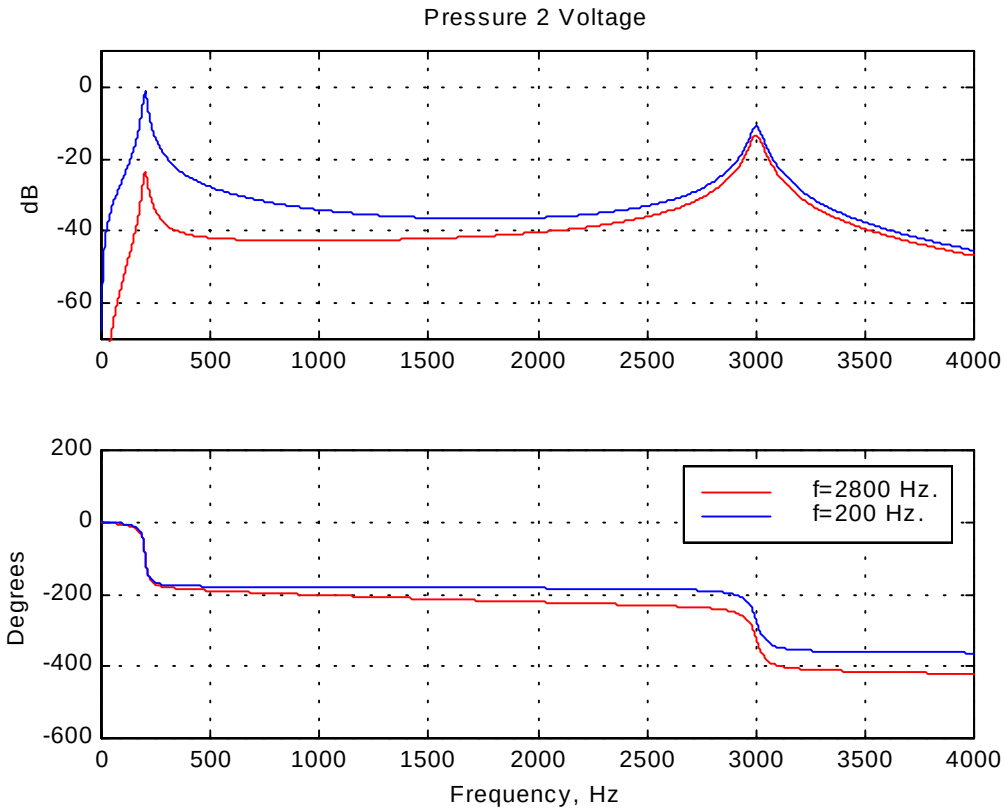

Figure 3.11 Acoustic impedance effects on pressure response

As shown in Figure 3.11, the actual acoustic impedance reduces the magnitude of the pressure response significantly. For this example, the system is reduced by 22 dB. The magnitude will decrease at 20 dB per decade before the corner frequency of the acoustic

impedance. Optimally, in order to get all of the magnitude from the mechanical system, the designer would specify the resonance above the corner frequency of the acoustic impedance. In order to be able to get full magnitude at 1000 Hz., it would seem that if no gain were to be added to the system, it would be advantageous to develop a speaker with a diameter that specifies a 1000 Hz. corner frequency. This can be done using equation 3.24.

$$f_{corner} = \frac{c}{2\pi r} \quad (3.24)$$

Where c is the speed of sound in m/s and r is the radius of the speaker. Thus for a 1000 Hz. corner frequency, a 4-inch speaker is necessary. While it is possible to construct a headset using a 4-inch speaker, it would be very awkward to wear. So the designer must be aware of how much gain will be required for the frequency they wish to control.

3.4.7 High frequency speaker modeling

Now that it has been demonstrated that the first mode can be modeled using a fourth order transfer function, the next task is to develop a multi-mode model. The framework above is expandable to a multi-mode model by inserting more accurate models for the electrical, mechanical and acoustical impedances. In fact, the simple electrical model is relatively accurate under normal driving conditions (under high power situations, thermal effects become significant to the electrical impedance and cause distortion). The acoustical model can contain more terms, but as the high pass filter shown in Figure 3.4 displays, there is really little to gain in terms of accuracy. The mechanical model is where the complexities begin. The simplification used represents a solid lumped mass connected to the driving force by a spring and damper. The actual system is a semi-rigid curved and textured diaphragm that is driven by at a radial distance from its center. The diaphragm is connected to a stiff frame by a compliant foam material. There is also an element near the center of the diaphragm to add damping.

Since the stiffness and damping of the diaphragm are functions of radius, r, and travel, x, very exacting mechanical properties must be known to evaluate. Also, due to the irregular shape of the basket, its resonant properties are very difficult to simulate. Due to the small size of the loudspeakers we wish to model, the adhesives and other bonding

agents (crimps, rivets, etc.) must be modeled with precision because small differences in bonding forces play a significant role as the speaker becomes smaller.

In order to evaluate this model, many approaches are available. First there are experimental methods that measure the pressure-to-voltage or velocity to voltage transfer functions. These techniques include laser vibrometry and pressure measurement. While not an analytical modeling technique, by curve fitting the data using a least squares or similar approach, a model can be created to characterize the data. Matlab contains a curve fitting scheme that can be run with the command "INVFREQS" that allows the user to input the number of poles and zeros and the tolerance for the curve fit. This model can then compared to an approximate model. This method will only be effective for the sample under test; it is not a generalized modeling method.

3.4.7.1 Axisymmetric Models

Perhaps the closest to a generalized high frequency modeling method, an axisymmertic model, presented by Murphy, [23], can be developed. With an extension of the lumped parameter method, the assumption that the loudspeaker's geometry and mode shapes are symmetric around the axis of vibration can lead to a multi-mode model. By assuming that the loudspeaker behaves axisymmetricly, each circumfrential section can be broken apart into multiple lumped parameters. As in all modeling methods, there are assumptions.

- The cone is straight sided, with uniform material properties and uniform thickness. If the speaker has a dust cap, it is hemispherical in nature.
- The cone is divided into multiple annular segments, which are equally spaced along the radius. The mass of each annular segment increases as the rings advance toward the outer rim of the speaker.
- The voice coil and the former are completely rigid, but there is a compliance where they join the dust cap, or base of the diaphragm. Each segment of the cone is assumed to be completely rigid.

- The forward acoustic radiation is calculated for the dust cap and all segments on the front facing surface. The rear acoustic radiation is only calculated for the cone segments, not the dust cap.
- The acoustic load for each annular segment is calculated as if the segment were a circular piston of equivalent area. There is not acoustic coupling between the segments.

The next section is a brief overview of the process:

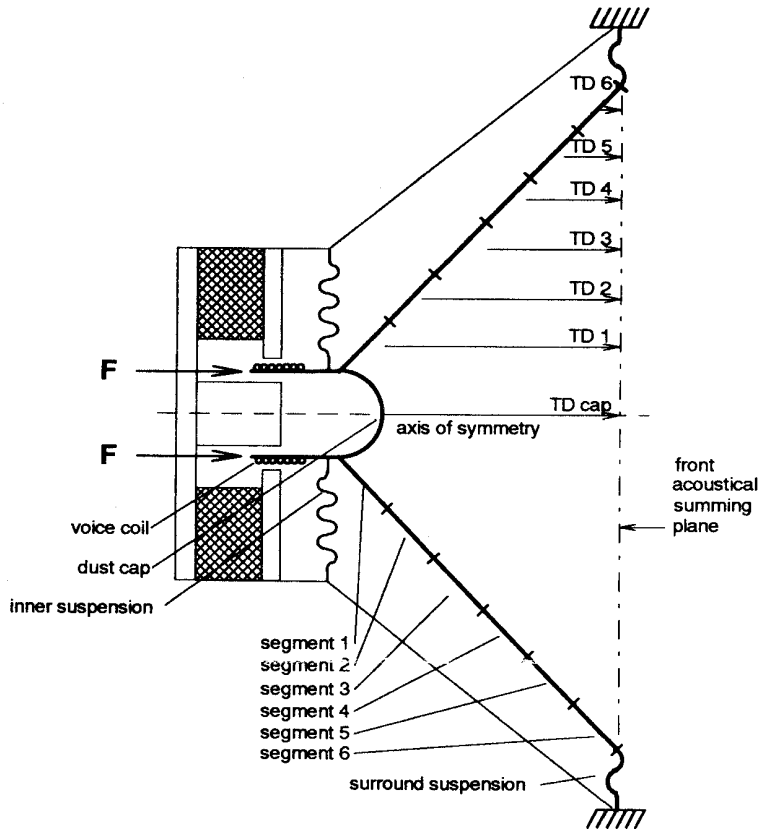

Figure 3.12 General arrangement of cone segments and acoustical summing plane for an axisymmertic model, courtesy [23]

The cone is thus divided into several "rings". Figure 3.12 is an illustration of how the cone is divided. Each of these rings has its own mass, stiffness and damping. These parameters are all estimated from the system parameters. The mass of each of the rings is

determined from the projected area of the cone segments. This assumes that the cone is straight sides and is formed with an oblique angle. The projection is onto the acoustical summing plane, as seen in Figure 3.12. Figure 3.13 shows a mechanical model that assumes axial symmetry.

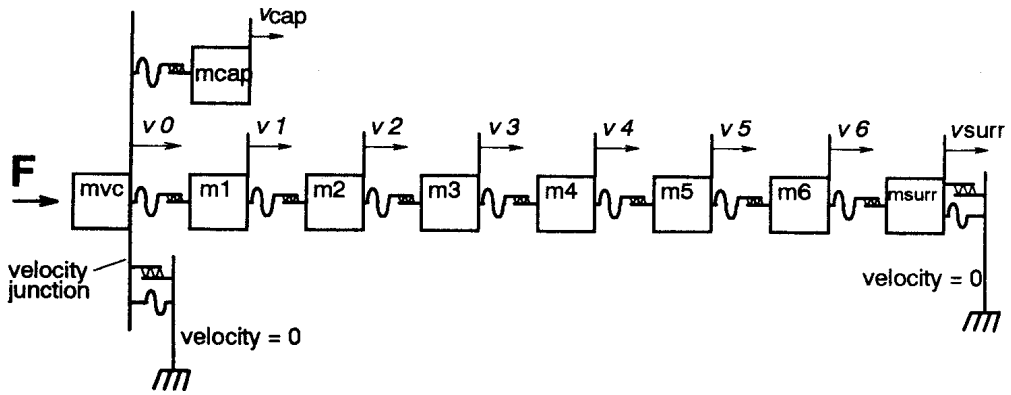

Figure 3.13 Mechanical representation of an axisymmertic model

The acoustic impedance is then calculated for each of the sections. Creating a circular piston with an area equivalent to the sectioned area does this. There is not acoustic coupling between the sections, each acoustic impedance is considered separately.

Next the compliance of each section is calculated. Unfortunately, the change between sections is quite complex that involves the elasticity of the cone material. Each segment experiences displacements in both axial and radial directions. Fortunately, the problem has been solved and has been termed the "Belleville washer". The deflection can be found by:

$$d = \frac{4W}{3\pi E t^3}\left(R_2^{\,2} - R_1^{\,2} + R_1 R_2 \ln\frac{R_2}{R_1} \right) \quad (3.25)$$

where

d = deflection, inches

W = load, pounds

E = modulus of elasticity, lb/in^2

R_1 = inside radius, inches

R_2 = outside radius, inches

t = plate thickness, inches

The compliance is equal to the deflection divided by the load, W. So by solving the equation for d/W and realizing that the term outside the brackets is a constant, the compliance for each ring can be determined by solving the bracketed expression. For systems with dust caps the innermost ring outside of the dust cap is usually determined empirically to represent the resonance of the voice coil. With the dust cap present, the terms determined by the Belleville washer solution must be normalized to the first segment. For systems without a dust cap, the center ring will have an innermost radius equal to zero. This leads to an infinite compliance for the center section. To solve this, the center section is given a value that is equal to the mean value of the outer sections. Then all of the sections are normalized to the total compliance of the system.

Unfortunately, the system damping cannot be divided between each segment. Determining the damping for each section requires determining the type of response (Q filter designation, see 3.5). After the response type is set, the damping is adjusted to the fit.

For demonstration purposes, a model for the example speaker in Section 3.4.2 will be created utilizing two sections. It will be assumed that the cone is a flat piston with uniform thickness and without a dust cap. The speaker has a radius of 0.75 inches and a diaphragm mass of 4.0e-4 Kg. The inside ring will have a radius of 0.25 inches. Assuming a uniform thickness across the cone, the mass for the inner section is then 4.444e-5 Kg. The outer ring then has a mass of 3.556e-4 Kg. The overall stiffness of the system is 300 N/m. Using the Belleville washer equation, the outside ring has a stiffness

of 7620 N/m. Since there are only two sections, the stiffness of the center section can be computed by a parallel combination relation such that the equivalent stiffness is equal to 300 N/m. With this, the center section has stiffness equal to 312 N/m. For this example we will assume that the damping is negligible.

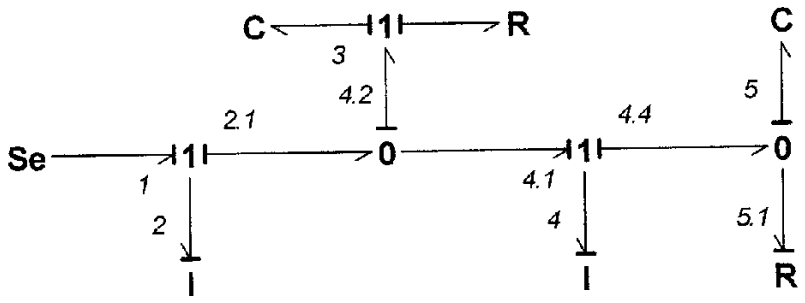

Figure 3.14 Bond graph for axisymmertic system showing causality

There are many ways to determine the natural frequencies for this model, for this example a Bond Graph was developed and the state equations were determined. Figure 3.14 shows the Bond Graph with causality determined. From the bond graph the state equations can be shown to be:

$$\begin{bmatrix} \dot{p}_1 \\ \dot{p}_6 \\ \dot{q}_4 \\ \dot{q}_9 \end{bmatrix} = \begin{bmatrix} 0 & 0 & \frac{-1}{C_4} & 0 \\ 0 & 0 & \frac{1}{C_4} & \frac{-1}{C_9} \\ \frac{1}{I_1} & \frac{-1}{I_6} & \frac{-R_3}{C_4} & 0 \\ 0 & \frac{1}{I_6} & 0 & \frac{-R_8}{C_9} \end{bmatrix} \begin{bmatrix} p_1 \\ p_6 \\ q_4 \\ q_9 \end{bmatrix} + \begin{bmatrix} 1 \\ 0 \\ 0 \\ 0 \end{bmatrix} S_e \quad (3.26)$$

Solving for the natural frequencies yields 135 and 2164 Hz. The experimental data in Figure 3.5 yields 137 and 2842 Hz, respectively. The differences in the second mode can be attributed to many things, the most influential being the geometry of the cone. While not extremely accurate, considering the severe simplicity of the model, the results are quite encouraging. With the introduction of varied geometry and damping, the model should be quite accurate, although due to the additional parameters, it becomes computationally expensive.

Taking the axisymmertic model one step further can be accomplished using finite element analysis. Instead of a few sections, the loudspeaker can be partitioned into thousands of sections, termed shells. Finite element models can be made exceedingly complex and multiple boundary conditions can be tested in a short time. The finite element model relies on accurate material properties and bonding forces. This model must then be compared to actual data and then can be modified to more closely fit that data. In actual studies [2, 27] finite element analysis can provide good results given that the computational resources are present. Again, this is not a generalized modeling method; each different speaker requires its own model. A definitive predictive model for high frequency dynamics does not exist at this time.

3.4.8 Mode Shapes

In the previous sections, the primary mode and first breakup mode have been mentioned several times. This terminology relates to the physical movement of the loudspeaker cone. At certain frequencies that are defined by the mass and stiffness, the cone will vibrate in particular patterns determined by the frequency. The mode shapes for loudspeaker cones are very difficult to discuss for all of the same reasons mentioned in the high frequency modeling section. The pressure response and the velocity of the cone are related by the characteristic impedance of the fluid (air) in the far field (where $ka>1$, k is the wave number and a is the radius of the speaker). The first mode shape is well understood and can be modeled accurately. At this resonant frequency, the entire diaphragm is vibrating in phase like a rigid piston. This is the primary, or plane wave mode. At the next higher resonant frequency, termed the first breakup mode, the cone now either develops a radial or circumferential region that is 180° out of phase with the rest of the surface. Whether the region is circular or radial depends on the geometry of the diaphragm. For a flat circular piston that is driven at the outer edge, Figure 3.15 shows the corresponding mode shapes for increasing frequency.

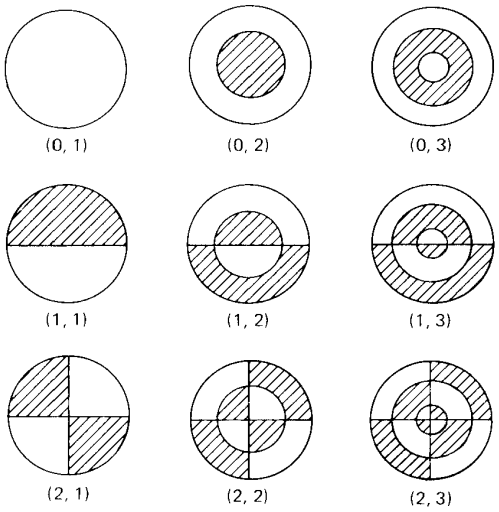

Figure 3.15 Circular membrane mode shapes, courtesy Kinsler et al. [8]

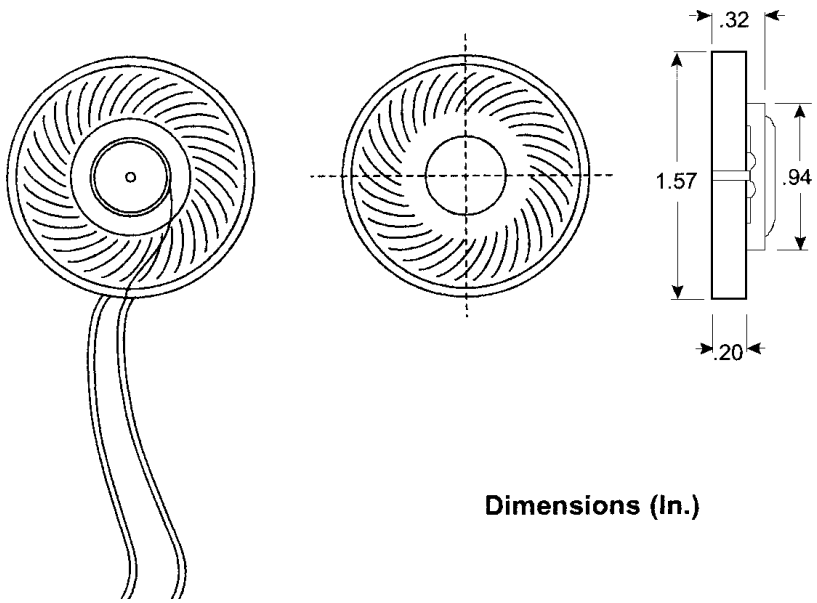

Figure 3.16 Headset loudspeaker schematic drawing, courtesy Korbitone

To complicate the issue, loudspeaker drivers are not flat pistons. In fact, for the speakers used in circumaural headphones, the designers have textured the diaphragm in such a way to accentuate the high frequency response. For the speakers that were examined for this thesis, they all had the similar characteristic that the diaphragm, which is made of plastic, is segmented into two rings. These can be seen in Figure 3.16. The outer ring that

attaches to the basket has spiral pleats that increase the stiffness of that region. These pleats are not on any radial or circumfrential axis and cover the majority of the area of the cone. The center ring begins where the voice coil attaches to the diaphragm at a radius of about 0.375 inches. The center ring is dome shaped and very flexible. At low frequencies the motor and the acoustic impedance limit the output while the speaker vibrates as a piston. At higher frequencies near the corner frequency of the acoustic radiation, the center ring begins to vibrate out of phase with the outer ring and since it has a much lower stiffness, with much greater amplitude allowing for higher output.

3.5 Loudspeaker Enclosures, Controlling Q

The primary purpose of designing an enclosure is to convert the loudspeaker from a dipole source to a monopole source. This is because the efficiency of a monopole is much higher than a dipole. The enclosure can also be used to modify the frequency response of the primary resonance, in terms of magnitude and location, and high frequency roll off. As explained earlier active noise control seeks to create as much gain as possible without additional phase at the primary resonance to increase closed loop suppression using feedback control. Secondly, by being able to design where the primary natural frequency shall fall allows the headset engineer the ability to tailor the headset to the specific environment it is to be used in.

3.5.1 Closed (Sealed) Enclosures

A rigid baffle is the simplest type of enclosure. It is a boundary that spans approximately one wavelength of interest away from the driver. The source effectively becomes a monopole, and all of the driver's characteristics remain intact. If this was to be used for active noise control, the bandwidth of interest begins around 50 Hz. This would require a baffle of 6.86 meters around the loudspeaker for perfect rejection. This is obviously ridiculous for any headset or even home audio use.

By enclosing one side of the driver into a sealed compartment, the acoustic output is completely defined by the volume velocity emitted by the driver. Traditional design methods have made the internal volume large enough such that the compliance of the air filling the enclosure is much greater than the compliance of the driver's suspension. This

system behaves much like an infinite baffle with the driver controlling the system's output. By thinking of the enclosure as an air-suspension, the compliance of the enclosure is made to be smaller and thus coupled with the driver's. So the overall acoustic output now becomes a function of the system, not just dependent on the driver.

Since the interest here is to use the primary resonance for control, the closed box system can be modeled using Richard Small's analysis [28-31]. This modeling scheme uses electrical and acoustical analogous circuits to develop quality factors for the mechanical, electrical and acoustical properties. The commercial market has adopted these quality factors to describe loudspeakers.

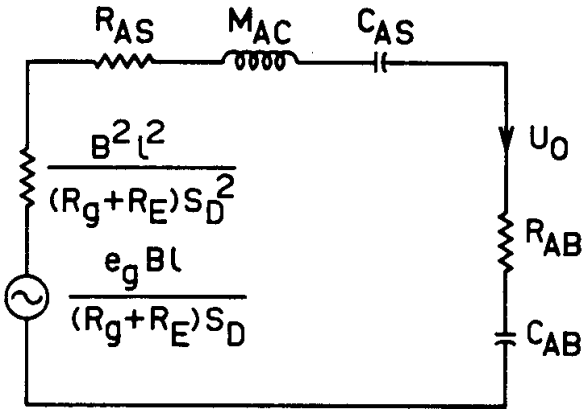

Figure 3.17 Acoustical analogous circuit for a closed-box loudspeaker, courtesy Small [29]

The assumptions made for this analysis are that the driver remains as a pure piston over the bandwidth, the inductive effects from the voice coil can be ignored, the amplifiers output resistance is zero, and the radiation impedance is negligible. With these assumptions the closed box loudspeaker system becomes a second order high pass filter. It must be noted that this analysis was developed modeling large low frequency woofers. At low frequencies large speakers show almost no inductance contribution at the primary resonance due to the large physical mass. For these large speakers, the systems natural frequency is its mechanical natural frequency. With the speakers of interest for the headset, they have a very small physical mass and thus exhibit a shifted natural frequency due to inductance effects.

Symbol	Description
ϕ	Equal to Bl, the force factor
V_{in}	Input voltage
R_g	Output resistance from the amplifier
R_E	DC resistance of the driver's voice coil
S_D	Surface area of the diaphragm
R_{AS}	Acoustic resistance of driver suspension losses
M_{AC}	Acoustic mass of driver diaphragm assembly including voice coil and air load
C_{AS}	Acoustic compliance of driver suspension
C_{AB}	Acoustic compliance of air in enclosure
R_{AB}	Acoustic resistance of enclosure losses
U_o	Output volume velocity of system

Table 3.3 Acoustical circuit analogous parameters

In order to determine quality factors for the mechanical and electrical properties, the circuit model is converted into acoustical and electrical forms. Figure 3.17 shows an acoustical analogous circuit for the closed box system. The total system compliance can be represented by

$$C_{AT} = \frac{C_{AB}C_{AS}}{C_{AB} + C_{AS}} \quad (3.27)$$

The total system resistance is

$$R_{ATC} = R_{AB} + R_{AS} + \frac{\phi^2}{R_E S_D{}^2} \quad (3.28)$$

For amplifiers with non-zero output resistance, replace R_E with the series combination of the two resistances'.

With these simplifications a transfer function can be found between the sound pressure and source voltage. Since this formulation ignores the acoustic output impedance, we are left with the normalized sensitivity. This transfer function is simply the combined impedance of R_{ATC}, M_{AC}, and C_{AT}. The complex algebra yields

$$G(s) = \frac{C_{AT} M_{AC} s^2}{C_{AT} M_{AC} s^2 + R_{ATC} C_{AT} s + 1} \quad (3.29)$$

The pressure-to-voltage transfer function can be simplified if the mechanical and electrical quality factors are found. The electrical equivalent model is found by taking the dual of the acoustic circuit and converting each element to its electrical equivalent [1]. The simplified parameters can be evaluated as

$$C_{MEC} = \frac{M_{AC} S_D^{\ 2}}{\phi^2} \quad (3.30)$$

$$L_{CET} = \frac{C_{AT} \phi^2}{S_D^{\ 2}} \quad (3.31)$$

$$R_{EC} = \frac{\phi^2}{(R_{AB} + R_{AS}) S_D^{\ 2}} \quad (3.32)$$

From these the resonant frequency and the quality factors can be determined
The resonant frequency (mechanical resonance)

$$\omega_c = \sqrt{\frac{1}{C_{AT} M_{AC}}} \quad (3.33)$$

For simplification the natural frequency is shown as a time constant, T_c, which will simplify the pressure to voltage transfer function greatly.

$$T_c = \frac{1}{\omega_c^{\ 2}} = C_{AT} M_{AC} \quad (3.34)$$

The mechanical quality factor is given by

$$Q_{MC} = \omega_c C_{MEC} R_{EC} \quad (3.35)$$

The electrical quality factor is given by

$$Q_{EC} = \omega_c C_{MEC} R_E \quad (3.36)$$

The total system Q at f_c is given by

$$Q_{TC} = \frac{Q_{MC}Q_{EC}}{Q_{MC} + Q_{EC}} = \frac{1}{\omega_c C_{AT} R_{ATC}} \quad (3.37)$$

Observing the terms in the pressure-to-voltage transfer function, it can be simplified by inserting Q_{TC} and T_c. With this arrangement it is now in the form that is advantageous for design. This form is analogous to classic high pass filter design. Now response types (Butterworth, Bessel, etc) can be specified and the parameters can be solved for. This form also aids the designer by making measurements simpler. The designer now only needs a small number of parameters to estimate the pressure response. The measurement process is summarized in [7].

$$G(s) = \frac{s^2 T_c^{\,2}}{s^2 T_c^{\,2} + sT_c / Q_{TC} + 1} \quad (3.38)$$

3.5.2 Reference Efficiency

A topic that is important for control is the efficiency of the driver. The efficiency is not only a way to judge the power characteristics of the speaker, but it is also a way to measure its bandwidth. The efficiency of the loudspeaker can be calculated by:

$$\eta(j\omega) = \frac{\rho_o}{2\pi c} \frac{B^2 l^2}{R_E S_D^{\,2} M_{AC}^{\,2}} \left| G(j\omega) \right|^2 \quad (3.39)$$

The reference efficiency is important for designers to determine the power necessary to drive the speaker to the appropriate levels. By plotting the efficiency it is possible to visualize the bandwidth of the speaker.

Most commercial speakers are given a rated sensitivity, which is the SPL of the speaker given a 1-watt (2.83 volts rms) input at 1 meter distance. To calculate the sensitivity of the speaker, an assumption will have to be made that the speaker will be radiating into a half space, or 2π space. 1 watt at 100% efficiency into a half space is equal to 112.2 SPL. For a driver that is less than 100% efficient (which is all drivers), the sound pressure level can be can be calculated by:

$$sensitivity = 112.2 - 10\log\left(\frac{1}{\eta_o}\right) \quad (3.40)$$

For the control engineer, the sensitivity is simply a measure of how much power will be required to drive the loudspeaker to the designated level.

3.5.3 Acoustic Output

The maximum acoustic output is an important parameter for the control engineer. This will dictate in what kind of environment the headset will be best suited for. As alluded to in 3.3.1, the maximum acoustic output is related to the maximum excursion, x_{max}. This is because the pressure response is linearly related to the velocity. When the derivative of the displacement is taken, the greater the value of x_{max} leads to a greater magnitude of the velocity, which then translates to more acoustic output. The maximum acoustic output can be calculated by [28]

$$P_{AR} = \frac{4\pi^3 \rho_o}{c} \frac{f_c^4 V_D^2}{\left|X(j\omega)\right|_{\max}^2} \quad (3.41)$$

Where f_c is the natural frequency of the closed-box system. V_D is the peak displacement volume of the driver that can be found by

$$V_D = S_D x_{\max} \quad (3.42)$$

Where x_{max} is the one-way maximum displacement of the loudspeaker. The normalized displacement can be found by integrating the frequency dependant velocity of the driver. From the acoustical circuit in Figure 3.17, the velocity can be determined by [29]

$$U_o(s) = \frac{V_{in} Bl}{R_E S_D M_{AC} s} \bullet G(s) \quad (3.43)$$

Next by integrating in the frequency domain and substituting the quality factors the normalized system displacement function can be determined.

$$X(s) = \frac{1}{s^2 T_c^2 + sT_c / Q_{TC} + 1} \quad (3.44)$$

The maximum acoustic power can answer two questions that apply to the open-air headset. First, what is the lowest natural frequency that can be used for an open-air headset? The determining factor is what sound pressure is available at that frequency. If the loudspeaker is driven to a level that requires a greater x_{max}, the magnetic field

becomes nonlinear, and distortion results. If the driver is further driven past x_{max}, it will eventually either push the voice coil past the magnet and will not play any louder, or on some speakers, solid end stops are placed to limit the cone displacement. If the speaker is driven at these levels for a significant amount of time, the voice coil will become thermally damaged.

Figure 3.18 shows the maximum sound pressure for a 1-inch speaker with a one-way x_{max} of 0.5 mm plotted against the driver's natural frequency. As the natural frequency is increased, the maximum sound pressure that is obtainable is increased. Most noise fields that active noise control would be suggested as a solution are greater than 95 dB. This would suggest that the lowest natural frequency for an open-air headset would be approximately 600 Hz, for this speaker with a 0.5mm x_{max}. Most 1-inch speakers have slightly less x_{max} than this example (0.2-0.4 mm), thus the lowest natural frequency approaches 1000 Hz. If the headset was to be used in a noise field that has a lower sound pressure level, a lower natural frequency could be chosen.

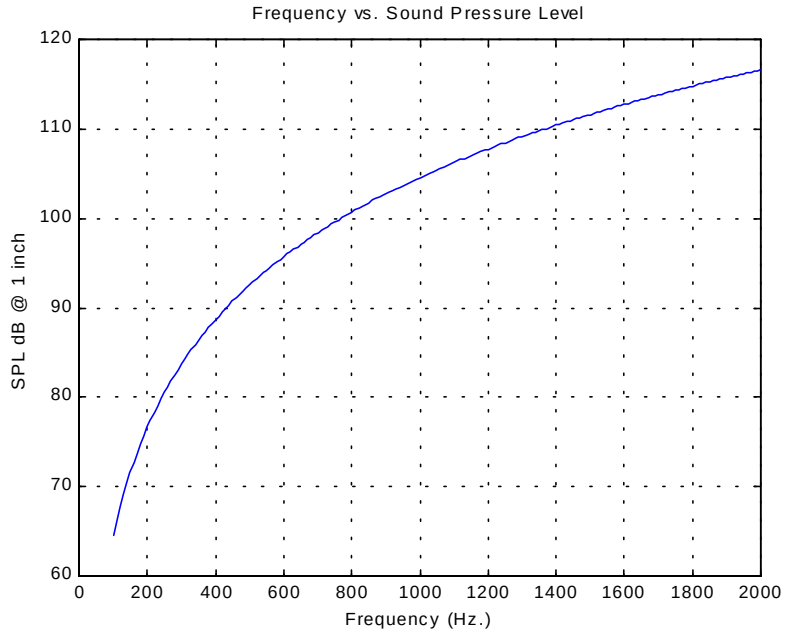

Figure 3.18 Natural frequency versus maximum sound pressure for a 1-inch loudspeaker (x_{max}=0.5 mm)

The second question for the engineer relates to the maximum excursion. From a design perspective, if a 1-inch speaker was to be chosen and the designer wanted to know what value of x_{max} was required to develop a particular sound pressure. Figure 3.19 plots x_{max} versus maximum sound pressure. The speaker used in Figure 3.18 with a natural frequency of 1000 Hz. was chosen as the starting point. If the engineer wished to increase the output by 6 dB, this would require an x_{max} that is more than 2 times the original x_{max} of 0.5 mm. Very large x_{max} parameters are difficult to generate due to the need for a very flexible surround material and long voice coil.

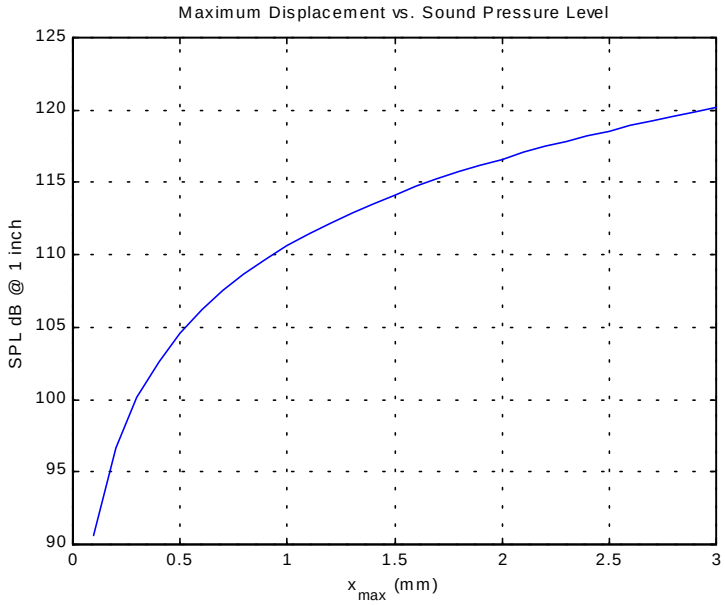

Figure 3.19 x_{max} versus sound pressure level for a 1-inch loudspeaker

3.6 Conclusions

There are many methods for modeling loudspeakers, but none of the available methods are particularly well suited for control applications. This is because an extremely accurate full bandwidth model would be necessary. Although the modeling techniques presented above cannot be placed into control schemes, the engineer can begin to appreciate how the loudspeakers parameters affect their data. For the design of new loudspeakers for control applications, the future is very bright. The axisymmertic modeling approach coupled with finite element techniques will give the designer the tools necessary to create accurate and robust models.

Chapter 4: Design Metrics for Open-Air, Active Noise Reduction Headset Modifications

This chapter deals with the overall scope of the design process for open-air ANR headsets. The questions presented are all to be compared to a baseline headset, but many are applicable to new designs. The designer must choose what the baseline parameters shall be. The goal is to have a way to evaluate each change implemented into the headset. By asking the following questions the designer can determine if the change will benefit the overall headset development process. These questions are necessary for most applications since many changes to the system are possible in the laboratory, but are not practical or possible for real-world systems.

This section defines the questions (metrics) that can be asked for any modification made to the headset. By clicking on the hyperlinks the reader can gain extra information about the topic.

Active Control Performance

- What is the overall improvement (or degradation) in performance from the reference in terms of maximum reduction, bandwidth of control, tonal reduction and/or overall loudness?
- What is the effect on the robustness of the headset with this performance improvement (or degradation)?
- What is the performance to cost ratio for this improvement over the reference? (dB/$, bandwidth/$, or sones/$)
- If the change is adding a linear dynamic system, can it be implemented through the controller? If yes, what other advantages does the dynamic system hold (user variability, manufacturing variability, cost)?

Power Requirements

- How much power is available?
- Will this change affect the form of the headset?
- With this change, does the power supply's stability affect the headset's robustness?
- Does this change require a more expensive power supply?

Robustness to Manufacturing Variation

- Does this change affect the robustness with respect to manufacturing variability?
- Will this change help performance in control or user variability?
- Assuming that this change improves manufacturing variability, what physical costs are involved? Are these costs acceptable?

Robustness to User Variability

- Does this change affect user variability? At what cost (control performance, power, other)?
- If there is an improvement in user variability, will the ergonomics of the headset be compromised by this change?
- Assuming that this change improves user variability, what physical costs are involved? Are these costs acceptable?

Manufacturability

- Can this change/design be mass-produced? Does it require a complicated manufacturing process?
- How much cost is involved with this change/design in terms of labor and materials?

Ergonomics / Form

- Will the comfort for the user be improved with this change?
- Will the ease of use for the user be improved with this change?
- Is the physical safety for the user improved with this change?
- Does this change meet approved standards for durability and environmental compatibility such as military specifications?

Performance

Control performance is dependant on the environment the headset is being used in and the goals of the designer. For example, if the headset were being used in an environment dominated by a single tone, then the designer would wish to achieve maximum suppression at that frequency. If the sound field contained broadband noise the designer might want a bandwidth of suppression, or if the sound field was a combination of tones and broadband noise, the designer might want to consider a loudness reduction.

Since there are so many choices of ways to measure control, it is very difficult to determine if the modification actually helps control performance. This issue becomes even more diluted if the modification is a linear dynamic system of low order that can be modeled by the controller. If the controller can obtain the same performance, why would the designer use it on the headset? It comes down to if the modification helps one of the other metrics, such as user variability.

Another issue is how to compare feedback controllers for performance alone. This is a very difficult task because it is always possible to create a higher order controller that will provide the exact performance the designer wants. If all of the other metrics were thrown out (cost, power, ergonomics, etc) and the designer just wanted to build a controller for his/her ears, it would be possible to get almost infinite control with a very large and complicated controller. Of course this is not practical, but it is an issue that

must be addressed. The best, not optimal, controller will be the one that will work on every user and have enough suppression to make the environment safe and comfortable.

Power

Power refers to the electrical power drawn by the speaker and controller while in use. If the power is supplied by an external power supply, this is usually not an issue unless there are many devices running off of the same supply. If the device is battery powered, or run off a limited power supply, then power consumption is of great importance. The more inefficient the design, the shorter the battery life, and the more often the user has to change or recharge batteries. Otherwise the user will have to carry large batteries, which then becomes an ergonomics problem. Another factor is power supply stability. The response characteristics of loudspeakers can change under varying power conditions. If the power supply cannot provide adequate power continuously, the performance could suffer or, worst case, the controller could go unstable.

Robustness to Manufacturing Variations

Due to the nature of mainstream audio, the quality of available headphone speakers is not adequate for control headsets. This is a two part cost issue. First, the tooling to build very small speakers is extremely expensive. Since the noise control headset market is not extremely large, loudspeaker manufacturers will not prototype and build a small custom loudspeaker that will only require several thousand units for a reasonable amount of money. Secondly, the general populous is not concerned with quality audio reproduction. Like in all industries, there are high-end manufacturers, but with headsets, they are a very small percentage and the drivers they use are not made available to consumers. So, the loudspeakers available are of low quality and have very large frequency response variations between examples.

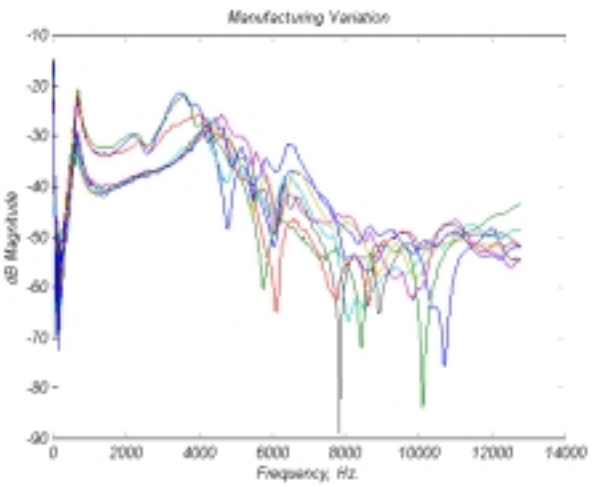

Figure 4.1 Manufacturing variation example

Figure 4.1 shows the variation in frequency response between several of the "same" loudspeaker from the same order. This is a problem any feedback controller. This requires the designer to either tune every controller for every loudspeaker used, or build a very simple low order controller that still may not be stable for all examples. The former is not practical for any type of production, and the second most likely will not provide the amount of control performance necessary.

Tolerances also have a role in manufacturing robustness. Changes in wall thickness, port diameters, and quantity of adhesives used or transducer placement can have drastic effects on the frequency response of the loudspeaker system. Either better quality speakers must be manufactured or methods to control variations must be developed to ensure control adequate performance, robustness and especially safety.

Robustness to User Variability

User variability refers to the change in the headsets frequency response when placed on the users head. Every user has a unique acoustic impedance for their ear canal that becomes coupled with the loudspeaker system. This relationship can be modeled by investigating HRTF's (Head Related Transfer Functions). As Figure 4.2 shows the headset impedance and the ear canal form a two-port network. With this series relation,

the pressure at the entrance to the ear canal can be determined by the pressure created by the headset.

$$\frac{P_6}{P_5} = \frac{Z_{Ear\ Canal}}{Z_{Ear\ Canal} + Z_{Headphone}} \quad (4.1)$$

The goal for a headphone system is to make $Z_{Headphone}$ as large as possible so that the pressure at the entrance to the ear canal is equal to the pressure at the loudspeaker. So, the sound that is reproduced is not distorted by the impedance coupling. This is the basis for binaural recording. For the ANR headset, the goal is the same, except the sound pressure at the microphone is to be the same as the sound pressure at the eardrum. This assures that the open loop frequency response of the headset does not change between users. Thus when controlled, the pressure transmitted would be optimally zero. The problem that arises is that every user has a unique ear impedance and it is difficult to make $Z_{Headphone}$ very large due to power constraints and acoustic phase.

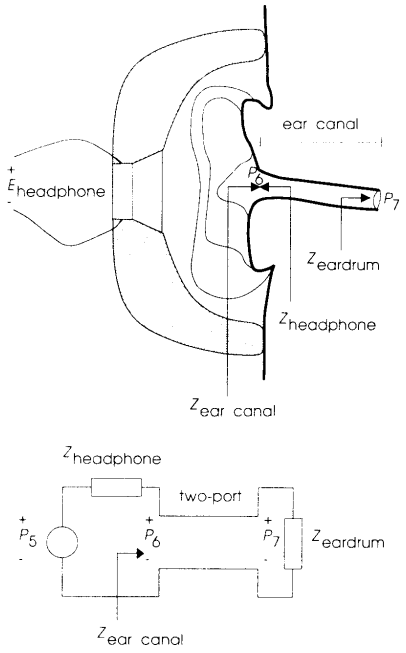

Figure 4.2 Two-port impedance network representing the headphone-ear coupling

Manufacturability

All of the parts included with the headset must be able to be manufactured in large quantities for as little cost as possible. Thus parts that require significant physical labor must either be changed to a simpler part or other route taken. The changes must be reproducible and consistent. This means that the same performance is easily achieved from one headset to the next. Although any headset design can be built, it is a matter of cost versus performance that ultimately decides if the headset is manufacturable.

Ergonomics

The ergonomics and form of the headset is what the end user interacts with. The headset must be comfortable, simple to operate and durable. Comfort relates to how the unit sits on the user's head and how the unit 'sounds' while it is active. If the unit has very good noise suppression but makes speech difficult to understand or makes speech sound very annoying, the user will probably not want to wear the unit for extended periods of time. Also, if the unit is heavy and makes head movement awkward and dangerous, the user will not wear the unit.

The operating procedure must be very simple. The unit should have a minimum of controls and adjustments to be made by the user.

The unit must be very durable. For military use, the unit must be robust to all environmental conditions and some degree of misuse. The headset must be able to handle slight shocks, such as being dropped, without fear of changes in stability of the controller. The headset should also be made of materials that can handle the wear and tear of everyday use.

Safety

The user's safety can be endangered in three ways, controller failures, mechanical failures, and user error. If the frequency response at the error microphone changes enough that the controller goes unstable the user may experience extremely loud pink

noise. This could cause hearing damage or total hearing loss. Secondly if the casing becomes damaged, sharp fragments may enter the ear and puncture the eardrum. Safety is thus tied to how robustly the headset performs under all conditions. Finally if the headset is difficult to use, the user will find a way to damage the set in some way that leads to personal injury. For any change made the designer makes, how robust the change is with respect to safety should be their first priority. Safety is of the utmost importance. See user variability and manufacturing variability

Chapter 5: Design Examples

5.1 Introduction

In this chapter, several alternative design features for open-air headsets will be examined. These design examples investigate the potential for improvements in terms of performance, user variability and manufacturing variability. The first three sections deal with modifications intended to increase control performance in each of the loudspeakers three domains, acoustical, electrical and mechanical. The first section explores exploiting the standing wave mode shapes that are created in a rigid pipe. Due to the size requirements of the headset, the analysis explores the effects of decreasing pipe length on the frequency response of the loudspeaker. The next two sections examine methods to reduce the high frequency magnitude by augmenting the electrical and mechanical properties. The loudspeaker's efficiency is a function of frequency and is influenced by the imaginary part of the electrical impedance. The inductance of the system was augmented with the goal of decreasing the efficiency at frequencies beyond the primary resonance with the result of reducing the system's magnitude with frequency. The mechanical properties were modified such that the extra inertia would decrease the efficiency at frequencies past the primary resonance.

The next two sections explore controlling manufacturing and user variability. Section 5.5 examines placing the speaker into a sealed enclosure. The compliance coupling between the loudspeaker and the enclosure is investigated as a means to control manufacturing variations. The effects of changing the microphone position and using a perforated screen for controlling user variability are illustrated in the next section. The final section departs from experimental methods of the chapter to synthesize a loudspeaker system using the details examined thus far.

5.2 Performance Experiments

5.2.1 Acoustical Design

The first design example examines the combined pipe-driver system. The resonance phenomenon that occurs inside sealed pipes creates high magnitude resonance peaks that provide high gain regions that are desirable for control. The first section first looks at the constitutive theory necessary to model these systems. In the second part, an experiment is conducted to determine how well the model created in this first section will apply when the length of the cavity decreases. A pipe-driver system is then augmented with a perforated end cap to allow transmission to the error microphone. The perforated end cap will also increase the acoustic impedance, compared to the impedance of the open speaker, with the goal of decoupling the system from the users ear.

When sound propagates inside of a rigid pipe, a resonance phenomenon occurs. If the wavelength of the traveling wave is much larger than the diameter of the cavity, the resonance properties will be governed by the pipe length and end conditions. When the wavelength becomes equal to, or smaller than the diameter of the pipe, two and three-dimensional standing waves can occur. By matching the impedance of the loudspeaker and the pipe at the end conditions, the resonant points can be calculated.

To begin, consider a pipe that is rigidly terminated at one end and is excited by a flat massless piston at the other. Assuming that the piston is used to drive only low frequency content so that it produces a constant volume velocity, only plane waves will be produced. The pressure will take the form:

$$p = Ae^{j(wt-kx+kL)} + Be^{j(wt+kx-kL)} \quad (5.1)$$

where A and B are determined by the boundary conditions.

At the rigid termination, continuity of force and particle velocity requires that the impedance of the traveling wave match the impedance of the termination, Z_{ml}.

$$Z_{mL} = \rho_o cS \frac{A+B}{A-B} \quad (5.2)$$

In order to solve for A and B, the impedance of the pipe must be known. The mechanical input impedance at x=0, where S is the surface area of the piston, is written as:

$$Z_{m0} = \rho_o c S \frac{Ae^{jkL} + Be^{-jkL}}{Ae^{jkL} - Be^{-jkL}} \quad (5.3)$$

By solving (5.2) for A and substituting in to (5.3), A and B can be eliminated and an expression relating Z_{mL} and Z_{m0} can be found.

$$\frac{Z_{m0}}{\rho_o c S} = \frac{\frac{Z_{mL}}{\rho_0 c S} + j \tan kL}{1 + j \frac{Z_{mL}}{\rho_o c S} \tan kL} \quad (5.4)$$

By making the substitution that Z_{mL} is equal to r+jx, and multiplying the expression by the complex conjugate of the denominator, and separating the real and imaginary parts yields:

$$\frac{Z_{m0}}{\rho_o c S} = \frac{[r(\tan^2 kL + 1) - j[x \tan^2 kL + (r^2 + x^2 - 1)\tan kL - x]}{(r^2 + x^2)\tan^2 kL - 2x \tan kL + 1} \quad (5.5)$$

What results is that resonance and anti-resonance occur when the reactance tends toward zero. The resonance condition occurs when the input resistance is small and anti-resonance when input resistance is large. The limiting case is when the impedance at x=L approaches infinity, this results in:

$$\frac{Z_{m0}}{\rho_o c S} = -j \cot(kL) \quad (5.6)$$

Thus the reactance is zero when cot(kL) =0 and resonance occurs.

For the headset application we must examine the coupled loudspeaker-pipe system. As shown in Chapter 3, the loudspeaker does not act as a rigid piston over the entire frequency range and adds considerable dynamics to the system. The analysis requires two steps, a mathematical model of the loudspeaker's impedance, and an impedance relationship for the tube that allows for near field calculations. Due to the sheer complexity of generating a multi-mode model, a single mode model will be used to represent the loudspeaker. This will allow us to examine the response of the system at low frequencies.

The first task involves finding the input impedance for both the driver and the pipe. In the following, it will be seen that with these two quantities a unified system model can be developed.

The solution that was solved earlier assumes that the pipe and the ends are completely rigid, with no absorption or losses. Since this is to be tested on a real system made of plastic, an absorption term, α, will be inserted to more correctly predict the conditions under test. By allowing the wave number **k** to now equal k- jα, and inserting this into the input impedance solution for the rigid walled pipe, dissipative effects in the model can now be included.

Setting **k** = k - jα:

$$Z_{m0} = -j\frac{\rho_o \omega\ S}{k - j\alpha}\cot\left[(k - j\alpha)L\right] \quad (5.7)$$

Multiplying the top and bottom by 1/**k**, dividing by the characteristic impedance and then expanding the cotangent:

$$\frac{Z_{m0}}{\rho_o cS} = -j\frac{1}{1 - j(\alpha/k)}\frac{\cos\left[(k - j\alpha)L\right]}{\sin\left[(k - j\alpha)L\right]} \quad (5.8)$$

Using a trigonometric substitution for cos(a-b) and sin(a-b) and then expanding the argument with the imaginary angle term by sin(*j*b) = *j*sinh(b) and cos(*j*b) = *j*cosh(b):

$$\frac{Z_{m0}}{\rho_o cS} = -j\frac{1}{1 - j(\alpha/k)}\frac{\cos(kL)(j\cosh(\alpha L)) + \sin(kL)(j\sinh(\alpha L))}{\sin(kL)(j\cosh(\alpha L)) - \cos(kL)(j\sinh(\alpha L))} \quad (5.9)$$

In order to remove the imaginary terms from the denominator, multiply the top and bottom by the complex conjugate of the denominator. With the Pythagorean identities this yields:

$$\frac{Z_{m0}}{\rho_o cS} = -j\frac{1 + j(\alpha/k)}{1 + (\alpha/k)^2}\frac{\cos(kL)\sin(kL) + j\cosh(\alpha L)\sinh(\alpha L)}{\sin^2(kL)\cosh^2(\alpha L) + \cos^2(kL)\sinh^2(\alpha L)} \quad (5.10)$$

Assuming that the driver consists of a rigid cone of mass M, a surround with stiffness K, damping C, and that it is driven by a harmonic force $f=Fe^{j\omega t}$, by Newton's Second Law a force relationship can be determined.

$$M\frac{d^2\xi}{dt^2} = -C\frac{d\xi}{dt} - K\xi - Sp(0,t) + f \quad (5.11)$$

where ξ is the displacement of the cone and p(0,t) is the pressure at the center of the pipe at x=0. It is also assumed that the resulting motion of the cone is harmonic, such that $\xi(t)=Ae^{j\omega t}$.

The mechanical impedance for the driver is then found by dividing through the above expression by the velocity of the mass, $u(0,t) = d\xi/dt$, which equals the complex particle speed at x=0. This yields:

$$\left[C + j\left(\omega M - \frac{K}{\omega}\right) + \frac{Sp(0,t)}{u(0,t)}\right]u(0,t) = f \quad (5.12)$$

The mechanical impedance at x=0 of the driver is:

$$Z_{md} = C + j\left(\omega M - \frac{K}{\omega}\right) \quad (5.13)$$

The input impedance of the pipe is then equal to:

$$Z_{m0} = \frac{Sp(0,t)}{u(0,t)} \quad (5.14)$$

The driver will then have a resonant frequency of $\omega = \sqrt{K/M}$ (this model does not take into account inductance shifting effects), this occurs when the reactance vanishes. The pipe has its own resonant frequencies when $\mathrm{Im}\{Z_{m0}\} = 0$. Since these are frequency domain characteristics, the resonant frequencies simply add to form system resonant frequencies. Thus:

$$\mathrm{Im}\{Z_{md} + Z_{m0}\} = 0 \quad (5.15)$$

Assuming a rigid termination at x=L, this results in:

$$\omega M - \frac{K}{\omega} - \frac{1}{1+(\alpha/k)^2}\frac{\cos(kL)\sin(kL)}{\sin^2(kL)\cosh^2(\alpha L) + \cos^2(kL)\sinh^2(\alpha L)} = 0 \quad (5.16)$$

A little rearrangement yields:

$$\frac{1}{1+(\alpha/k)^2}\frac{\cos(kL)\sin(kL)}{\sin^2(kL)\cosh^2(\alpha L)+\cos^2(kL)\sinh^2(\alpha L)} = akL - \frac{b}{kL} \quad (5.17)$$

Where: $a = \frac{M}{S\rho_o L}$ *and* $b = \frac{KL}{S\rho_o c^2}$ (5.18)

It should be noted that *a* is the ratio of the mass of the driver versus the mass of the air in the pipe. Similarly, *b* is the ratio of the stiffness of the diaphragm versus the stiffness of the fluid in the pipe.

5.2.1.1 Experimental SCP Testing

Two sets of measurements were taken. The first examines the changes in the frequency response as the length of the pipe decreases. This will be done to check the validity of the model created for non standing wave conditions. The second examines the pipe-driver system with a porous end cap. The porous end cap will be termed the speaker cover plate or SCP.

To test the model, four lengths of pipe, 36, 12, 6 and 1 inches respectively, will be tested to see how greatly the near field and other effects deviate from the model's prediction. The pipe that was used was 1 1/2" dia. PVC with a 3/16" wall thickness. The driver was a 1 1/2" membrane – mylar cone speaker taken from a Radio Shack® Nova 57 headset. The pipe was sealed at the far end with a PVC pressure cap that a hole had been drilled in its center for a microphone to record the pressure at the center of the end cap plane. The microphone used was a Panasonic condenser omni-directional microphone with a 1.2 V inline preamp. The speaker was driven by a 2 V. peak random noise signal sourced from a HP 36656 frequency analyzer. Each frequency trace shown in the following figures contains 1600 lines of resolution and is a composite of 25 averages.

Figure 5.1 shows the measured and predicted (single mode) pressure response of the loudspeaker when mounted in an infinite baffle. The first resonant frequency occurs around 135 Hz., and the second resonance at 3100 Hz. The loudspeaker model predicts

that the model for the tube's response will be valid to approximately 600 Hz. After that point the loudspeaker no longer behaves as a piston source.

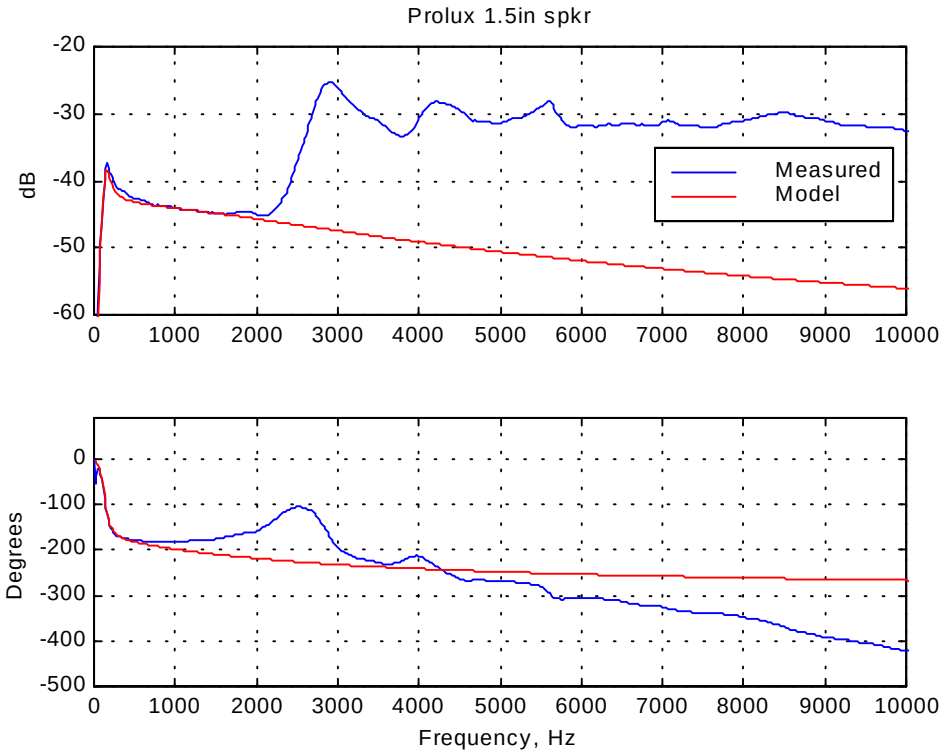

Figure 5.1 Modeled and experimental pressure response for a 1.5 inch speaker

Figures 5.2 and 5.3 show the predicted and measured magnitude and phase response in the linear range for the 36, 12, 6 and 1 inch pipes respectively. As the tube becomes shorter the resonant peaks become spaced further apart. The model was created using the assumption that the entire pipe was rigid, so there was not any absorption. The model predicts the resonant peaks with good accuracy for the 36 and 12 inch pipes and with only reasonably well for the 6-inch pipe. The one-inch pipe does not obey the model; all agreement is lost. Upon observing the entire bandwidth for the one-inch pipe, it becomes clear that the pressure response is no longer dominated by the impedance of the tube. It is postulated that radial modes and near field acoustic effects begin to become significant. Also, the mode shapes of the driver become begin to become significant. Figure 5.4 displays the entire bandwidth for the one-inch pipe.

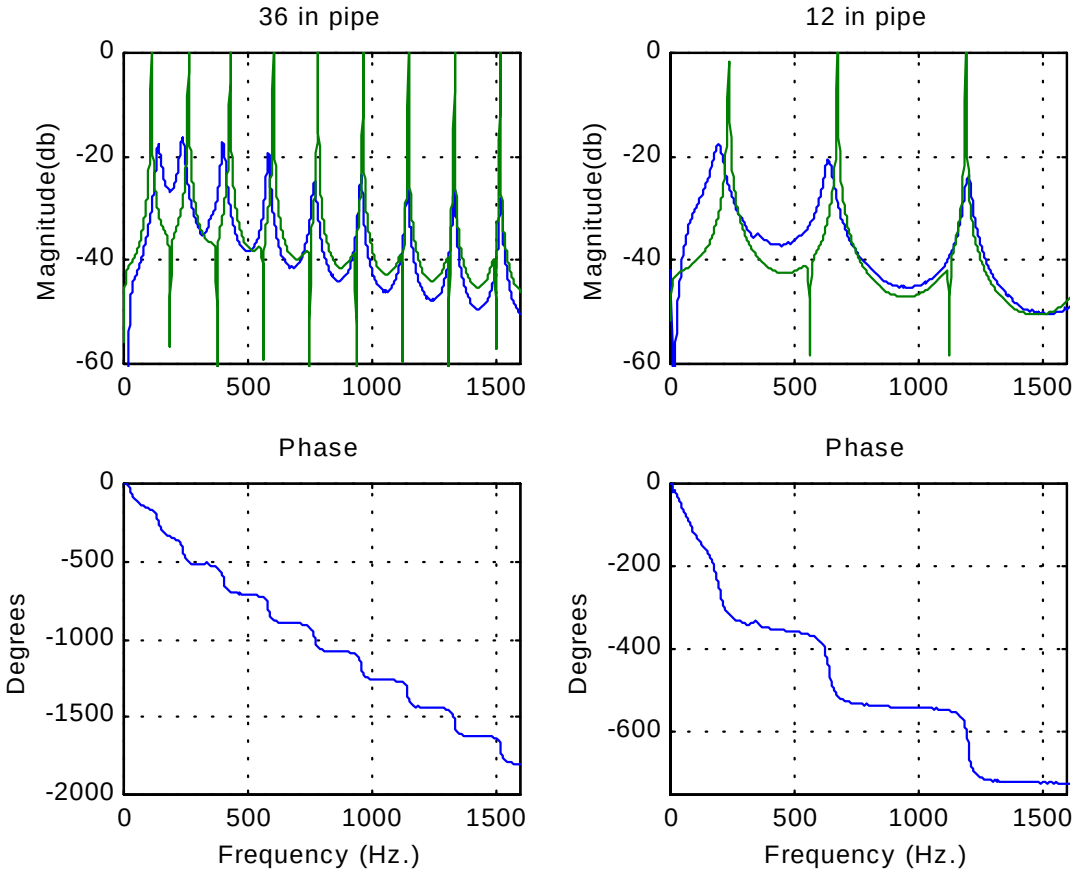

Figure 5.2 36 and 12 inch pipe pressure response, theoretical (green) experimental (blue)

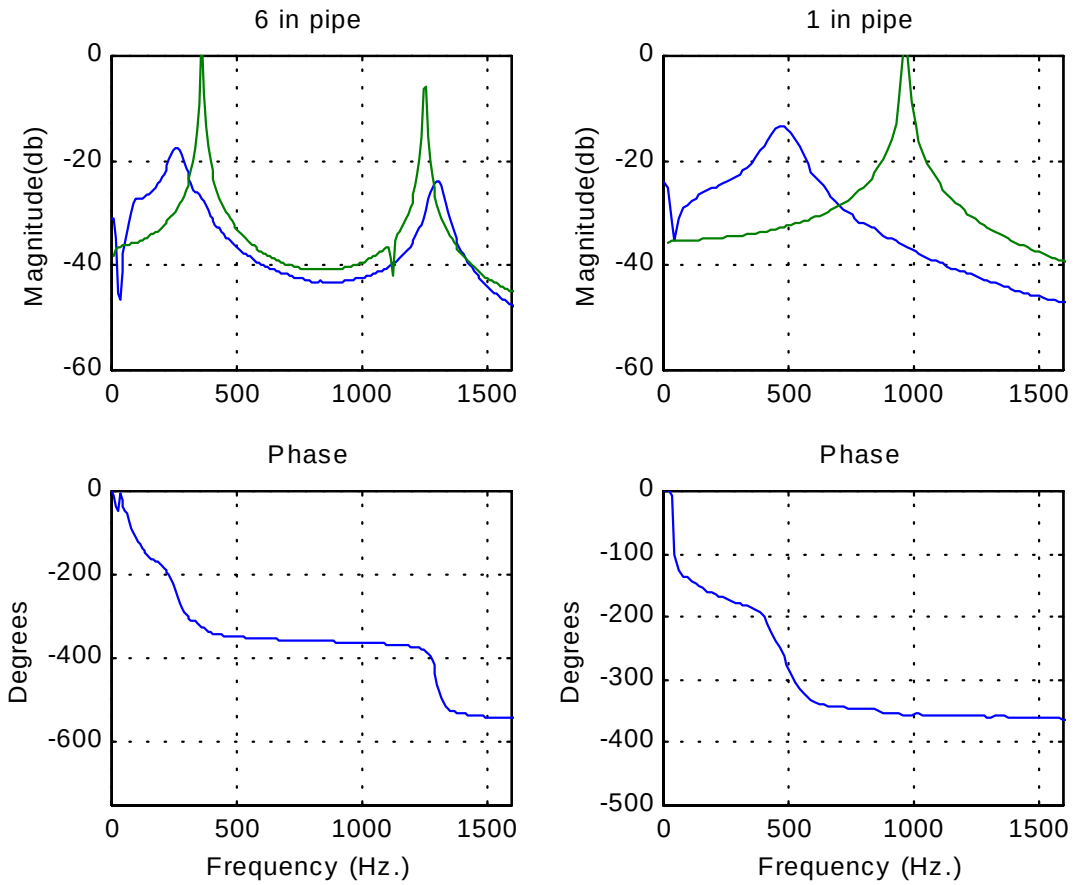

Figure 5.3 6 and 1 inch pipe pressure response, theoretical (green) experimental (blue)

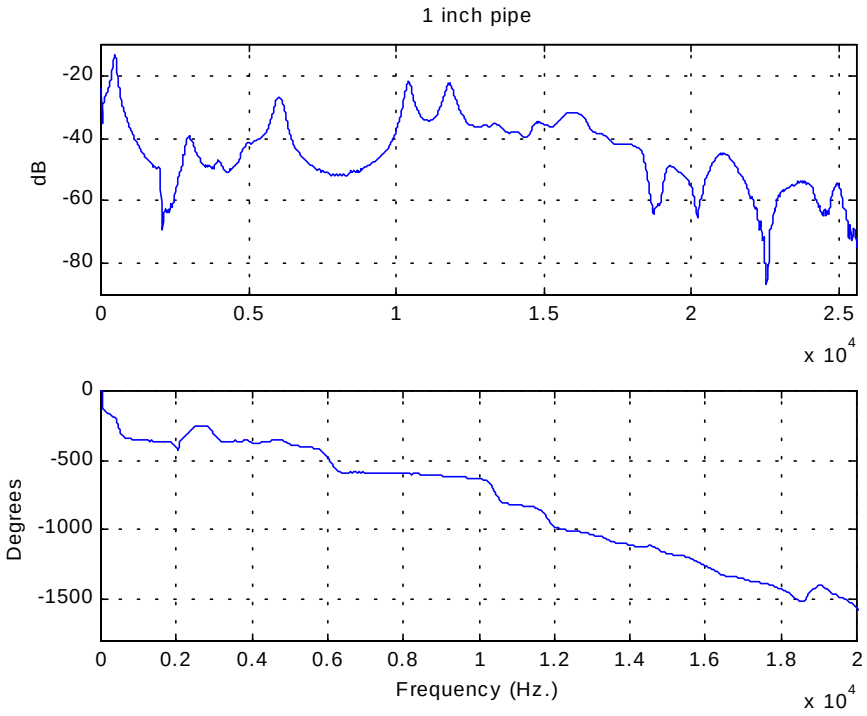

Figure 5.4 1-inch pipe pressure response

Figure 5.5 shows the results of the left-hand side of the closed pipe-driver equation. The places marked with a '+' correspond to the resonant peaks on the data shown in Figure 5.2. The red line corresponds to the right-hand side of the closed pipe driver equation. 'a' and 'b' were determined the manufacturers specifications for the speaker, but were slightly modified using an iteration process. This was done until the line fit as many data points as possible.

'a' and 'b' were determined to be 0.4 and 3 for the 36 inch pipe. This results in a mass of 0.350 grams and a stiffness of 370 N/m. This is compared to the manufacturers specifications of 0.4 grams and 300 N/m. A way to check the mass value is to determine the theoretical weight by multiplying the density by the volume. Approximating the volume of the cone with a circle of radius of 1.587 cm (0.625 inches) and 0.5 mm thickness and assuming that the material is a polyproplyene (common plastic), that has a density of 900 kg/m^3 (Manufacturing Processes for Engineering Materials, Kalpakjian, 1997). This results in a mass of 0.356 grams.

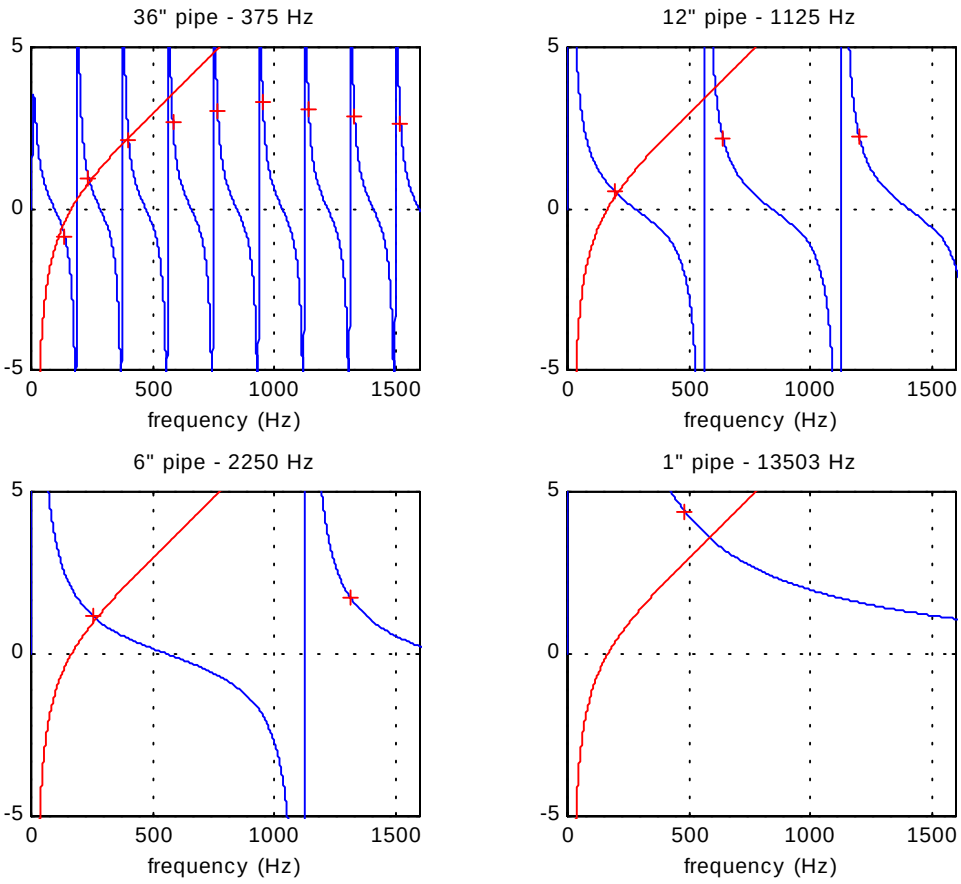

Figure 5.5 Theoretical resonant frequency mapping

With the addition of the absorption, which also includes leakage, Figure 5.5 shows good agreement with the model. Even for the one-inch case, the model comes within 150 Hz. The model begins to deviate severely when the loudspeaker's phase deviates from the model at frequencies past 500 Hz, which can be seen in Figure 5.1. While this is not an extremely accurate model for short tube lengths, it can provide a good starting place to begin a more complicated study.

As stated earlier, the model used a lumped parameter simplification to facilitate model simulation. The first major deviation for the model is the loudspeaker's dynamics. The actual loudspeaker contains at least three distinct modes over the frequency band of interest. Each mode introduces 180 degrees of phase and a related magnitude, which are unaccounted for by the single mode model developed above. The speaker used in this

test also has a significant damped zero just past the first mode. This causes the phase of the data to begin to deviate from the model rather substantially without affecting the magnitude greatly. The second deviation is in the tube's length. The equations developed all depend on having a relatively long length. As the tube length diminishes, the number of half wavelengths (within the audible range, 20-20,000Hz.) that can fit inside the tube becomes very small. The pipe-driver model requires that the boundary conditions at the sealed end resolve to be a pressure maximum for each frequency's half wavelength. As the overall length becomes shorter, all half wavelengths longer than the tube violate this criterion, and the incomplete half wavelengths excite a series of longitudinal modes. At this point the pressure distribution is deemed the near field. The near field can be approximately defined by kL<1, so for the 1-inch pipe (0.03175m) all frequencies below 18,913 Hz. are considered in the near field.

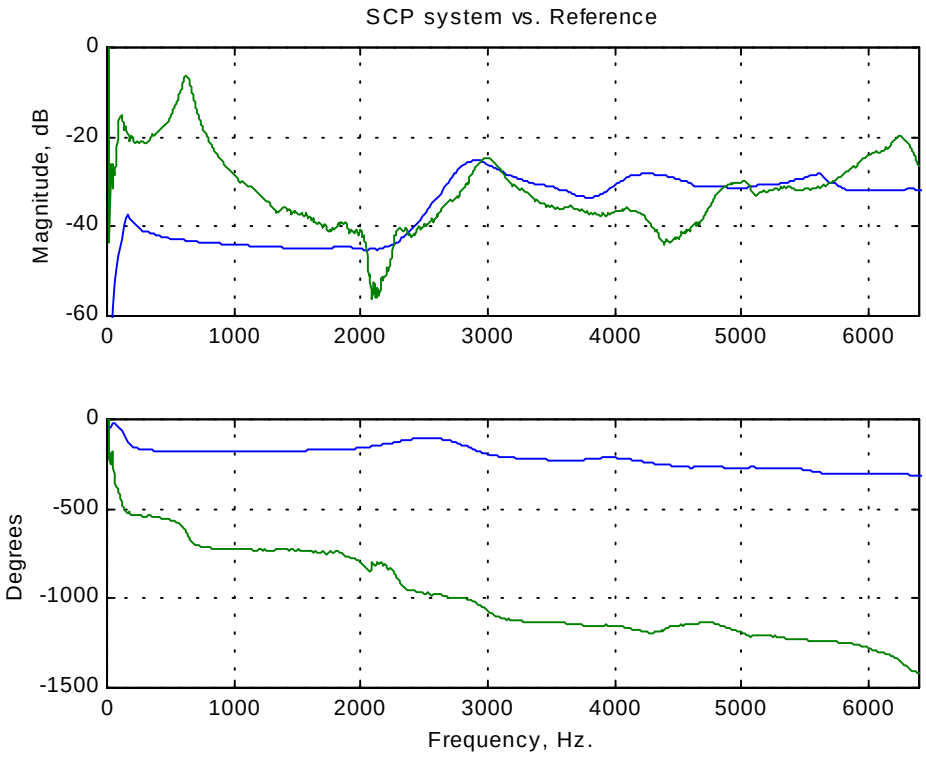

Figure 5.6 SCP, 1/8-inch hole, versus infinite baffle reference response

The second part of the test was to remove the rigid end cap and replace it with a perforated cap, or SCP. Figure 5.6 shows the pressure response of the system with the

SCP and the response of the driver alone. The magnitude is increased a maximum 35 dB at 750 Hz. In the region of the tubes first resonance, there is 360° of phase lag. For feedback control, this system would be unstable in the closed loop for a full bandwidth controller. For an ANR headset system that utilized a feedforward controller, this could be a viable option because the feedforward algorithm does not rely on phase for performance.

5.2.1.2 Results and Conclusions

The gain created by the longitudinal waves is very attractive for control purposes. Unfortunately the effect that is occurring is not an enforcement of the driver's natural frequency, it is determined by the geometry of the tube. For the 36 inch tube the response is dominated by the acoustic impedance of the tube, and for each resonance, there is an additional 180° of phase. As the microphone moves closer to the driver, or the tube becomes shorter, the driver's impedance begins to become significant. At 1 inch the pressure response at the microphone is a signal modified by both the tube and driver's impedance. The result is that at the first tube resonance the magnitude mismatch makes the magnitude response appear like it is only the tube's response, but in the phase response it is visible that it is truly a summation of the tube and driver's response. This adds up to over 360° of phase that can be attributed to the region near the first resonance of the loudspeaker (see Figure 5.6). For feedback control application, the control loop only has 360° of phase to work with per resonance. With out additional compensation, this system would be unstable. Thus this system is not applicable for feedback headset designs.

5.2.2 Electrical Design

The second design example examines modifying the electrical impedance. When driven by a constant voltage amplifier, the acoustic output efficiency is a function of the imaginary part of the electrical impedance. This is due to the current storage capacity of the inductance in the voice coil. The first part of this section derives the acoustic output

and illustrates the affect of modifying the electrical impedance. The second half of this section looks at the experimental results from modifying the loudspeaker's inductance.

In order to determine the acoustic power output, the mechanical and electrical impedance terms must be recalled from Chapter 3.

Although a high pass filter in Chapter 3 approximated the acoustic impedance, here the Bessel functions will be evaluated. The acoustic radiation impedance can be separated by its real and imaginary components. The real component is termed the radiation resistance and the imaginary, the radiation reactance.

$$Z_r = R_r + jX_r \quad (5.19)$$

$$R_r = \pi\rho_o c R_1(2ka) \quad (5.20)$$

$$X_r = \pi\rho_o c X_1(2ka) \quad (5.21)$$

Where R_r is a Bessel function of the first kind, and X_r is the Sturve function of order one. This becomes very computationally extensive for large numbers of frequency points, so for transfer function analysis, as shown in Chapter 3, a simple high pass filter is more appropriate.

With all of the impedance terms it is now possible to determine the acoustical output. The acoustic power radiated in to the fluid can be determined by:

$$\Pi = R_r u^2 \quad (5.22)$$

For the constant current source the velocity, u, can be determined from the transfer function developed in Chapter 3 for velocity to current. Solving for u and allowing the current to be come constant yields:

$$u = \frac{Bli}{Z_m + A^2 Z_r} \quad (5.23)$$

The power for a constant current source can then be calculated as:

$$\Pi_{cs} = R_r \left(\frac{Bli}{Z_m + A^2 Z_r} \right)^2 \quad (5.24)$$

For the constant voltage source, the velocity must be determined by another relation because the current, i, varies with frequency. By multiplying the velocity to current relation found in 5.23 by the inverse of the electrical impedance, a function relating the velocity and input voltage can be determined.

$$u = \frac{BlV}{Ze(Z_m + A^2 Z_r} \quad (5.25)$$

The power is then calculated by:

$$\Pi_{vs} = R_r \left(\frac{BlV}{Ze(Z_m + A^2 Z_r} \right)^2 \quad (5.26)$$

Figure 5.7 shows the differences in the acoustic output when driven by a constant voltage and constant current source. If the electrical reactance is then augmented, the output power of the constant voltage source decreases substantially. Figure 5.8 shows the acoustic output before and after being modified for both types of sources, and Figure 5.9 shows the resultant change in the electrical impedance. If driven by a constant current source, the inductance stores a constant amount of power at all frequencies and only acts as a constant decrease in gain over all frequencies.

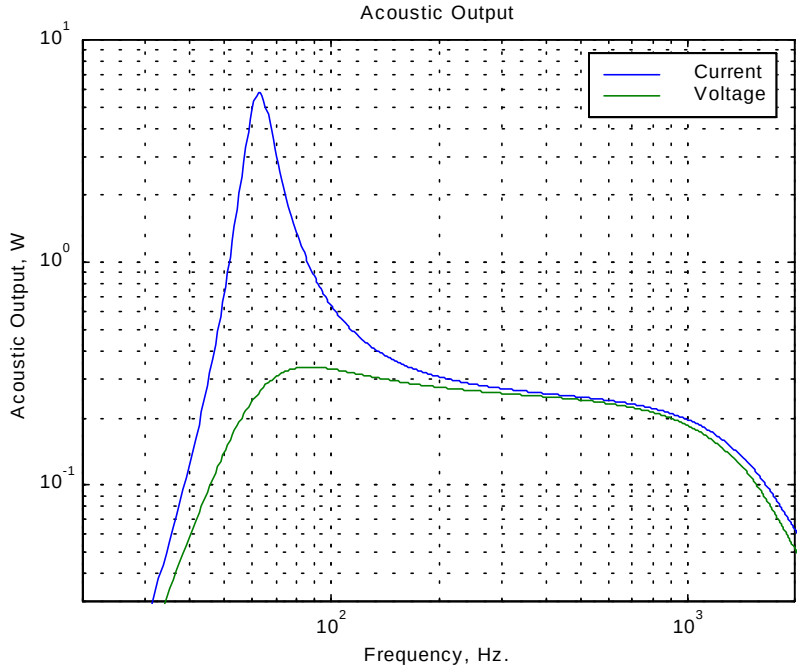

Figure 5.7 Frequency response driven by a constant current and constant voltage source

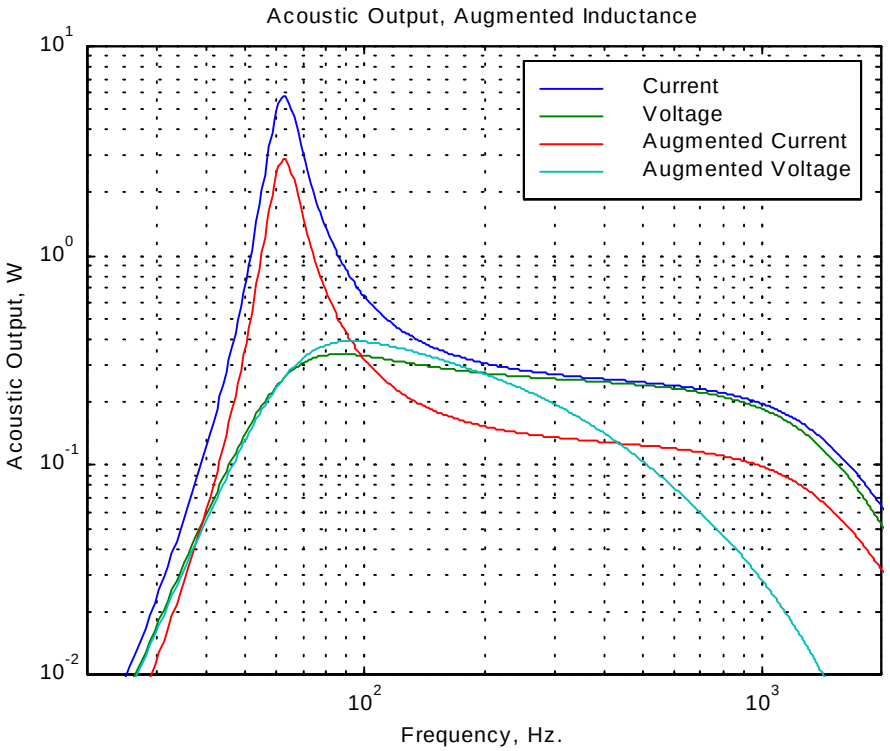

Figure 5.8 Augmented reactance frequency response, constant current vs. constant voltage source

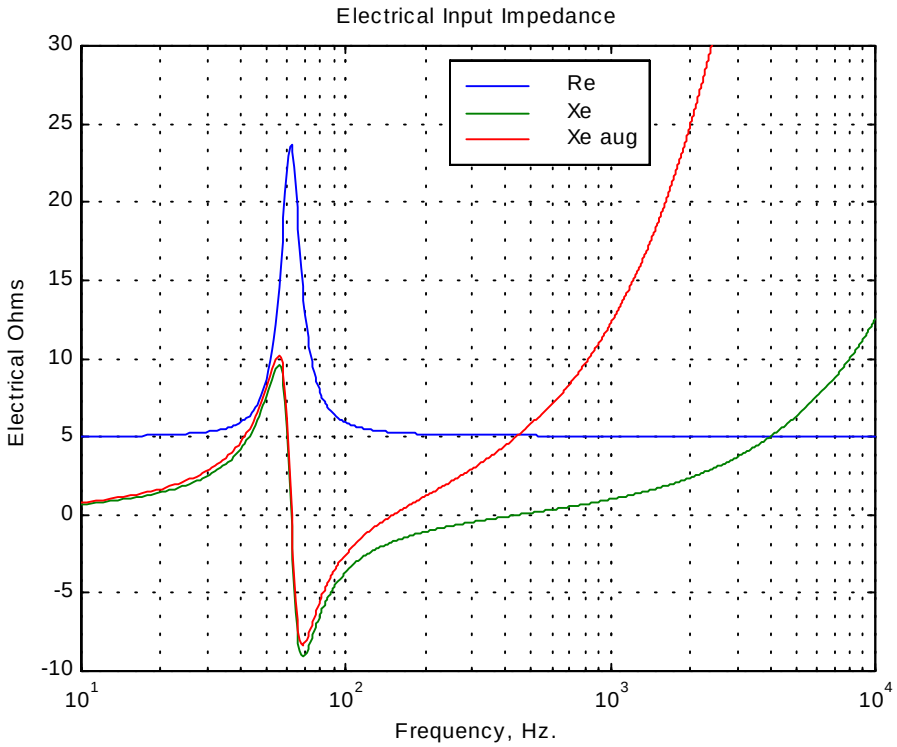

Figure 5.9 Electrical impedance with augmented reactance

5.2.2.1 Experimental Results

For the experiment a 1.1mH inductor (that also has 16.5 Ω resistance) was placed in series with the speaker and the frequency response was measured. The loudspeaker was driven by a constant voltage source. Three measurements were taken, without the inductor, with the inductor and the response of just the inductor (V_{in}/V_{out}). Then these results were compared to the theoretical model. The electrical impedance in the model was augmented with the added impedance and the results can be seen below.

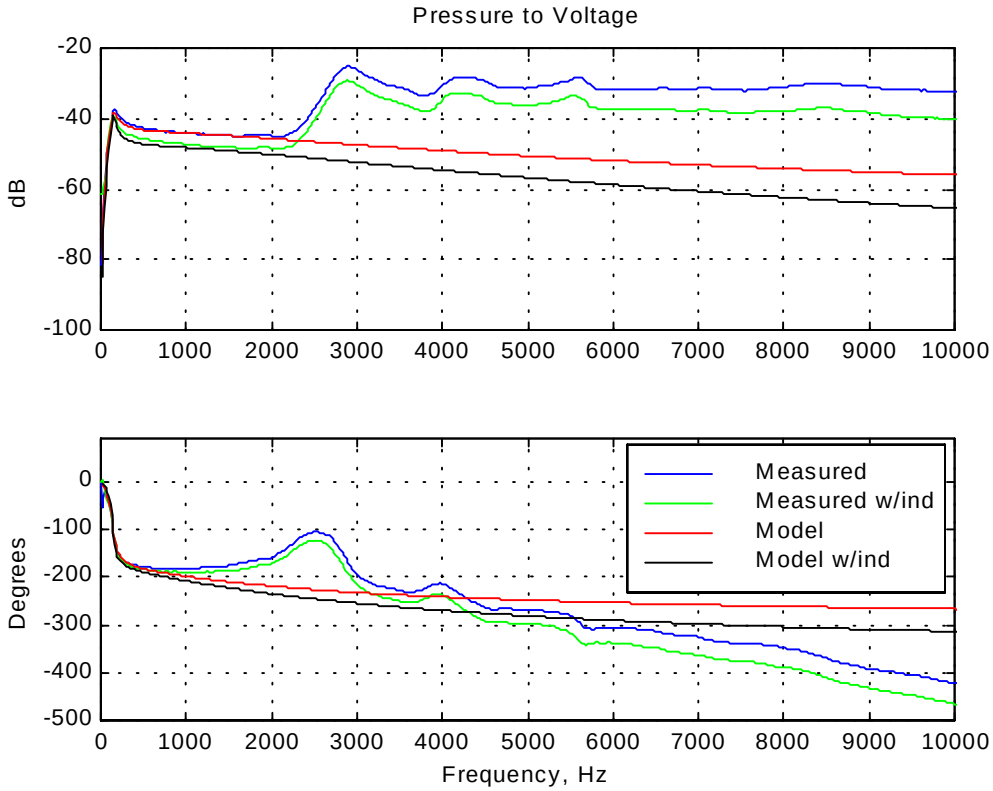

Figure 5.10 Added inductance model

Figure 5.10 shows that the model predicts the experimental data well for the primary mode shape. As predicted there is a frequency dependant reduction in pressure. By 10,000 Hz. there is a 9dB drop in magnitude. With the chosen inductance value (1.1 mH) the amount of power absorbed by the inductor becomes significant. The electrical power in to the inductor can be found using equation 5.27.

$$p = vi = Li\frac{di}{dt} \quad (5.27)$$

Since the nature of acoustics is dynamic, the value of the current feeding the speaker will be constantly varying (unless the amplifier has a constant current source output, like Bob Carver's Sunfire) and thus the inductor will continually be dissipating power. The rate of change in current is frequency dependant that increases exponentially. This is in total agreement with the theoretical case examined previously.

The first resonant peak is also affected by the added inductance. As predicted in Chapter 3, the quality factor is increased and the frequency is shifted downward. By increasing the quality factor, when placed in a closed loop system, could allow the system to benefit from additional reduction. This is possible if the system has adequate stability margins at primary crossings.

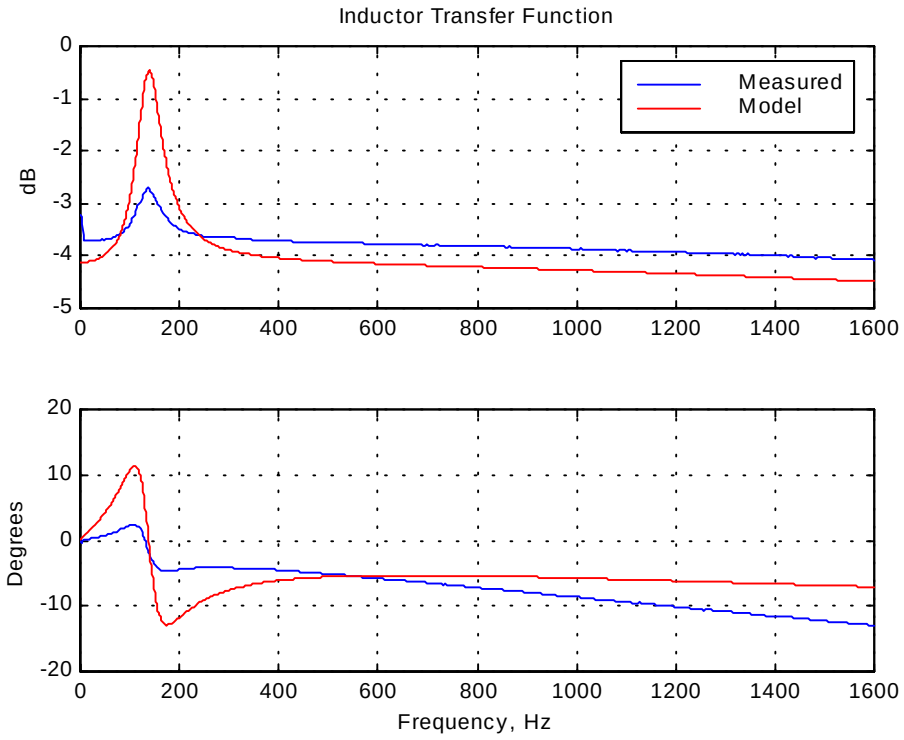

Figure 5.11 Added inductance transfer function

The question that remains is how does the added inductance compare with what can be constructed using a compensator. By placing a pole in the compensator at 3000 Hz. a 10 dB reduction by 10,000 Hz. is possible, but with the compensator pole comes an additional 90 degrees of phase lag plus an additional dynamic. The inductor only introduces 56 degrees of phase at 10,000 Hz. This is somewhat deceiving also because

the inductor is only shifting the response; it is not an added dynamic. Depending on the number of dynamics found in the bandwidth past the first resonance, the less phase added to the system is usually beneficial. For systems without power restrictions this modification will help transform the system closer to the open loop response goal.

Figure 5.11 shows the transfer function for the inductor alone. Investigating the zero-pole mapping it is found that the low pass shape is due to a pole that has moved to $(R_o+R_l)/L_l$, which for the given speaker (Pro-Luxe) is found to be 43,455 rad/sec (7000 Hz.). There is also a high frequency zero that can be found at $3.25x10^5$ rad/sec that does not seem to affect the frequency response.

5.2.3 Mechanical Design

Chapter 3 demonstrated that by increasing the mass to stiffness ratio increased the system's Q factor. This increase should also decrease the acoustic output at high frequencies due to the increased inertia. With the proper choice of extra cone material it should be possible to maintain the same natural frequency and not add significant damping which would reduce the gain of the first resonance Without a complete high frequency model, it is not possible to predict these effects.

For this experiment, mass was added directly to the cone of a plastic speaker. This not only increased the mass of the diaphragm but also changed the stiffness and damping properties significantly. The driver was augmented in two ways. First the driver was coated with a spray acrylic. The acrylic did not add a significant amount of mass but changed the driver's stiffness and damping slightly. The changes were not significant to the frequency response. Secondly a driver was coated using rubber cement. This was chosen for its ability to be applied evenly over the entire surface. Unfortunately, this did not add a constant mass to stiffness ratio, and the damping much higher than expected. Figures 5.12 and 5.13 show the frequency response results.

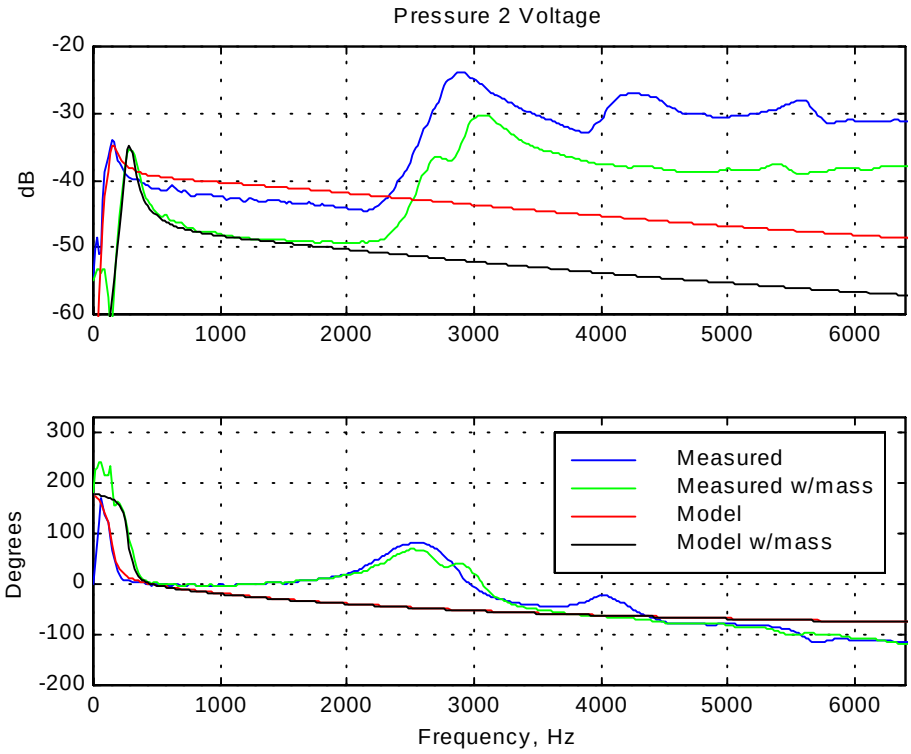

Figure 5.12 Mechanical property modifications

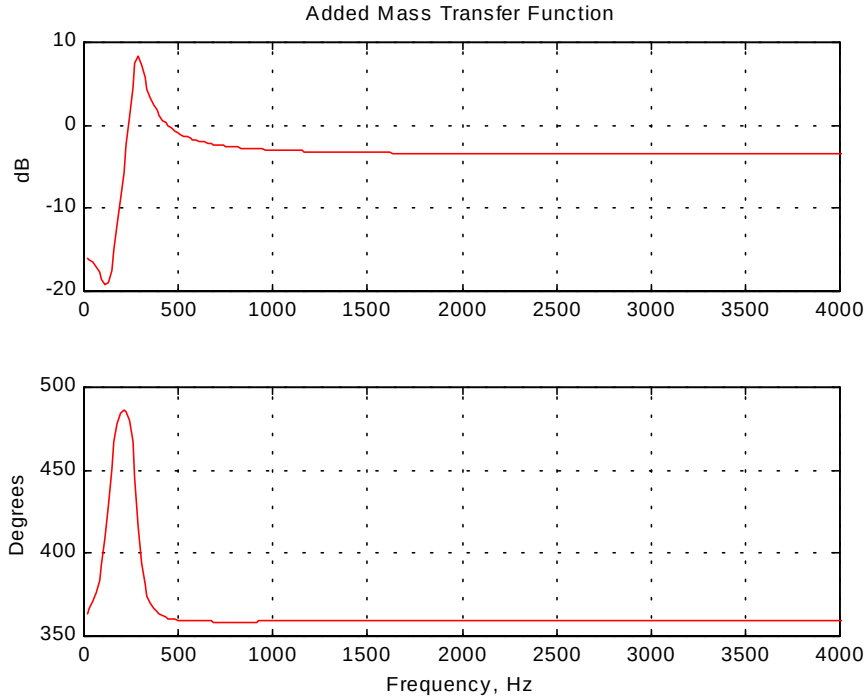

Figure 5.13 Augmented mechanical properties transfer function

Since the mass to stiffness ratio was not fixed for the rubber cement system, the natural frequency was changed, but the results are quite good. The system Q was significantly increased, as predicted. The system is reduced in magnitude by 10 to 20 dB over the frequency range past the first resonance. The added damping only decreased the first resonance by 3 dB. It should be noted that during the short time the driver was under test, the magnet began to become warm. This could become a significant problem if the driver was used in a sealed enclosure that is filled with acoustic damping material. The life of the driver would certainly be decreased.

5.3 Design for Parameter Variation

5.3.1 Closed Box Effects on Manufacturing Variation

As discussed in Chapter 4, variation in the frequency response due to manufacturing variations is a major problem for fixed gain controllers. Sealed enclosures have properties that are beneficial for control, these include higher output and increased quality factor. The goal of this investigation is to determine if the enclosure interaction with the loudspeaker is beneficial for manufacturing variations. Figure 5.14 is another example of manufacturing variation from all identical speakers.

Assuming that the walls of the enclosure are rigid and do not have any mechanical mode shapes within the bandwidth of interest, the only design parameter for the enclosure is its volume. This volume of air inside of the enclosure has an acoustic compliance equal to

$$C_{AB} = \frac{V_{AB}}{\rho c^2} \quad (5.28)$$

$$C_{Total} = \frac{C_{AS} C_{AB}}{C_{AS} + C_{AB}} \quad (5.29)$$

Where C_{AB} is the compliance of air inside the enclosure and C_{AS} is the total compliance of the speaker cone. Since the total compliance of the system is found through a voltage divider relation, 5.29, as the compliance becomes smaller, the enclosure will control the system. The compliance changes many characteristics of the loudspeaker. The natural

frequency of the system will be shifted higher (as predicted by 5.28) as the volume becomes smaller. The system Q is also increased.

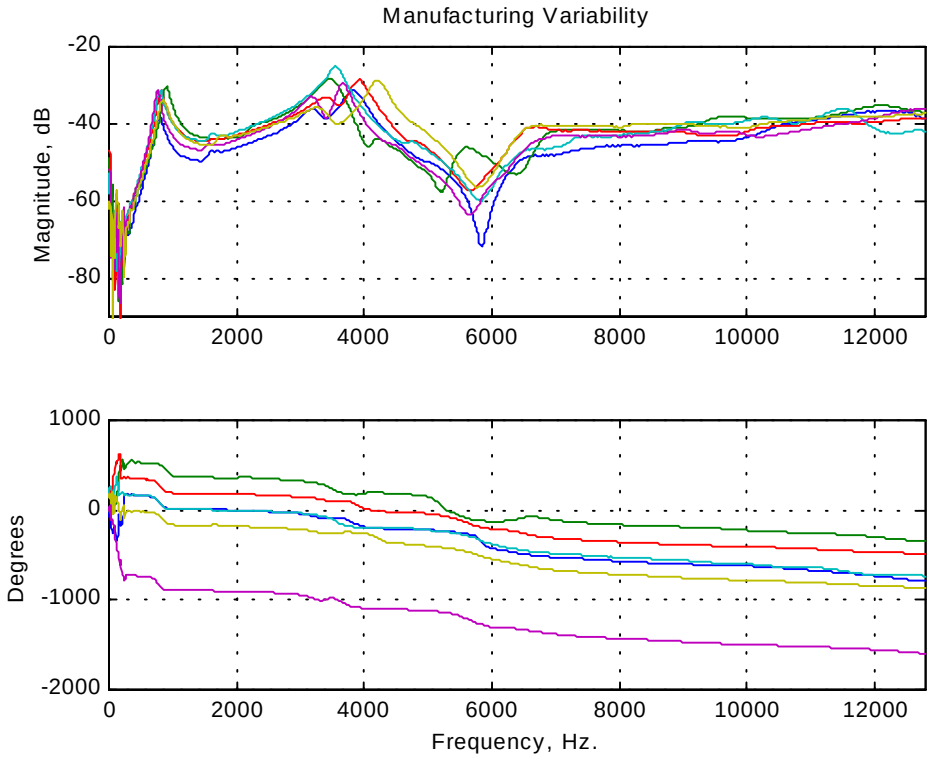

Figure 5.14 Manufacturing variability, infinite baffle response

For this simulation, large variations in natural frequency and damping of the primary resonance were invoked. By placing the loudspeakers into various enclosures, the variation in resonant frequency decreases as the enclosure volume decreases. Figure 5.15 is a simulation of a 20-cm^3 enclosure where the variation in natural frequency went from 172 Hz. to 36.2 Hz., which is a 79% decrease in variation. The system's total Q originally varied between .99 and 3.1, by adding the enclosure the total Q was drastically increased and the variation was minimized to 9.6 to 10.0. Another benefit from the enclosure is the added gain (magnitude). The 20-cm^3 enclosure exhibited a 10 dB increase over the free air response.

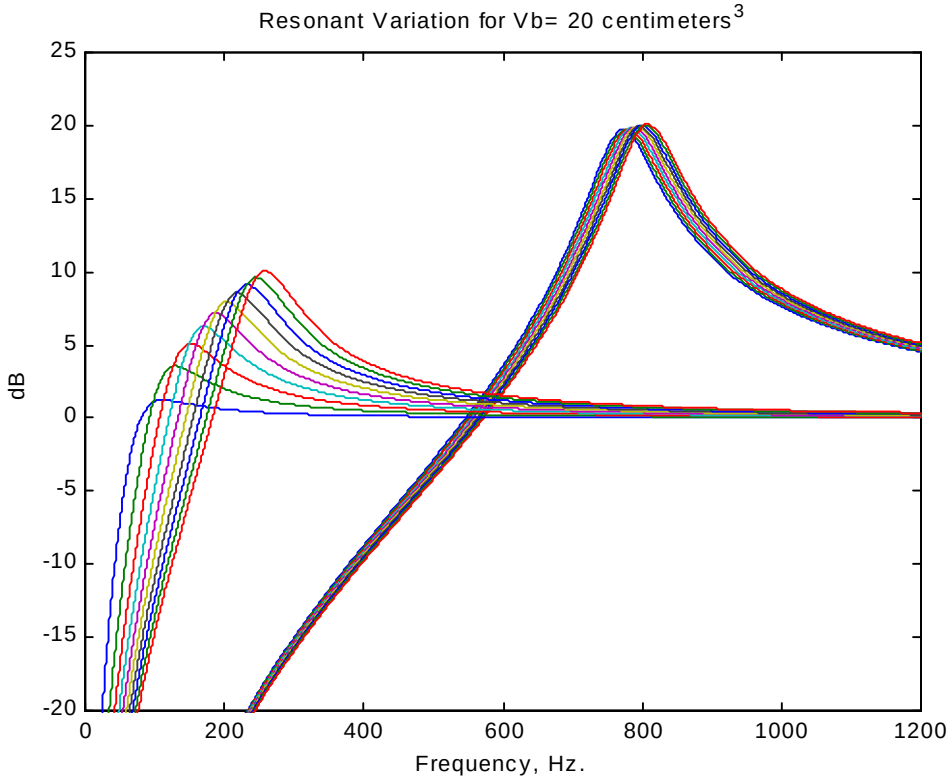

Figure 5.15 Closed box resonance variation control - simulated

To test the effects of loudspeaker enclosure size several enclosures of different volumes were constructed. Figure 5.16 shows data taken using enclosures of approximately 20, 40, 60 cm^3 and the free air case is approximated by 2 m^3. In this figure, the dotted lines represent the theoretical model and are scaled to unity gain. The theoretical model was constructed using Small's methods and this requires an additional assumption that the radiating area is equal on both sides of the loudspeaker. The differences shown in damping can be attributed to an imperfect enclosure seal and because the speaker under test had an disproportionate radiating surface between the front and back of the speaker. The differences in frequency can be attributed to slight variances in enclosure volume. During the construction of the test enclosures, the volume of the wire leads and sealant were not considered when the volumes were calculated. Since the size of the enclosures under test are quite small, these variations, ~1.5 cm^3, become significant. Even with these oversights, the model does predict the resonant frequency should be higher than the theoretical simulation. The magnitude disagreement is because the test was done without

a permanent test rig, and the microphone distance was only approximately the same for each of the traces. Also the microphone used was not calibrated. However, even with the tests shortcomings, the model does show good correlation with the experimental data.

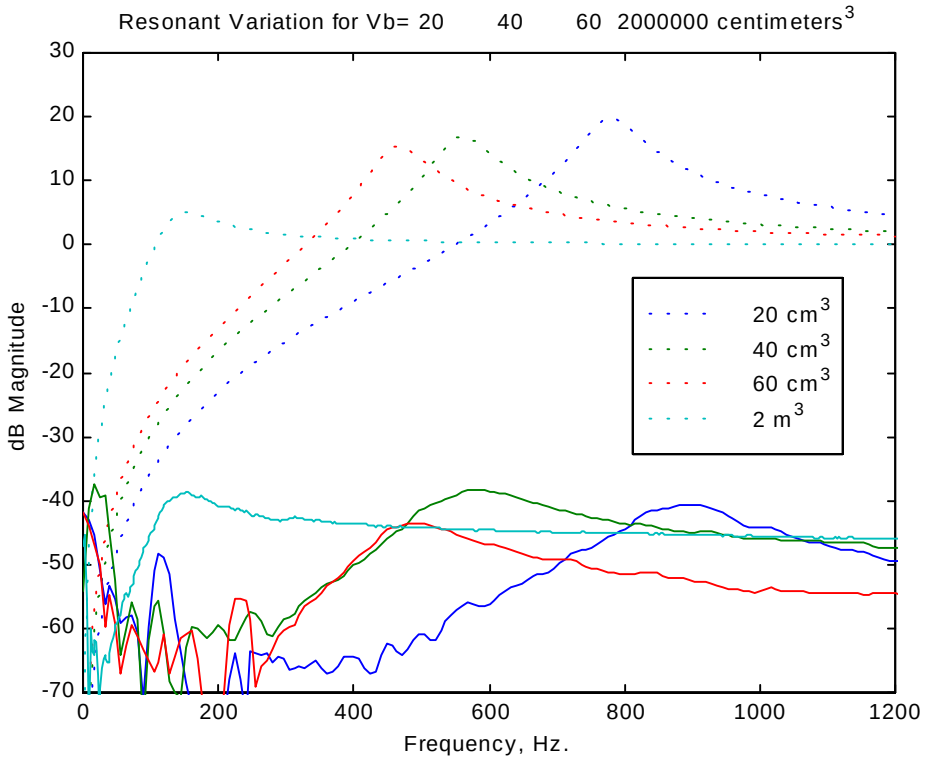

Figure 5.16 Resonant frequency variation with Vb

With the results of the previous test, the 20 cm^3 enclosure was chosen and the 20 drivers shown in Figure 5.17 were placed into this enclosure. Figure 5.17 shows the frequency response with selected drivers with and without the enclosure. The natural frequency was increased by 200 Hz and the average magnitude gain was 8 dB. This enclosure accounts for a 70% decrease in variation in frequency and a 50% decrease in variation of magnitude.

In terms of its effect on control, manufacturing variation can cause fixed gain controllers to become unstable. Due to manufacturing variations, most designers do not attempt to directly cancel unwanted dynamics because the variations between samples may cause the system to go unstable. The second resonance in the speaker shown in Figure 5.17 is problematic for control. The 20 cm^3 enclosure reduce the variation in resonant frequency

by 41% which allows the resonant peak to be successfully canceled in the control design of Chapter 6.

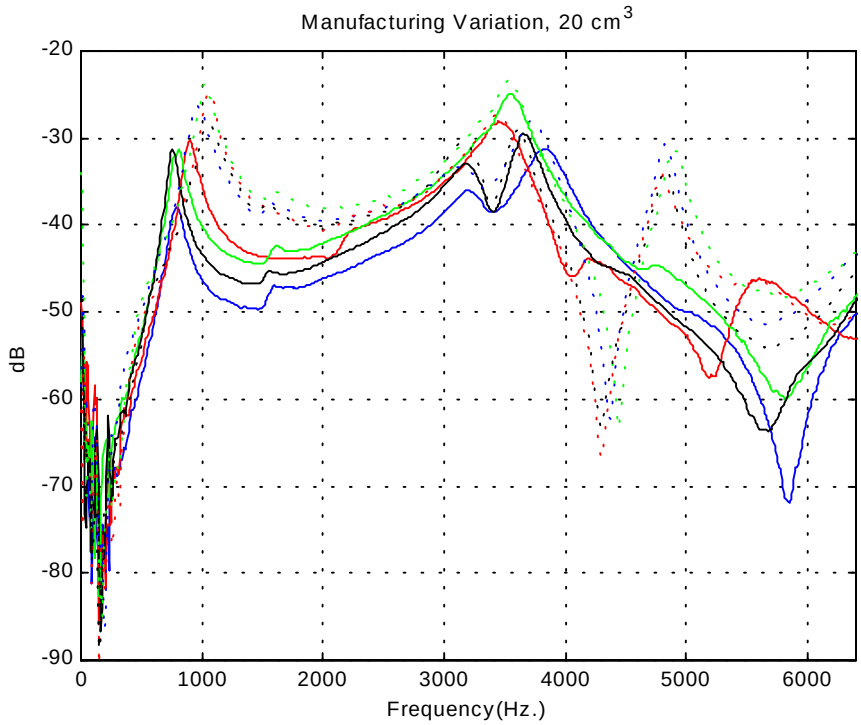

Figure 5.17 Manufacturing variation with (dashed) and without (solid) a 20 cm^3 closed-box enclosure

5.3.2 User Variability Control

User variability is the result of the coupling of the loudspeaker system with the characteristic impedance of the human ear. As explained in Chapter 4, by increasing the acoustic impedance of the loudspeaker system significantly, the headset's response will dominate the coupling and the pressure response will not be skewed by the ear's impedance. Due to the extremely complex nature of the near field acoustics between the loudspeaker and the ear, the analysis presented here will be experimental.

The control engineer has two design choices that will affect user variability. The first is the position of the microphone, how far it is positioned from the ear and how far it is positioned from the loudspeaker. In this thesis only the variance in frequency response will be considered, issues pertaining to the zone of silence around the microphone must

be examined, but that task will be left for future work. The second choice is augmenting the system with a modification to increase the acoustic impedance, such as a port or screen. As shown in 5.2.1, placing an enclosure with a port in front of the loudspeaker increases the acoustic impedance such that significant magnitude can be extracted from the tube's dynamics, but with a phase penalty that makes the system uncontrollable for feedback systems.

Another option to increase the acoustic impedance is to place a permeable boundary at some distance in front of the loudspeaker. This boundary will act as an acoustic low pass filter. Suitable candidates for this boundary include mesh screens and woven cloth. The filter shape can be determined by investigating transmission through panels [8]. Since the fluid on both sides of the screen is the same (air), the transmission coefficient can be determined by:

$$T_I = \frac{1}{1+\frac{1}{4}\left(\frac{r_2}{r_1}-\frac{r_1}{r_2}\right)^2 \sin^2 k_2 L} \quad (5.30)$$

where:

r_1 is the characteristic impedance of the screen

r_2 is the characteristic impedance of the screen

k_2 is the wave number for the screen's material

L is the thickness of the screen

The short inherent length of the screen assures the engineer that there will be a relatively small phase lag associated with this filter. The characteristic impedance of the boundary is dependant on the material used and the mesh spacing. As the thickness increases, more energy is lost transmitting through the medium due to absorptive effects, and the overall gain of the system decreases. Also if the mesh spacing is too fine, the reflection coefficient will increase thus decreasing the system's gain.

Although magnitude of change in the acoustic impedance due to the acoustic screen will be small until the corner frequency, after the corner frequency, the acoustic impedance

will begin to increase helping to decouple the headset from the ear. What this means is that around the frequencies of control (low frequencies) the screen will not be significantly effective for reducing user variability.

5.3.2.1 Experimental Results

Experiments were performed to determine the effects of different microphone positions and whether the acoustic screen provides any benefit for user variability control. Only centrally located microphone positions were investigated. This was accomplished by mounting the microphone onto a frame that was suspended in front of the loudspeaker. The acoustic screen was formed into a hemispherical shape and was applied over this frame enclosing both the loudspeaker and microphone. In the following figures, "near" refers to having the loudspeaker module in contact with the ear, as close as the frame or acoustic screen would allow. "Far" refers to distance of approximately 20 mm from the entrance to the ear canal. The loudspeaker was mounted onto a modified construction helmet with a boom to allow hands free steady measurements. Two users were subjected to each test.

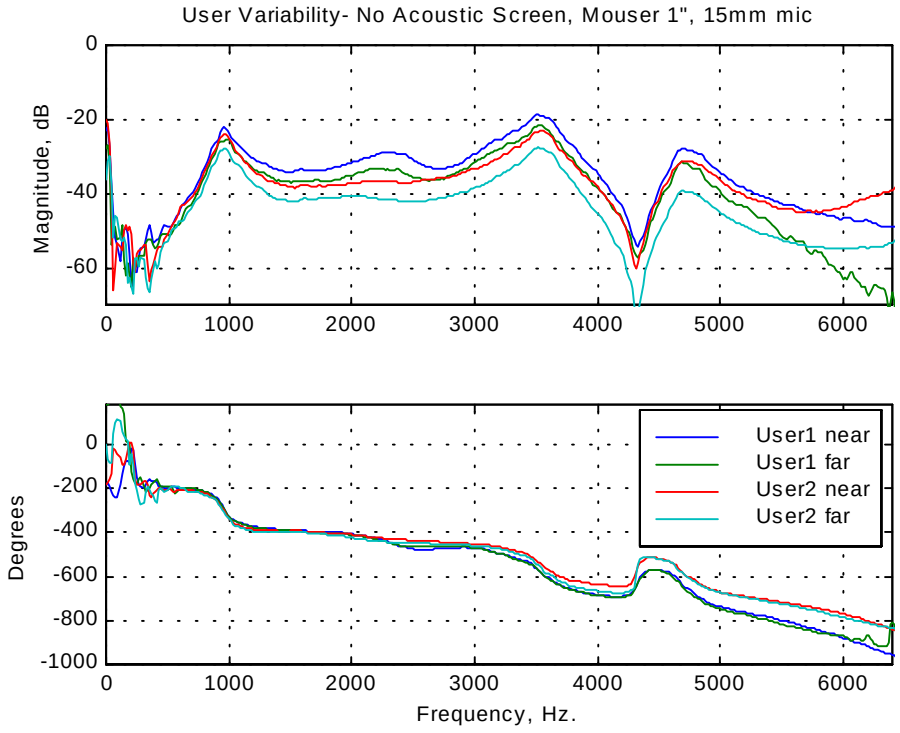

Figure 5.18 User variability for 2 users, 15 mm microphone position

Figure 5.18 shows the frequency response with a 15 mm microphone to loudspeaker spacing. There is little correlation between the two users for the two positions. The gain at the first resonance is nearly equal for all cases. This feature is important because it ensures stability in the bandwidth of the first resonance. Of particular concern is the rise in magnitude at 2500 Hz., there is a 8.5 dB increase between the users.

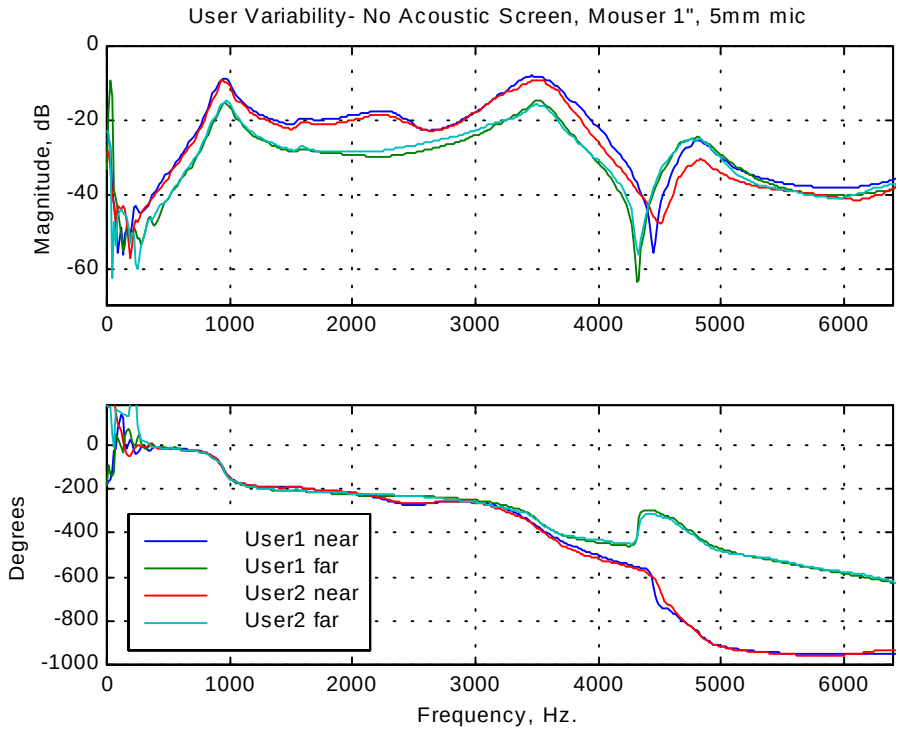

Figure 5.19 User variability for 2 users, 5 mm microphone spacing

Figure 5.19 shows the frequency response with a 5 mm microphone to loudspeaker spacing. There is very good agreement between users until approximately 4000 Hz. with the only difference being the damping on the zero near 4500 Hz. The gain at 2500 Hz. is still present, but at most points, the gain is approximately constant at a 6 dB increase. There is an increase in gain at the primary resonance that could be problematic for stability in the closed loop system.

Figure 5.20 shows the frequency response with a 5 mm microphone to loudspeaker spacing with an aluminum mesh screen. The screen used has a mesh spacing of approximately 1/64 of an inch. There is very good agreement between the two users throughout the frequency band. The gain at the primary resonance is reasonably equal

for all cases and the gain at 2500 Hz. is not present. The previous tree figures show clearly that this combination of 5mm microphone spacing and use of an acoustic screen yields the most consistent frequency response results for the tests performed.

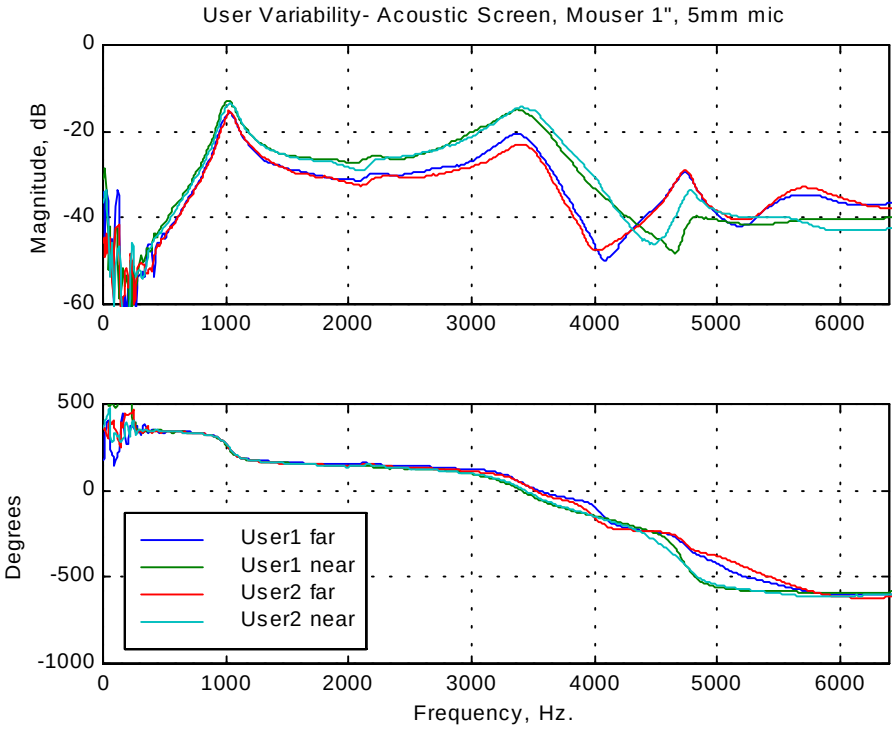

Figure 5.20 User variability for two users, acoustic screen and 5 mm microphone spacing

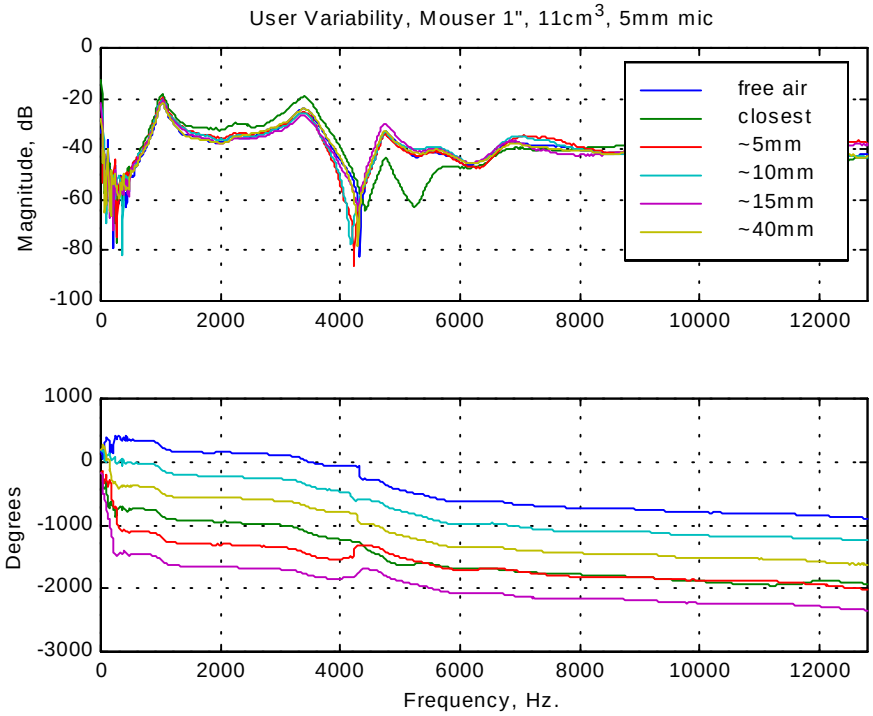

Figure 5.21 User variability for multiple microphone to ear distances

With this combination, other microphone to ear canal spacings were tested. The construction helmet's boom to hold the loudspeaker system was modified such that it could be affixed at various distances from the users ear. Figure 5.21 shows the variance between these spacings. The trace labeled "closest" was with the loudspeaker module placed in contact with the ear yielding a microphone to ear canal opening spacing of about 3 mm, the approximate diameter of the frame members. This is as close as possible to the entrance to the ear canal for the microphone, and is very painful for the user. For all distances, with the exception of "closest", there is very good agreement.

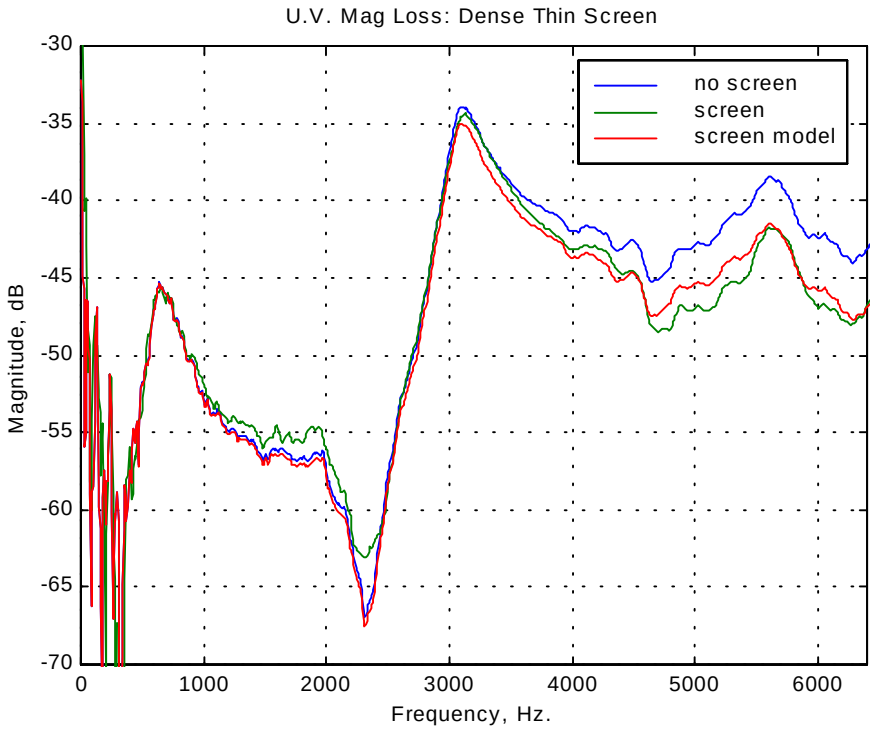

Figure 5.22 Frequency response with the acoustic screen

He final test was to determine what effect the acoustic screen had on the frequency response and how much power it dissipated. Figure 5.22 shows the open-air frequency response with and without the acoustic screen. The microphone was placed outside of the screen for this test. The acoustic screen acts as a low pass filter with a corner frequency of approximately 4000 Hz. The screen was modeled using equation 5.30 using an approximate hole size to determine the characteristic impedance of the screen.

The acoustic screen not only helps with user variability, but also acts as protection for the loudspeaker. This is important because both the loudspeaker and microphone are fragile and can be damaged with misuse. The screen also creates a minimum distance between the microphone and the ear canal the user can position the loudspeaker module such that variations as in Figure 5.21 are minimized.

5.4 Loudspeaker Synthesis

Using the results from the experiments and simulations in this thesis thus far, an attempt will be made to develop a loudspeaker for control applications. This chapter will not try

to determine how to reach the parameters or ideas conveyed; for that is a matter for a materials scientist or someone learned in solid mechanics to determine what materials are necessary to achieve those goals. By drawing conclusions from the simulations performed in Chapter 3 and the experiments done in this chapter, theoretical parameters can be chosen that should yield performance approaching the goal set in Chapter 1.

Before a new loudspeaker can be designed many other factors besides pressure response shape must be determined. For a 1-2 inch loudspeaker, the primary resonance should be located near 700 Hz. When placed in a cabinet this will increase to 740-760 Hz. depending on alignment. The ear is very sensitive to content between 500 and 2000 Hz. [21] and with a good feedback design the controller's 3 dB point should fall around 1300Hz, so the design will cover most of that band. Also the zone of silence around the microphone becomes very small at frequencies approaching 2000 Hz. Since the open-air set floats away from the ear, the microphone cannot be positioned as close to the ear canal as in a circumaural set.

Secondly the loudspeaker should have a weatherproof diaphragm. Many headsets are for military or commercial applications that require very rugged components. Also the basket and electrical contacts should be plated with materials that resist corrosion.

The diameter should be as large as possible. I would propose as large as 2.5 inches. At 2.5 inches, the corner frequency of the acoustical impedance is approximately 1720 Hz. Thus at 800 Hz., the response will only be penalized by about 10 dB of magnitude. The larger diameter will also allow the speaker to include a surround and spider, which give the designer better control over the mechanical properties.

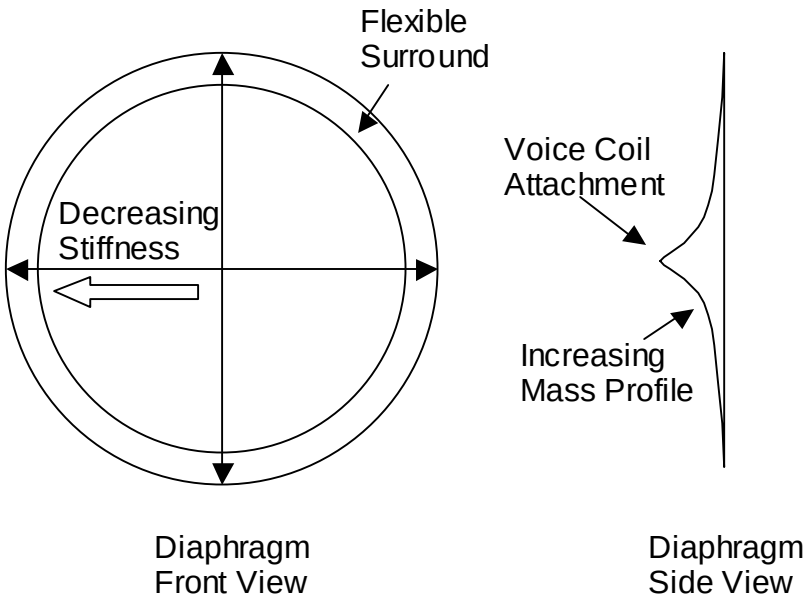

Figure 5.23 Proposed ANC headset loudspeaker

The magnet size should be determined by the mechanical properties. The mass and stiffness values should be quite large, to allow the system to be underdamped. The magnet size should then be picked to allow for this underdamped response. The geometry of the cone plays a significant part in the response as well. As discussed in Chapter 3, the center section on many headphone speakers has a much lower stiffness and mass than the surrounding cone to increase the high frequency output. For control, the opposite would be beneficial. By creating a very stiff and massive center section, while outside of the voice coil radius the stiffness decreases until it connects with a very flexible surround. This design should encourage good low frequency performance with very little high frequency output. This is because as the frequency increases on a conventional speaker, the effective radiating area and effective mass become smaller, so the voice coil can drive the speaker more efficiently. For the new design, by increasing the mass of the center, as frequency increases the effective area will decrease, but the effective mass will change very little, which will limit the output. This design is illustrated in Figure 5.23.

The electrical inductance should be made considerably large, to evoke the effects shown in 5.2.2. It would also be beneficial to used two voice coils. This allows for several impedance combinations and gives the designer more overall flexibility.

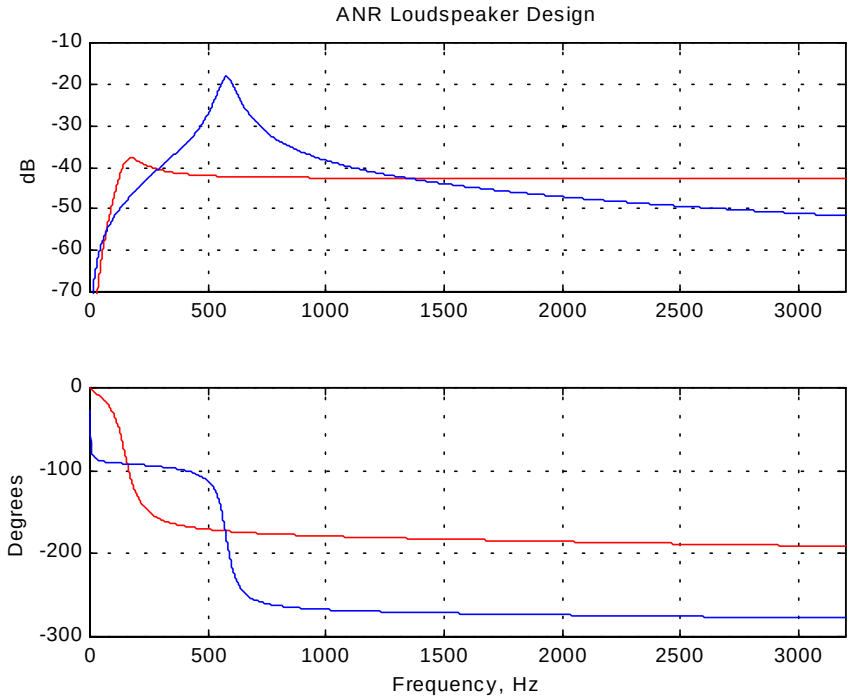

Figure 5.24 Synthesized ANR loudspeaker design (blue) and current headphone loudspeaker (red)

Although many more parameters would have to be specified in order to prototype this driver, the goals set above allow for some rough simulations to be done. Figure 5.24 shows a simulated speaker using the goals specified above against a current headphone speaker.

5.5 Conclusions

This chapter illustrated five experiments that addressed at least parts of all of the major areas of concern in open-air headset design. It was shown that modifying the electrical inductance and the mechanical properties will roll off the plant at high frequencies. Each of these methods has their accompanying trade offs, namely higher power consumption. For systems where power is not a major concern, or where the additional inductance or mass does not change the power characteristics greatly, these ideas will allow the

designer to move closer to the goals set in Chapter 1. Partial control over manufacturing variations was achieved by placing the loudspeaker into a sealed enclosure. The compliance coupling between the loudspeaker and the enclosure allows the designer to make the enclosure a major contributor the response of the speaker, thus reducing variations. User variability decreased by positioning the microphone near the loudspeaker and introducing a transmission loss barrier between the loudspeaker system and the user's ear. The acoustic screen and a microphone placement close to the driver will allow the engineer to build a significantly more robust plant.

Chapter 6: Open-Air Headset Control

6.1Introduction

The preceding chapters have been a guide to creating a plant that can be successfully controlled. Once an open loop frequency response function has been developed that is robust to both user and manufacturing variations, the plant can be shaped for control. Alternatively, if the plant design has achieved the goal set in Chapter 1, simple gain feedback is sufficient to control the system. There are many ways to develop a frequency domain feedback controller, including loop shaping techniques and optimal H_∞ designs. Digital designs will not be discussed here, but the designs are very challenging due to the extra phase from the required anti-aliasing filters and smoothing filters. A strictly analog feedback design will be vastly more cost effective because it can be built using inexpensive components. If a type of heteronomous controller (feedforward and feedback) [34], is to be used the design tradeoffs can also take into account the shape of the noise field.

The first part of this chapter is a short description of the methods available to the control engineer for supra aural headsets. The second part of this chapter is a short summary of the control theory necessary to design a supra aural headset. It will focus on path determination and the Bode gain-phase relationship. It will also explain the response of poles and zeros in the frequency domain and will examine the response of a few basic compensator designs. The third section addresses a method for developing a compensator for a supra aural headset. In this method, termed loop shaping, the designer chooses poles and zeros to shape the desired open loop frequency response to comply with the Bode gain-phase margins while seeking to maximize the open loop gain. A controller will be designed for a selected loudspeaker system and test data will be analyzed.

6.1.1 Methods of Control

Analog fixed gain feedback control is the most common type of design for active noise reducing headsets seeking to achieve broadband noise reduction. For the headset a loop shaping frequency domain approach will be used. Control is accomplished by compensating the control to error path to achieve disturbance in the closed loop. It can be built using relatively inexpensive and common integrated circuits. This type of controller design will be the basis for this control discussion.

Optimal feedback designs (H_2, etc) are state variable methods. These methods try to minimize a cost functional based on a relationship between the states that is defined by the engineer. The large number of calculation and the need for an exact model for the system require that these methods are to be implemented using digital hardware. This introduces the sampling process, anti-aliasing and smoothing filters and machine delay into the control loop. There has been very few successful digital feedback headsets implemented in industry due to hardware limitations. Digital feedback will not be discussed here.

Feed-forward designs make of use digital hardware and adaptive signal processing, particularly the LMS algorithm. Feed-forward control has excellent success in environments that contain tonal noise fields because a coherent and uncontrollable reference signal is often available. Feed-forward methods will not be discussed here.

6.2 Feedback Control

6.2.1 Block Diagram Analysis

The first step to every control problem is to identify the variables in the model. The components of the model in Figure 6.1 were discussed in Chapter 1. To review, the microphone detects pressure fluctuations in the environment and converts that pressure to an electrical voltage. The microphone output voltage, d(t), is passed to a compensator H, which outputs a voltage, V_{in}, to the plant G. The plant creates an acoustic pressure, $P_p(t)$, that is received by the microphone and transformed into a voltage, $V_p(t)$. The

superposition of d(t) and $V_p(t)$ is the error signal, e(t), which is the direct result of feedback. For the moment we will assume that the superposition adds the two signals together, which is termed positive feedback. The system then exists in closed loop form. The pressure is minimized as e(t) tends toward zero. In terms of Laplace transforms the model can be described by

$$E(s) = D(s) + G(s)H(s)E(s) \quad (6.1)$$

By rearranging, we can determine the disturbance to error path.

$$\frac{E(s)}{D(s)} = \frac{1}{1 - G(s)H(s)} \quad (6.2)$$

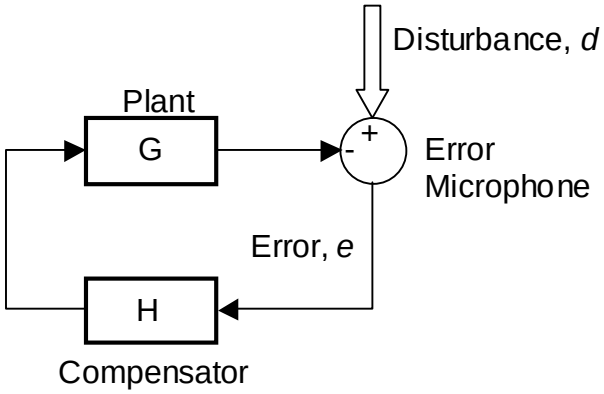

Figure 6.1 Open-air headset block diagram

Although the problem now appears trivial, several complications are present. First, the compensator we create must be realizable. The filter must not produce an output prior to its input; it must have a causal impulse response. Secondly, the closed loop system must be stable (only the closed loop needs to be stable, it is possible to have a unstable open loop system, that is stable in the closed loop). Finally, the design must be able to be constructed. While it is possible to build improper systems, often at high frequencies the gain becomes unmanageable.

6.2.2 Relative Stability and Bode Diagrams

For a system, suppose that the closed loop transfer function is known. Then stability can be determined by simply inspecting the roots of the denominator. If the roots of the denominator are all contained within the left half of the s-plane, the system is stable.

However, for the headset, and for most systems, the closed loop transfer function is not known. Fortunately it is possible to determine the stability by evaluating the open loop frequency response. This is only possible if the open loop system is stable. Open loop stability can be determined by the final value theorem, this will tell if the system has a bounded response. Alternatively, if a bounded input results in a bounded output, the following technique can be applied. Using root locus methods, it is possible to predict the closed loop response from the open loop transfer function as a function of gain. It has been determined that the neutral stability points for the root locus have the following properties (assuming that the system uses negative feedback).

$$\left|KG(s)\right| = 1 \quad and \quad \angle G(s) = \pm 180° \pm k360°,\ k = 0,1,2,... \quad (6.3)$$

By converting these statements into the frequency domain, by replacing s with jω, these statements must hold for the open loop Bode plots as well. Now if the gain K is to be increased, the stability conditions must be revised. To illustrate these changes Figure 6.2 shows a system with multiple gain cases. With K=2 the system is at neutral stability, and it can be seen that any value of K less than 2 will yield a stable system. For values greater than 2 the system becomes unstable because at the gain crossover the phase is no longer equal to or less than -180°. So the neutral stability conditions become [35]:

$$\left|KG(j\omega)\right| < 1 \quad at \quad \angle G(j\omega) = \pm 180° \pm k360°,\ k = 0,1,2,... \quad (6.4)$$

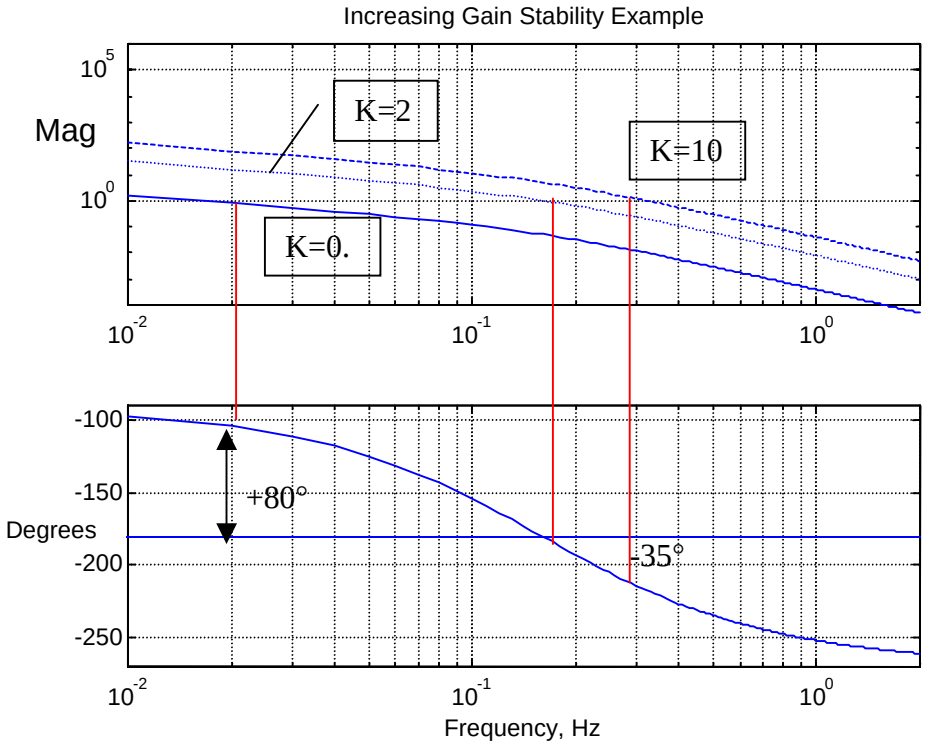

Figure 6.2 Increasing gain instability example

These conditions are the Bode stability criteria for negative feedback and apply for minimum phase systems, or systems where all of their dynamics are contained in the left half of the s-plane. For non-minimum phase systems (systems that contain zeros in the right half of the s-plane) or systems with a large number of dynamics, these conditions must be modified again. The designer must ensure that for every point beyond -180° (for negative feedback systems), the magnitude remains less than unity. So the designer must examine each phase crossing throughout the entire bandwidth of control. For negative feedback systems this becomes:

$$\left|KG(j\omega)\right| < 1 \quad at \quad \angle G(j\omega) = -180° - 360°(n-1)\ n = 1,2,... \quad (6.5)$$

Where n is the number of phase crossings in the bandwidth of interest. For positive feedback systems, the conditions similarly become:

$$\left|KG(j\omega)\right| < 1 \quad at \quad \angle G(j\omega) = 0° - 360°(n-1)\ n = 1,2,... \quad (6.6)$$

Quantitative measures of stability for negative feedback systems can be defined from the Bode criteria. The gain margin is the factor by which the magnitude is less than unity at

all of the -180° crossings in the phase plot. Another measure of relative stability is the phase margin. It is the amount by which the phase exceeds -180° at the unity gain crossing. For the headset system developed in this paper, there will be two phase margins (the system crosses unity twice) and a gain margin for each phase crossover point. Figure 6.3 illustrates the gain and phase margins for a typical headset system.

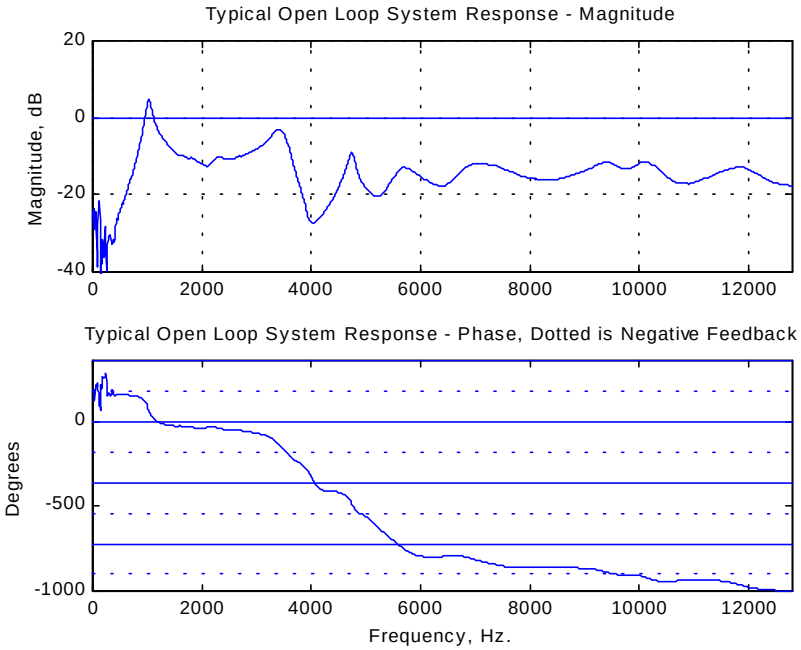

Figure 6.3 Typical open-loop frequency response

Many designers will suggest the Nyquist criteria when multiple stability margins are present. The Bode criteria cannot predict stability for some plants, such as the double integrator. Nyquist has fewer limitations in the type of plant evaluated, but it requires an accurate model of the plant, which includes the number of open loop poles in the right half plane. As Chapter 3 explained, an accurate model for the loudspeaker alone is a very difficult task, not withstanding the enclosure and the acoustic medium between the speaker and microphone. For the headset systems, the plant is represented by measured frequency response data at points of good coherence. Bode stability analysis allows the designers to implement actual measured data in their simulations.

6.3 Loop Shaping

Loop shaping is a trial and error process where the designer places poles and zeros based on their frequency response characteristics in order to shape the open loop response to a desired goal. As discussed in Chapter1, the desired goal that will be investigated is the complex conjugate pair of poles. The amount of control is limited by the Bode gain and phase margins. There is not a set technique; loop shaping relies on the skill and experience of the designers and their knowledge of how poles and zeros interact in the frequency domain. So, the first step is to understand how poles and zeros can be used in the frequency domain.

6.3.1 Frequency Domain Characteristic Filters

Figure 6.4 shows a single pole and two complex conjugate poles, one lightly damped and one heavily damped. A single pole has unity magnitude until it reaches its corner frequency (also called the break point), which is defined by a 3 dB decrease in magnitude. After its corner frequency, the response will continue to decay at -20 dB per decade. Each pole also brings with it -90° of phase and in the limit to the corner frequency, the phase will be 45°.

Complex conjugate poles start at unity magnitude and then increase to a point that is proportional to the damping of the pair. Complex conjugates have a corner frequency equal to the natural frequency of the pair. The natural frequency is equal to the distance away from the origin in the complex s-plane. After the corner frequency the pair decays at –40 dB per decade. Each pair also contributes -180° degrees of phase to the system. The phase will be -90° at the corner frequency.

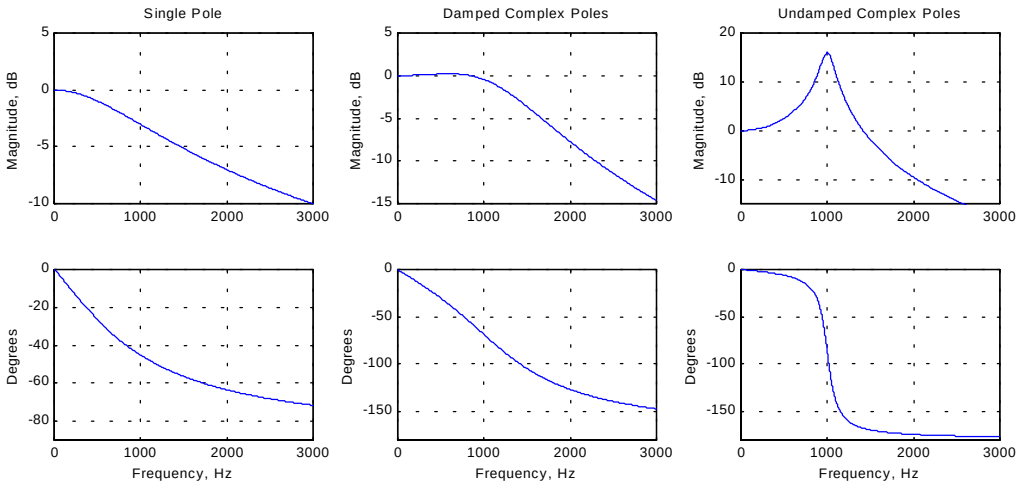

Figure 6.4 Frequency response – Poles

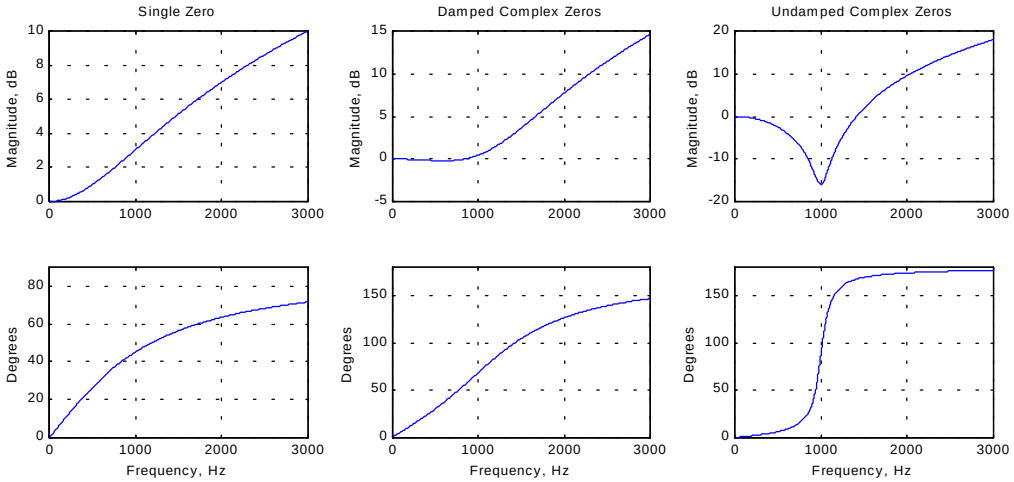

Figure 6.5 Frequency response – Zeros

Figure 6.5 shows a single zero and two complex conjugate zeros, one lightly damped and one heavily damped. Each type of zero has exactly the opposite response as its corresponding pole. A single zero has unity magnitude until it reaches its corner frequency. At the corner frequency, the magnitude is increased by 3 dB. After the corner frequency, the magnitude increases at 20 dB per decade. Each zero also has +90° of phase. Like the pole at the corner frequency, the phase will be at 45°.

Complex conjugate zeros decrease in magnitude until a maximum that is proportional to their damping that occurs at their natural frequency. They then increase in magnitude at a rate equal to +40 dB per decade. They contribute +180° of phase and have increased +90° at their natural frequency.

Once each individual component is understood, it is helpful to understand several pole-zero combination relationships. This section is not a detailed explanation of the design procedure for the controllers presented; it simply shows the general frequency response characteristics and what is required to design compensators for supra aural headsets. If the reader wishes more detail, it can be found in any feedback control text [11]. In general, only a basic understanding of what controls the features of each filter is sufficient to successfully design a loop shaped controller.

The general compensator network that will be employed for the headset is of the form:

$$H(s) = K\frac{s+z}{s+p} \quad (6.7)$$

Provided that the pole and zero are real and in the left half plane, the transfer function can be said to be minimum phase. This will minimize the contribution to the overall loop phase, but will allow for the magnitude to roll off at higher frequencies (once the phase shift passes 360°).

With this transfer function two types of responses can be specified. The first involves placing a zero closer to the origin than the pole. This is termed a lead controller. The response is simply the summation of a zero and a pole (as it well should be). It was shown that the phase margin is related to the damping of the system, thus a lead controller is often used for systems to increase the damping. Figure 6.6 shows the magnitude and phase response of this filter. The frequency of maximum phase gain (lead) can be determined by

$$\omega_{\max,\, phase} = \sqrt{|z||p|} \quad (6.8).$$

To determine the values of the magnitude and phase increases it is helpful to represent 6.7 as

$$H(s) = K\frac{Ts+1}{\alpha Ts+1} \quad (6.9)$$

where

$$T = \frac{1}{2\pi * freq_{zero}\,(Hz)} \quad (6.10)$$

and $1/\alpha$ is the lead ratio. α is simply the frequency ratio between the pole and zero. For a lead controller α is always less than one. Referring to Figure 6.6, the maximum phase increase is equal to

$$\phi_{\max} = \sin^{-1}\frac{1-\alpha}{1+\alpha} \quad (6.11)$$

The maximum magnitude can be found by

$$mag_{\max} = \frac{K}{\alpha} \quad (6.12)$$

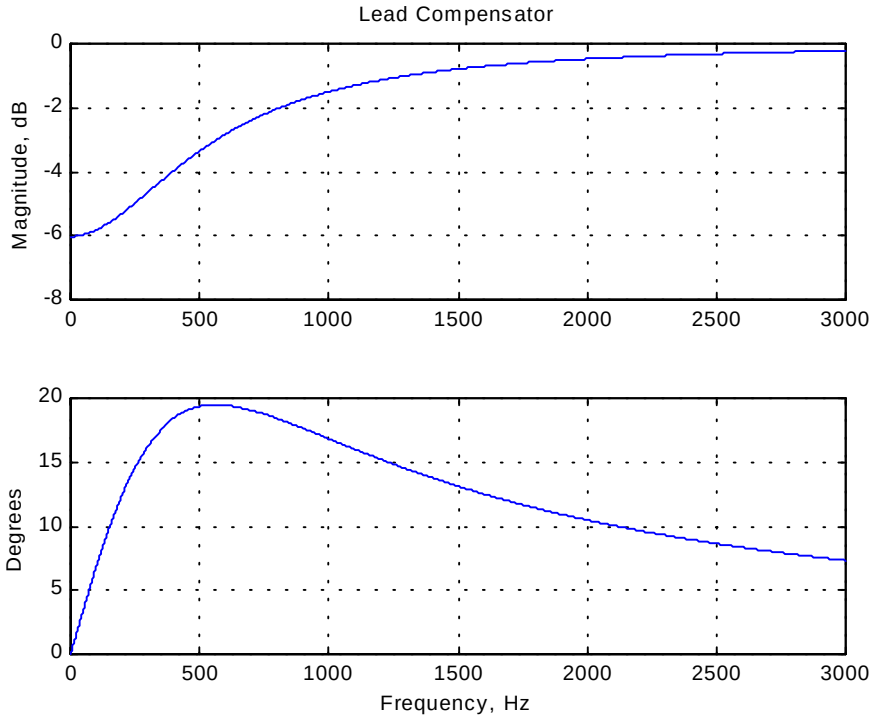

Figure 6.6 Frequency response – Lead compensator

For most systems the maximum phase increase is approximately 60°. If more phase lead is needed the designer may simply construct a second filter with the same specifications

and multiply these together, this results in having twice the maximum phase increase. In the frequency domain, multiplying filters together results in their composite being a summation of their individual responses. Figure 6.7 graphically illustrates this point.

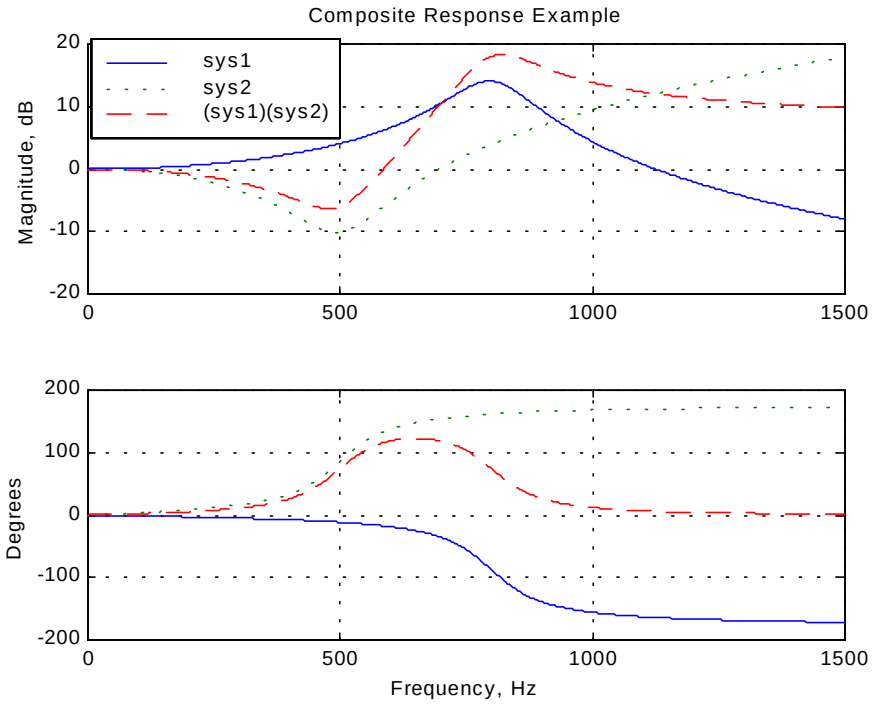

Figure 6.7 Frequency domain addition

The other case for the transfer function in equation 6.7 is placing a pole closer to the origin in the s-plane. This is termed a lag controller. A lag controller creates a high, low frequency gain and a phase decrease (lag), which is shown in Figure 6.8. The lag controller performs very similarly to a PI (proportional-integral) controller (Figure 6.8) that is used to reduce steady state error. The lag controller has the advantage over a PI controller that it has a smaller phase decrease that can leave a sufficient phase margin for stability. The lag controller also affects the DC gain of the system allowing for improved steady state response characteristics. The lag controller's transfer function can be represented using the form

$$H(s) = \alpha \frac{Ts + 1}{\alpha Ts + 1} \quad (6.13)$$

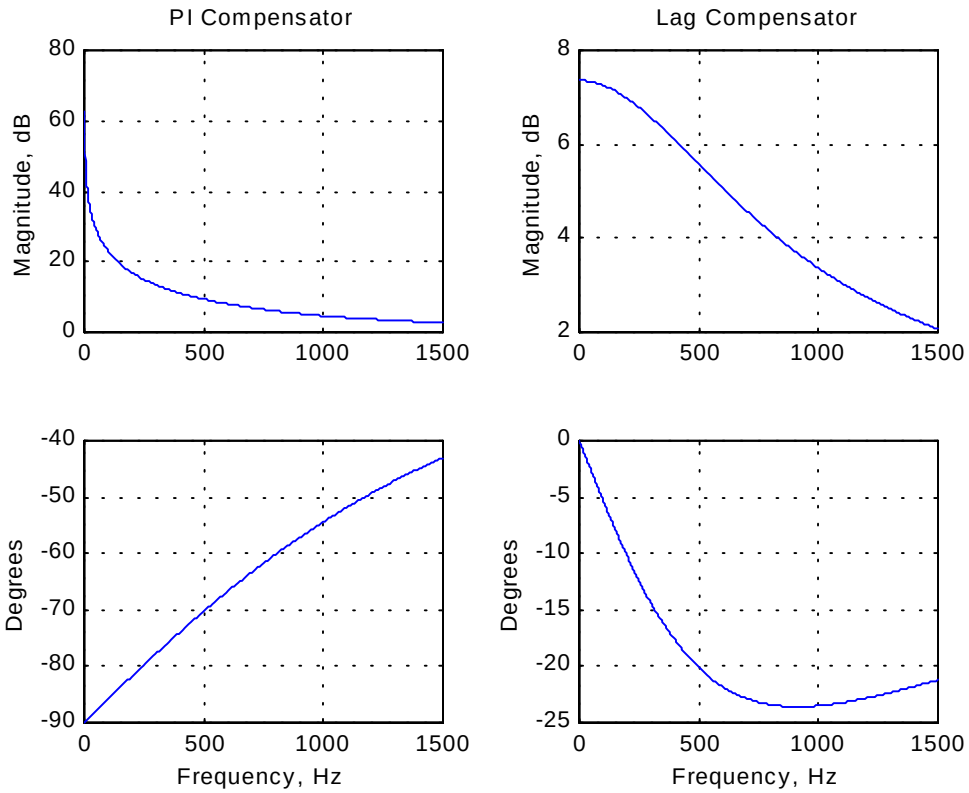

Figure 6.8 Frequency response –PI and Lag compensators

The value of α should now be greater than 1 signifying that the pole is nearer to the origin than the zero. The maximum gain is now simply α (or 20logα in dB units) and the maximum phase decrease is calculated using equation 6.11. The frequency of the maximum phase lag is found using equation 6.8.

A third type of filter that should be considered uses a set of complex poles and zeros. Its transfer function can be modeled as

$$H(s) = K\frac{(s+z)(s+z^*)}{(s+p)(s+p^*)} \quad (6.14)$$

Where the natural frequency of the poles is less than that of the zeros. The frequency response and pole zero map are found in Figure 6.9. This filter allows the designer to add gain to the system with a reduced phase penalty. In 1987 Carme (ref) made a comprehensive study of various compensation filters. It was his conclusion that this filter was the most appropriate for headset design. The advantage is that significant gain can

be achieved with no net phase [34]. Another advantage of this filter is that it can be implemented using the standard "bi-quad" architecture. A description of the bi-quad circuit can be found in [33].

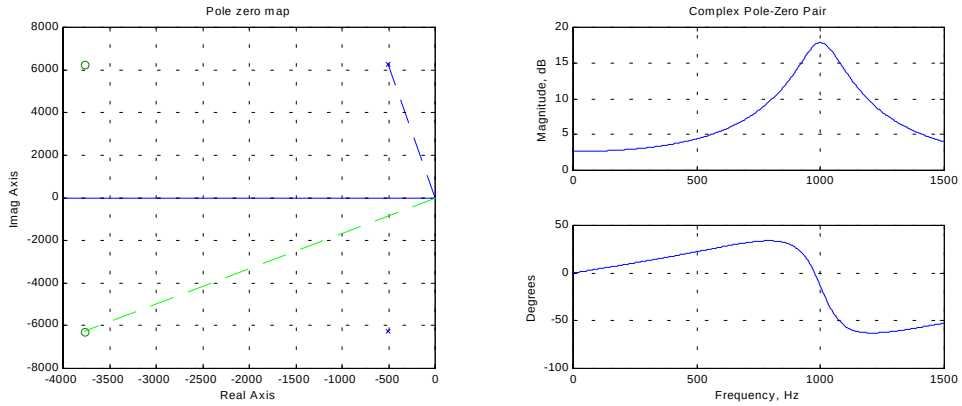

Figure 6.9 Frequency response –Complex pole-zero pair

6.3.2 Open-Air Control Realization

Now with the frequency domain tools in place, it is time to design a compensator. The goal for this compensator is to achieve maximum open loop gain with maximum gain and phase margins to minimize unwanted amplification in the closed loop [34]. After completing all of the experimentation in Chapter 5, a plant was designed that utilized all of the ideas deemed advantageous according to the metrics developed in Chapter 4. The next step was to measure the frequency response data on and off the head for several different subjects. Although methods to control user variability have been built into the plant, having multiple data sets will ensure that the compensator that is built will be stable. The compensator was then simulated until the designer believes that they have built the optimum controller (or they just get sick of it and quit …). Finally the controller was constructed out of analog components and tested.

6.3.2.1 Plant Description

The plant was developed with the minimization of user variability and manufacturing variability as the main goals. The speaker that was selected was from Mouser

Electronics. It was a 1.0” diameter Mylar speaker with a rated sensitivity of 98 dB. The speaker was placed in a 20 cm^3 enclosure which was demonstrated in Chapter 5 to reduce resonant peak variability by 79%. User variability was improved by using a 5 mm microphone spacing and a aluminum mesh screen. The mesh screen served two purposes, to increase the acoustic impedance across the boundary between the microphone and the ear canal, and to physically protect the microphone and loudspeaker from physical damage. The added inductance was not used because the open-air headset has a good possibility of being battery powered and the increased power consumption was deemed unsatisfactory.

6.3.2.2 Compensator Design

The compensator was developed using thirty different open loop frequency response functions representing both manufacturing and user variability. This included eleven different speakers and three frequency ranges. The simulation was done using Matlab. The most varied response was chosen and used to develop the controller. Figure 6.10 shows the open loop averaged uncompensated frequency response. In order to more easily recognize the Bode phase crossover points; horizontal lines are inserted into the phase response: red is for negative feedback and occurs at multiples of 180°, blue represents positive feedback and occurs at multiples of 360°.

This next section outlines the process to design a compensator. It is only one approach and is not claimed to be the optimal design. Other designers with more experience may be more successful.

Referring to the data taken during the manufacturing variation experiments, the enclosure chosen reinforces the second resonance and reduces its variation in frequency significantly (41%). This resonant peak is reducing the amount of overall system gain that would be possible for control. Using a least squares curve fit on all of the data traces, the poles for the second resonance average value are nearly -100±3400i (in Hz.). These will be the first zeros for the compensator. In order to keep the compensator proper, two poles are added at 12,000 Hz to ensure the plant rolls off. Also by placing the poles so far from the origin, they will have only a small effect on the dynamics around the primary resonant peak, which will be the center of control. Referring to Equation 6.2, the open loop response is simply GH. The compensator and open loop response can be seen in Figure 6.10.

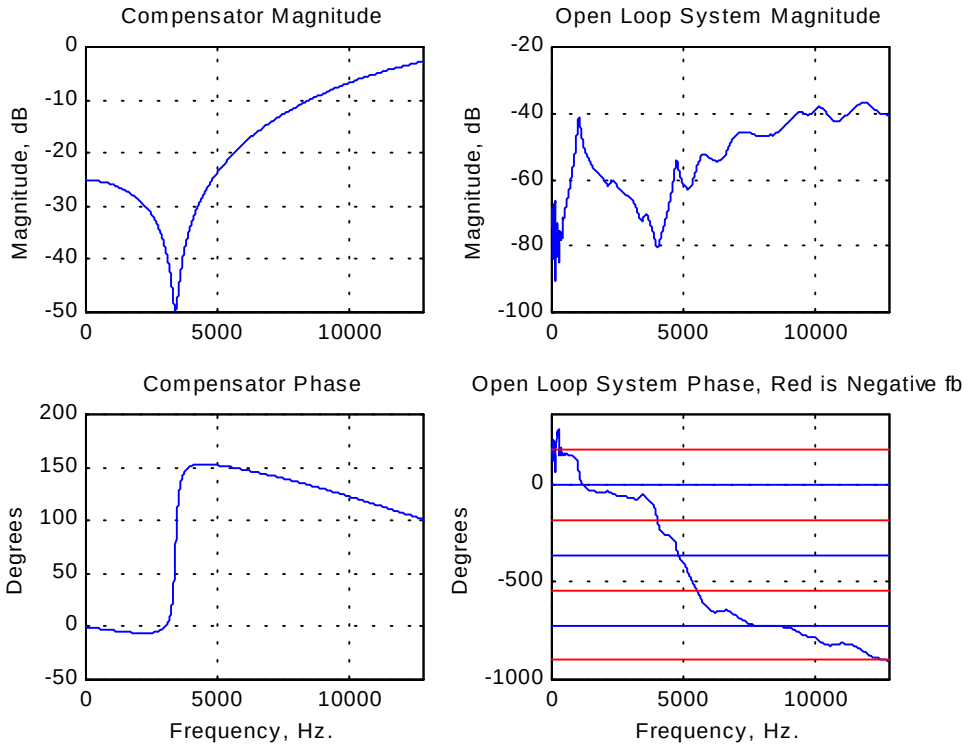

Figure 6.10 Open-loop compensated response (1)

In order to control the magnitude of the complex zeros, a pole was placed near the origin. This has the effect of shifting the response down at 20 dB per decade. To finally break the complex zeros back to unity gain (remember that responses add in the frequency

domain, two zeros plus two poles equal unity gain), a pole was placed at 4500 Hz. The compensator and open loop response are plotted in Figure 6.11.

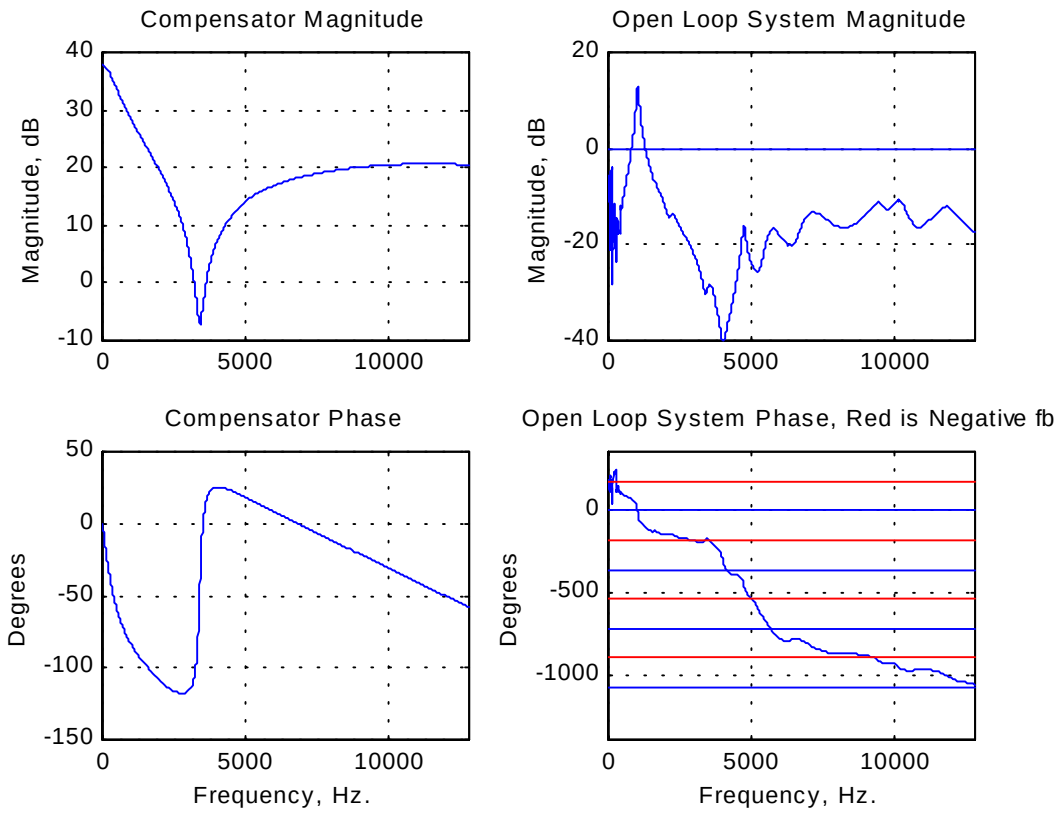

Figure 6.11 Open-loop compensated response (2)

Now the open loop frequency response is beginning to look like the desired response. The gain and phase margins show that the system is stable, so the next step is to close the loop on the system. Gain must be added to the system and is controlled again by the phase margin. For this system the gain added is equal to 100,000,000,000. This number should not be alarming, for when constructed with actual analog electronics, the gain is inherent in the dynamic design. The closed loop system is found using equation 6.2 and is plotted in Figure 6.12. While the reduction looks very promising, the system shows some magnification at the higher frequencies making the system marginally stable. This amplification is sometimes called “spillover” and is the result of having very shallow

slopes at the Bode crossover points. For most headset systems a maximum amplification rule of thumb is around 3 dB [34].

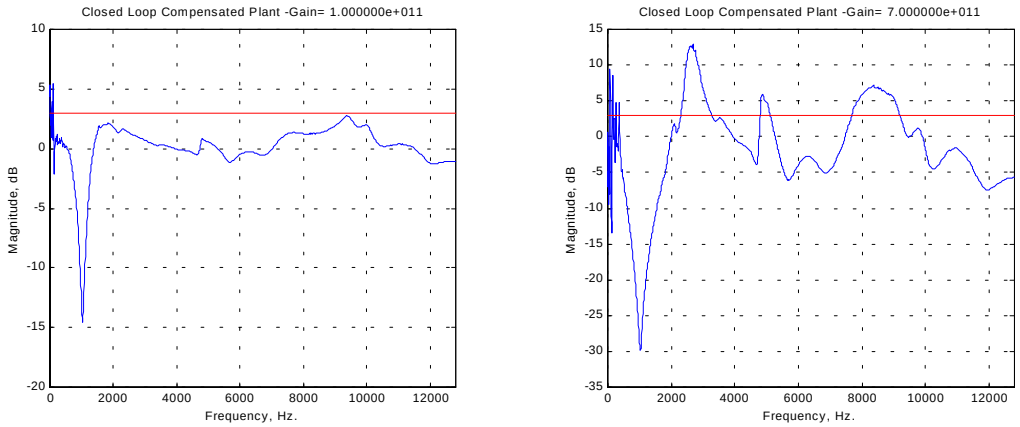

Figure 6.12 Closed-loop response, 2 gain cases

While the spillover around 10,000Hz is less than 3 dB at this gain, when the gain is slightly increased, the system goes unstable at 2,500 and 8,000 Hz (Figure 6.12). To control this, a set of complex zeros is placed at 10,000 Hz. This will increase the phase margin to allow for greater gain and suppression. With the complex zeros a set of complex poles was also added at 14,000 Hz. to equalize the magnitude gain from the zeros and to allow the system to continue to roll off from the poles at 400 and 4500 Hz. Figures 6.13 and 6.14 show the open loop and close loop response of this system.

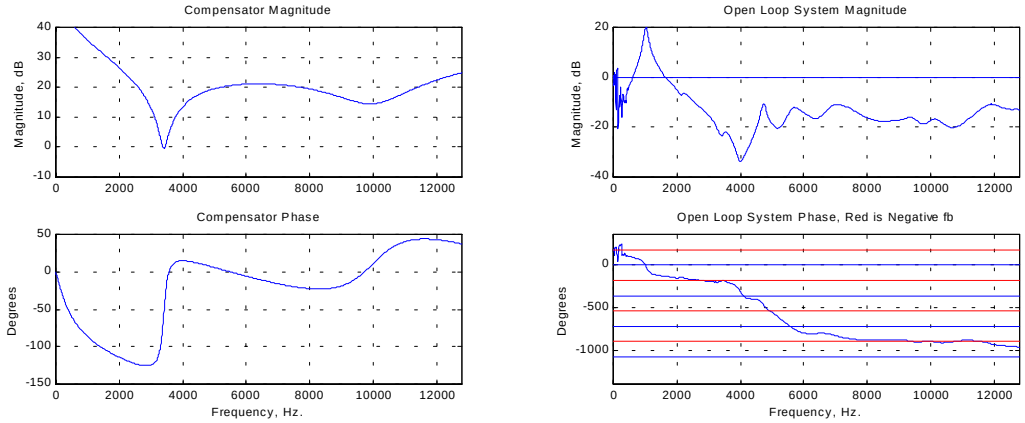

Figure 6.13 Open-loop response – Final Compensator

The results for this compensator are very favorable, 21 dB reduction at 1016 Hz and less than 3 dB spillover after 4000 Hz. It should be noted that at no time during the design process were the gain or phase margins calculated. By observing the Bode diagrams it is possible to inspect for stability.

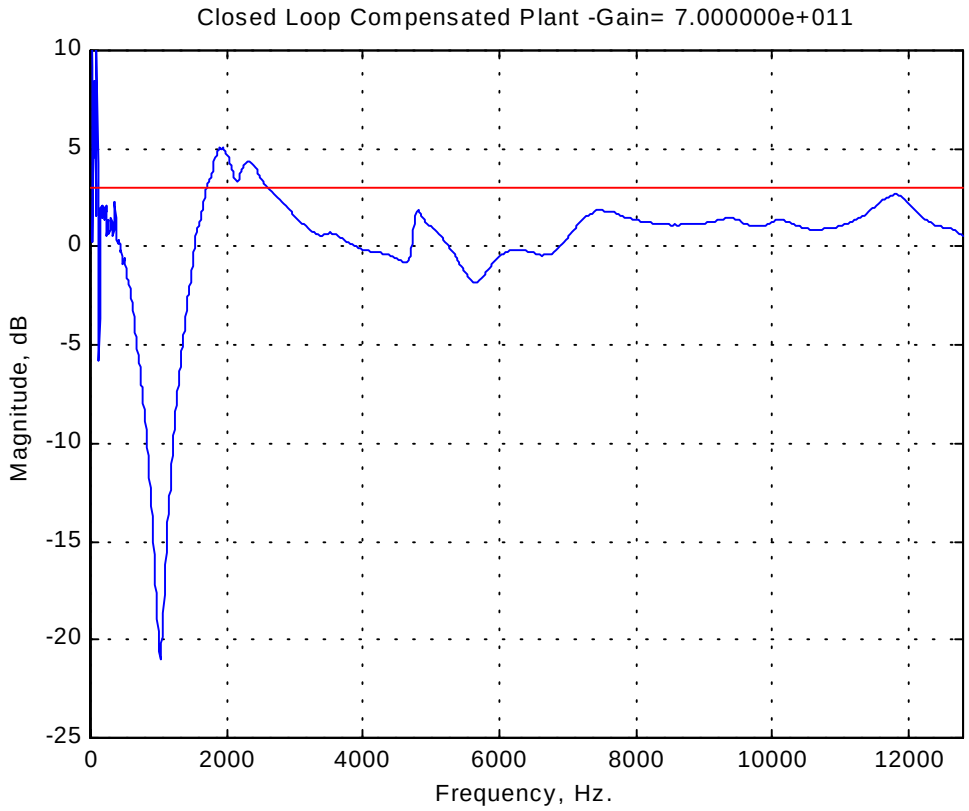

Figure 6.14 Closed-loop response – Final compensator

Since the controller was designed using a composite of all of the test cases, it was simulated for a final time using the individual test cases. These cases included data taken on and off the subject's head and at varying distances from the entrance to the ear. For all cases, the controller remained stable with less than 5 dB of spillover across the entire bandwidth. The case with 5 dB of spillover was one where the loudspeaker system module was inserted as far as possible into the user's ear. This raised the gain slightly on the second resonance and thus reduced the gain margin and increased spillover. Figure 6.15 shows a sampling of closed loop responses.

At this point the theoretical compensator design was deemed successful.

The next step in the process is constructing the compensator out of analog components. As stated earlier it is possible to build a zero alone, but it is often difficult to control the high frequency gain. It is quite easy to build a set of complex poles and complex zeros together. This is the bi-quad circuit [33]. Table 6.2 is a list of the final pole zero locations.

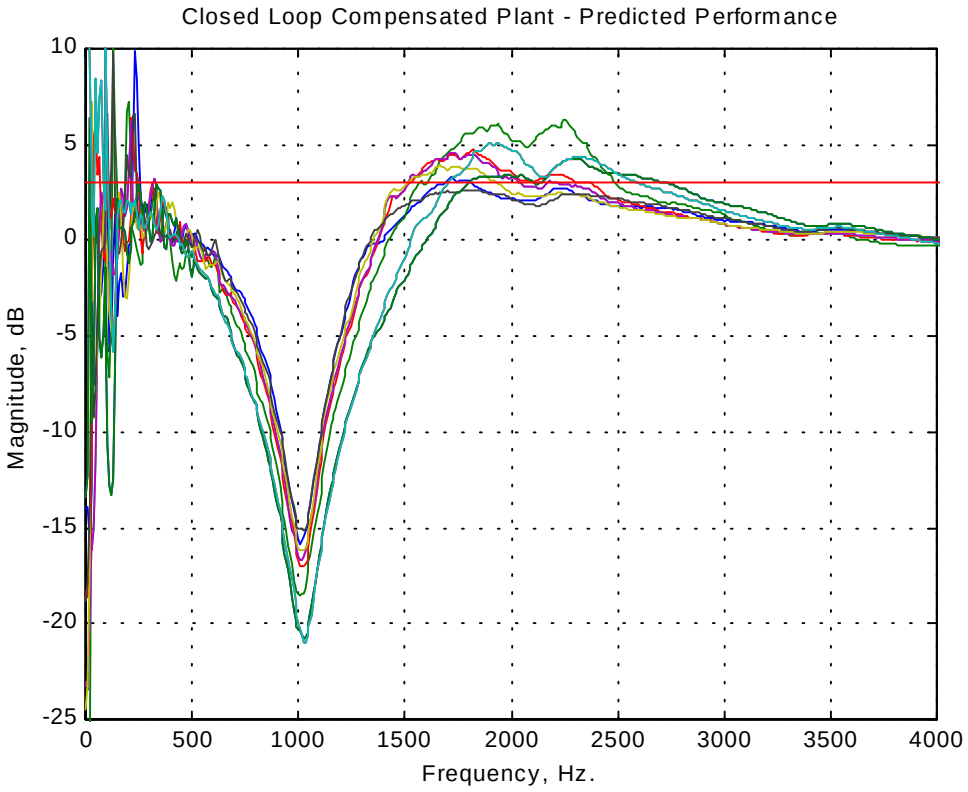

Figure 6.15 Closed loop frequency response – Multiple cases

Poles	Zeros
-400	-100+3400i
-4500	-100-3400i
-8000+12000i	-1000-10000i
-8000-12000i	-1000-10000i
-10000+14000i	
-10000-14000i	

Table 6.1 Compensator pole-zero list – All values in Hz.

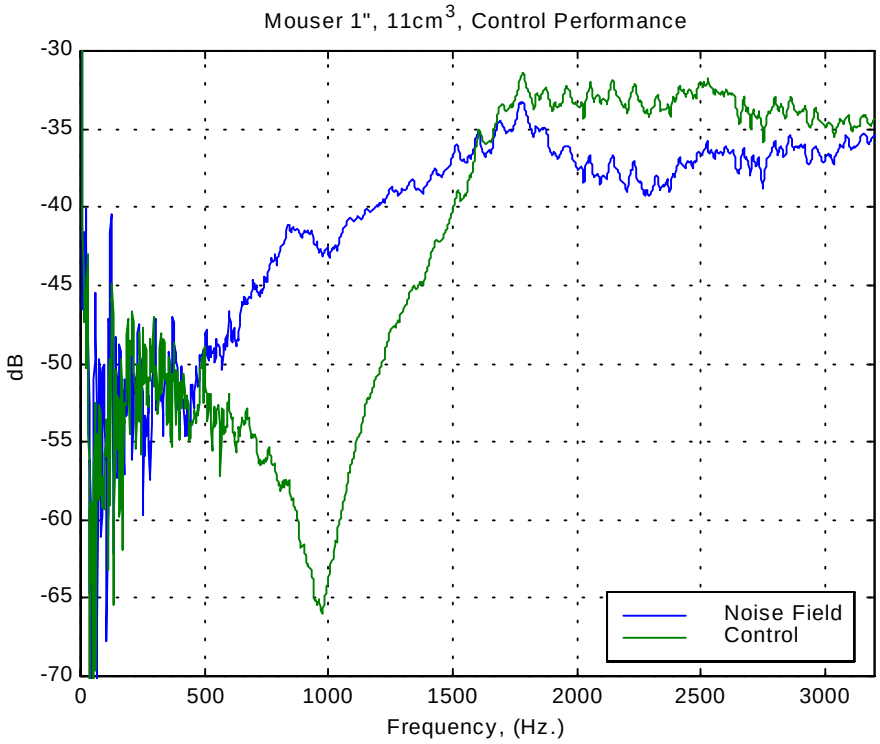

Figure 6.16 Experimental control performance (1)

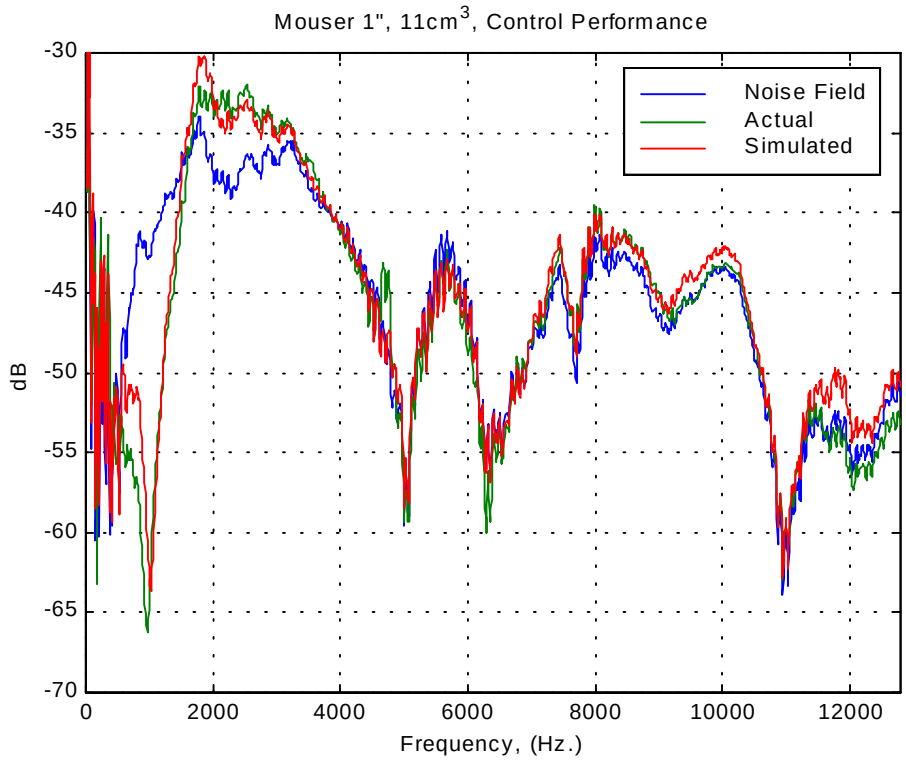

Figure 6.17 Experimental and simulated control performance (2)

6.3.2.3 Experimental Results

The system was subjected to white noise sourced from a 4-inch loudspeaker operating as a dipole. The noise field was then measured using the error microphone on the headset with the controller off and then on. Figure 6.16 and 6.17 plot the results of both the simulated and experimental results. Table 6.2 displays a list of performance measurements.

Max dB Reduction	21
Bandwidth (-3dB)	1008 Hz
Maximum Spillover	4.7 dB
Gain Margin (multiple phase crossings)	12.7 dB, 18.2 dB
Phase Margin	46°

Table 6.2 Performance and stability measurements

While the experimental results match the theoretical model almost exactly, when the loop was closed the loudspeaker began to produce audible distortion. This occurred because

the control simulation does not account for the power handling of the loudspeaker. The control simulation is based on the uncompensated open loop data, which is taken without the gain from the compensator. If the loudspeaker is overdriven the coherence will decrease due to distortion. In Figures 6.16 and 6.17, the frequency response plots have very poor coherence below 700 Hz. This is due to distortion from the loudspeaker. Observing the response shape of the compensator in Figure 6.13 shows that the low frequency gain is greater than +35 dB at 100 Hz. For underdamped systems the loudspeaker reaches its maximum excursion at its resonant frequency. As shown in Chapter 3, it requires a doubling of the maximum excursion to increase the sound pressure 6 dB at frequencies at and below the resonant frequency. For the gain selected there are many points below the resonant frequency where the compensated gain is greater than 6 dB above the nominal system. What results is that the loudspeaker exhibits audible distortion from being driven past the linear region of the voice coil.

While the experimental results indicate a 21 dB reduction in sound pressure level, this system is not realizable for actual implementation due to the distortion at low frequencies. One solution is to reduce the overall gain into the system. This decreases the bandwidth of suppression and focuses control around the resonant frequency where the maximum excursion is located, so distortion should be minimized. Figure 6.18 shows the controlled system with approximately one half the gain of the previous system. Notice that the response has good coherence throughout the frequency band. The maximum suppression is now 10 dB at 1016 Hz., but the driver does not exhibit any audible distortion at this gain.

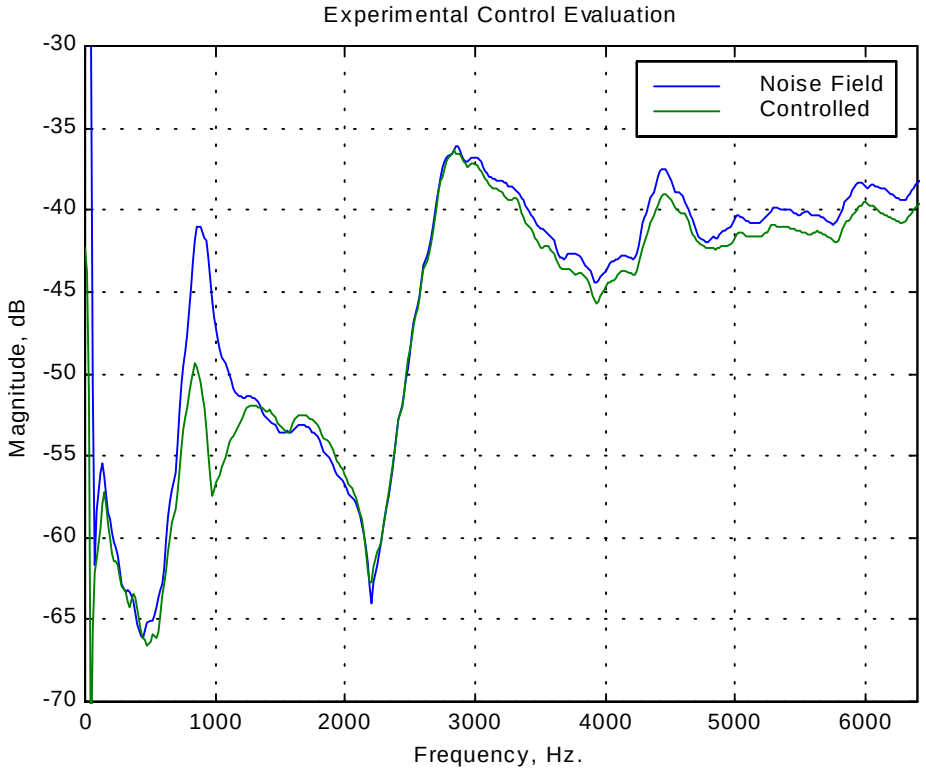

Figure 6.18 Reduced gain control, minimal distortion

A more elegant solution would be to redesign the controller by placing a zero near the origin. This would ensure that the compensators gain would be minimized as the frequency approaches DC.

6.4 Conclusions

By using the metrics of Chapter 4, and the results of the testing in Chapter 5, it was possible to construct a robust controller for an open-air headset. Although loop shaping is not considered to be a robust control design method, creating a plant that is robust to manufacturing and user variations allows robust control performance to be achieved. Once robustness is established, successful loop shaping is a process of becoming familiar with how poles and zeros interact in the frequency domain. The engineer must also consider the power handling characteristics of the loudspeaker in order to avoid low frequency distortion and physical damage to the speaker.

The controller that was developed relies on the speaker enclosure to reinforce and stabilize the second mode shape allowing the designer to successfully cancel those dynamics. For most designs, without a robust plant, error margins would have to be placed on the controller to make the system robust to the plant's changes. If the plant is considered to be sufficiently robust, the designer is then free to develop a controller that attempts to achieve the goals set in Chapter 1, which may require cancellation of loudspeaker dynamics that normally have variations in frequency and magnitude.

Chapter 7: Conclusions and Future Work

7.1 Conclusions

A summary of the main conclusions from this research follows:

- Using conventional loudspeakers and analog electronics, it is not possible to obtain flat magnitude and flat phase response over all frequencies, thus the optimal control solution is not possible. A sub-optimal response must be generated with the "complex pole solution" being very effective.
- There is not a generalized full bandwidth loudspeaker-modeling scheme that is suitable for open-air control applications. Using axisymmetric assumptions and the finite element method, future engineers will likely be able to develop a full-bandwidth design tool.
- The lowest frequency for peak control for a headphone-sized loudspeaker (1.5 inches or less) is approximately 600 Hz. This is limited by both the power handling of the speaker and the acoustic impedance.
- Augmenting the electrical reactance can improve control performance by increasing Q of the primary resonance and reducing the magnitude of the plant at high frequencies at the expense of higher power consumption.
- Closed-box enclosures can help reduce the effects of manufacturing variations in headset speakers' frequency response. This is attributed to a coupling of the compliance of the enclosure and the driver. The magnitude of the projected SPL is also increased because the source effectively becomes a monopole.
- Microphone positions near the loudspeaker and acoustic screens are an effective way to reduce user variability effects. The acoustic screen increases the acoustic impedance of the headset system, so that the headset dominates the coupling with the ear. However, the screen must be chosen carefully because it can cause a power loss for the system.

- Loop shaping is an effective control method when dealing with a robust plant. Successful controller design for open-air ANR headsets requires building the required robustness into the plant.

7.2 Future Work

- Prototype a loudspeaker based on the parameters discussed in Chapter 5. Develop a robust manufacturing process that minimizes variations in the frequency response.
- Further understand the dynamics of the human ear and develop new methods to decouple the loudspeaker system from the ear's impedance.
- Investigate optimal microphone positions for minimization of user variability without degrading the spatial extent of the zone of silence surrounding the controlled microphone.
- Examine adaptive feedforward control applications and digital feedback control using an optimal algorithm such as H_∞.

References

[1] Beranek, L. L. 1954 *Acoustics.* Ney York, NY: McGraw Hill.

[2] Binks, L.A., D.J. Henwood and M.A. Jones. 1991. "Finite Element Methods Applied to the Analysis of High-Fidelity Loudspeaker Transducers," *Computers and Structures*. Vol. 44, No. 4, pp. 765-772

[3] Bose, A. G. and J. Carter. "Headphoning," U.S. Patent No. 4,455,675

[4] Brissaud, M., P. Gonnard, J. C. Bera and M. Sunyach. 1996. "Active Control Headset Protector Using Piezoceramic Material Actuator," *Proceedings of the SPIE – The International Society for Optical Engineering*

[5] Clark, R. L. and S. Lane. 1998 "Improving Loudspeaker Performance for Active Noise Control Applications," *Journal of the Audio Engineering Society*, Vol. 46. No. 6. pp. 508-518

[6] Clatterbuck, D. C. 1998. *An Investigation of Performance Limitations in Active Noise Reduction Headsets*. MS Thesis, Virginia Polytechnic Institute and State University

[7] Colloms, M. 1998. *High Performance Loudspeakers*. Fifth Edition. Chichester, England: John Wiley and Sons

[8] Coppens, A., A. Frey, L. Kinsler and J. Sanders. 1982. *Fundamentals of Acoustics*. Third Edition. New York: John Wiley and Sons.

[9] Elliot, S. J. and P. A. Nelson. 1992. *Active Control of Sound*. London, England. Academic Press LTD.

[10] Fahy, F. 1985. *Sound and Structural Vibration*. London, England: Academic Press LTD.

[11] Franklin, G. F., J. D. Powell, and A. E. Emami-Naeini. 1994. *Feedback Control of Dynamic Systems*. Third Edition. Reading, MA: Addison-Wesley

[12] Gardner, M. B. and M. S. Hawley. 1973. "Comparison of Network and Real-Ear Characteristics of the External Ear," *Journal of the Audio Engineering Society*. Vol. 21, No. 3. pp. 158-165

[13] Geaves, G. P. 1996. "Design and Validation of a System for Selecting Optimized Midrange Loudspeaker Diaphragm Profiles," *Journal of the Audio Engineering Society*. Vol. 44, No. 3. pp. 107-118

[14] Gogate, S. and C. Radcliffe. 1992. “Identification and Modeling of Speaker Dynamics For Acoustic Control Applications,” *Active Control of Noise and Vibration* ASME. Vol. 38, pp. 295-300

[15] Harley, R. 1998. *The Complete Guide to High-End Audio*. Second Edition. Albuquerque, NM: Acapella Publishing

[16] Howard, R. C. 1972. “Acoustical Circuits Revisited,” *Journal of the Audio Engineering Society*. Vol. 20, No. 3. pp. 185-197

[17] Kagawa, Y., T. Yamabuchi, K. Sugihara and T. Shindou. 1980. “A Finite Element Approach to a Coupled Structural Radiation System with Application To Loudspeaker Characteristic Calculations,” *Journal of Sound and Vibration*. Vol. 69, No. 2. pp. 229-243

[18] Kalpakjian, S. 1997. *Manufacturing Processes for Engineering Materials*. Third Edition. Menlo Park, CA: Addison-Wesley

[19] Lagö, T. L. and S. Johansson. 1997. “Analysis of Helicopter Sound for the Development of A New Generation Active Headset,” *Proceedings of the International Modal Analysis Conference*, Vol. 2.

[20] Leo, D. J. and D. Limpert. 1998. “A Self Sensing Technique for Active Acoustic Attenuation,” VPI&SU

[21] Møller, H., C. B. Jensen, D. Hammershøi and M. F. Sørensen. 1995. “Design Criteria for Headphones,” *Journal of the Audio Engineering Society*. Vol. 43, No. 4. pp. 218-232

[22] Møller, H., C. B. Jensen, D. Hammershøi and M. F. Sørensen. 1995. “Transfer Characteristics of Headphones Measured on Human Ears,” *Journal of the Audio Engineering Society*. Vol. 43, No. 4. pp. 203-217

[23] Murphy, D. J. 1993. “Axisymmetric Model of a Moving-Coil Loudspeaker,” *Journal of the Audio Engineering Society*. Vol. 41, No. 9. pp. 679-690

[24] Rafaely, B., S. J. Elliot and J. Garcia-Bonito. 1998. “Broadband Zones of Quiet in Active Headrest,” *Journal of the Acoustical Society of America*, Vol. 106. Issue 2. pp. 787-793

[25] Rao, S. S. 1995. *Mechanical Vibrations*. Third Edition. Reading, MA: Addison-Wesley

[26] Sapiejewski, R. “Headphone With Sound Pressure Sensing Means,” U.S. Patent No. 4,644,581

[27] Shepard, I. C. and R. J. Alfredson. 1985. “An Improved Computer Model of Direct-Radiator Loudspeakers,” *Journal of the Audio Engineering Society*. Vol. 33, No. 5. pp. 322-329

[28] Small, R. 1972. “Direct-Radiator Loudspeaker System Analysis,” *Journal of the Audio Engineering Society*. Vol. 20, No. 5. pp. 383-395

[29] Small, R. 1972. “Closed-Box Loudspeaker Systems Part 1: Analysis,” *Journal of the Audio Engineering Society*. Vol. 20, No. 10. pp. 798-807

[30] Small, R. 1973. “Closed-Box Loudspeaker Systems Part 2: Synthesis,” *Journal of the Audio Engineering Society*. Vol. 21, No. 1. pp. 11-17

[31] Small, R. 1972. “Simplified Loudspeaker Measurements at Low Frequencies,” *Journal of the Audio Engineering Society*. Vol. 20, No. 1. pp. 28-33

[32] Tokhi, M. O. 1999. “The Design of Active Noise Control Systems For Compact and Distributed Sources,” Journal of Sound and Vibration. Vol. 225, No. 3. pp. 401-424

[33] Van Valkenburg, M. E. 1982. *Analog Filter Design*. New York, NY: Holt Reinhart and Winston.

[34] Vaudrey, M. A., "Modifications to ANR Communication Headsets for Improved Attenuation and Speech Intelligibility", Phase I SBIR Final Report, May 1998.

[35] Vaudrey, M. A., W. R. Saunders, "Active Noise Reduction Headphones for In-Situ Audiometry Testing", Phase I SBIR Final Report, January 1998.

[36] Vaudrey, M. A., W. R. Saunders, and B. A. Eisenhower, "A Test Based Methodology for Apriori Selection of Gain/Phase Relationships in Proportional, Phase-Shifting Control of Combustion Instabilities", Proceedings of the IGTI 2000.

[37] Saunders, W.R., M.A. Vaudrey, B.A. Eisenhower, U. Vandsburger, and C.A. Fannin, "Perspectives on Linear Compensator Designs for Active Control", AIAA 99-0717, 37th AIAA Aerospace Sciences Meeting, Reno, NV, Jan. 11-14, 1999.

Appendix: Matlab Code

---

1 Acoustic_power_limiting.m

```
================================================================
%This m-file plots the sound pressure level for various values of xmax

close all
clear all
%radius in millimeters
r = .5*.0254;
%surface area of piston
Sd = pi*r^2;
%set range of xmax
xmax = .0001:.0001:.003;
%total Q for the system
Qt = 8;
%primary resonant frequency
fs = 1000;
%calculate the acoustic power output
par = .437*((fs^4)/(Qt^2)).*(Sd.*xmax).^2;

SPL = 20*log10(sqrt(2*1.21*343.*par)./20e-6);

figure

plot(xmax.*1000,SPL+15),xlabel('x_m_a_x (mm)'),ylabel('SPL dB @ 1
inch');
title('Maximum Displacement vs. Sound Pressure Level'),grid
%15 dB is added to go from 1 m to 1 inch reference


%this section plots the sound pressure versus frequency for a given
xmax
xmax = .0005;
freq = 100:10:2000;
par = .437*((freq.^4)/(Qt^2)).*(Sd*xmax).^2;

SPL = 20*log10(sqrt(2*1.21*343.*par)./20e-6);

figure

plot(freq,SPL+15),xlabel('Frequency (Hz.)'),ylabel('SPL dB @ 1 inch');
title('Frequency vs. Sound Pressure Level'),grid
```

2 Mechanical_modifications.m

```
==============================================================
%This m-file varies the mass, stiffness and damping to
%evaluate their effect on the frequency response

clear all
close all

r = (.75*2.54/100);  %radius of speaker, m
L = .0001;           %inductance of the voice coil, H
R = 31.3;            %resistance of the voice coil; ohms
l = 2.5;             %length of wire in the voice coil, m
B = 1;               %magnetic field, T
bl= B*l;

A = pi*r^2;          %area of the diaphragm
b = 2*pi*2800;       %corner frequency of the acoustic impedance for a
1.5" speaker
c = 415;             %characteristic impedance of air


natural_freq = (sqrt(s/m))/(2*pi)

freq=1:1:3000;

m = [1e-4 5e-4 9e-4 13e-4 17e-4 21e-4];   %variation in the mechanical
mass, Kg
s = m.*(1000*2*pi)^2;                     %mechaincal stiffness,
computed to keep a
                                          %constant natural frequency
Rm = [.001 .05 .1 .5 1 2];                %variation in mechanical
damping, N-s/m
num = [-bl*A*c -bl*A*c 0];                %numerator of the p2v tf
for g=1:length(m)
   for h=1:length(Rm)
      den = [L*m(g) (L*m(g)*b+L*Rm(h)+R*m(g))
(L*Rm(h)*b+L*s(g)+R*m(g)*b+R*Rm(h)+(bl^2))
(L*s(g)*b+R*Rm(h)*b+R*s(g)+b*(bl^2)) R*s(g)*b];
      [mag,phase]=bode(num,den,2*pi*freq);
      M(:,g,h) = 20*log10(mag);
      P(:,g,h) = phase;
end
end

figure
subplot(221),plot(freq,M(:,1,1),freq,M(:,1,2),freq,M(:,1,3),freq,M(:,1,
4),freq,M(:,1,5),freq,M(:,1,6))
```

```
title(['m=',num2str(m(1)),', s=',num2str(s(1))])

subplot(222),plot(freq,M(:,2,1),freq,M(:,2,2),freq,M(:,2,3),freq,M(:,2,
4),freq,M(:,2,5),freq,M(:,2,6))
title(['m=',num2str(m(2)),', s=',num2str(s(2))])grid,axis([0 3000 -80 -
20]),xlabel('Frequency, Hz.'),ylabel('dB')

subplot(223),plot(freq,M(:,3,1),freq,M(:,3,2),freq,M(:,3,3),freq,M(:,3,
4),freq,M(:,3,5),freq,M(:,3,6))
title(['m=',num2str(m(3)),', s=',num2str(s(3))]),
grid,axis([0 3000 -80 -20]),xlabel('Frequency, Hz.'),ylabel('dB')

subplot(224),plot(freq,M(:,4,1),freq,M(:,4,2),freq,M(:,4,3),freq,M(:,4,
4),freq,M(:,4,5),freq,M(:,4,6))
title(['m=',num2str(m(4)),', s=',num2str(s(4))])
grid,axis([0 3000 -80 -20]),xlabel('Frequency, Hz.'),ylabel('dB')
```

3 Magnetic_modifications.m

```
================================================================

%This m-file varies the force factor, bl to determine its effect on
%the frequency response

clear all
close all


m = 4e-4;            %mechanical mass, kg
r = (.75*2.54/100);  %radius, m
s = 300;             %stiffness of diaphragm, N/m
Rm = .001;           %mechanical damping, N-s/m
L = .0001;           %inductance of the voice coil, H
R = 31.3;            %resistance of the voice coil; ohms
l = 2.5;             %length of wire in the voice coil, m
B = 1;               %magnetic field, T
bl= B*l;

A = pi*r^2;          %area of diaphragm
b = 2*pi*2800;       %corner frequency of acoustic impedance for a 1.5”
                     %loudspeaker
c = 415;             %characteristic impedance of air


freq=1:1:750;

bl = [.5  1.5  2.5  3.5 4.5 5.5];


for g=1:length(bl)
      num = [-bl(g)*A*c -bl(g)*A*c 0];
```

```
      den = [L*m (L*m*b+L*Rm+R*m) (L*Rm*b+L*s+R*m*b+R*Rm+(bl(g)^2))
(L*s*b+R*Rm*b+R*s+b*(bl(g)^2)) R*s*b];
      [mag,phase]=bode(num,den,2*pi*freq);
      M(:,g) = 20*log10(mag);
      P(:,g) = phase;
end

figure
plot(freq,M(:,1),freq,M(:,2),freq,M(:,3),freq,M(:,4),freq,M(:,5),
freq,(:,6)),title('Variation in Bl'),
legend('Bl=0.5','Bl=1.5','Bl=2.5','Bl=3.5','Bl=4.5','Bl=5.5',4)
grid,xlabel('Frequency, Hz.'),ylabel('dB'),axis([0 750 -80 -20])
```

4 Electrical_modifications.m

```
================================================================
%this m-file varies the resistance, R and inductance, L and plots the
results
clear all
close all


m = .0038;     % mass of driver,kg
a = .1;        % radius of driver, m
s = 900;       % stiffness N/m
Rm=.1;         % mechanical resistance Ns/m
Lo = .0235;    % inductance of the voice coil, H
Ro = 6.2;      % resistance of the voice coil; ohms
l = 4;         % length of wire in the voice coil, m
B = 1.15;      % magnetic field, T
bl= B*l;
A = pi*a^2;
a = 0;
b = 2*pi*1000; % 4 inch speaker
c = 415;
natural_freq = (sqrt(s/m))/(2*pi)
num_nom = [-bl*A*c -bl*A*c 0];
den_nom = [Lo*m (Lo*m*b+Lo*Rm+Ro*m) (Lo*Rm*b+Lo*s+Ro*m*b+Ro*Rm+(bl^2))
(Lo*s*b+Ro*Rm*b+Ro*s+b*(bl^2)) Ro*s*b];

freq=1:1:500;
[mag_nom,phase_nom]=bode(num_nom,den_nom,2*pi*freq);

L = [0.001 0.005 0.01 0.015 0.020 0.025 0.03 0.035 0.04 0.045 1 0.1];
R = [0.001 1 2 3 4 5 6 7 8 9 10 100];

num = [-bl*A*c -bl*A*c*a 0];
for g=1:length(L)
   for h=1:length(R)
      den = [L(g)*m (L(g)*m*b+L(g)*Rm+R(h)*m)
(L(g)*Rm*b+L(g)*s+R(h)*m*b+R(h)*Rm+(bl^2))
(L(g)*s*b+R(h)*Rm*b+R(h)*s+b*(bl^2)) R(h)*s*b];
```

```
      [mag,phase]=bode(num,den,2*pi*freq);
      M(:,g,h) = 20*log10(mag);
      P(:,g,h) = phase;
end
end
x = ones(length(freq))*natural_freq;
%create a vertical line at the natural frequency
y = zeros(length(freq)); y(1) = -60; y(length(freq)) = 25;

%=====================================================
figure

subplot(321),plot(x,y,':')
hold on
plot(freq,M(:,1,1),freq,M(:,1,3),freq,M(:,1,5),freq,M(:,1,7),freq,M(:,1
,9),freq,M(:,1,11))
title('L = 1mH, vs R'),legend('R=0.001','R=2','R=4','R=6','R=8','R=10')
hold on
plot(freq,20*log10(mag_nom),'k'),axis([0 500 -50 25]),grid,ylabel('dB')
hold off


subplot(322),plot(x,y,':')
hold on
plot(freq,M(:,3,1),freq,M(:,3,3),freq,M(:,3,5),freq,M(:,3,7),freq,M(:,3
,9),freq,M(:,3,11))
title('L = 10mH, vs
R'),legend('R=0.001','R=2','R=4','R=6','R=8','R=10')
hold on
plot(freq,20*log10(mag_nom),'k'),axis([0 500 -50 25]),grid,ylabel('dB')
hold off

subplot(323),plot(x,y,':')
hold on
plot(freq,M(:,5,1),freq,M(:,5,3),freq,M(:,5,5),freq,M(:,5,7),freq,M(:,5
,9),freq,M(:,5,11))
title('L = 20mH, vs
R'),legend('R=0.001','R=2','R=4','R=6','R=8','R=10')
hold on
plot(freq,20*log10(mag_nom),'k'),axis([0 500 -50 25]),grid,ylabel('dB')
hold off

subplot(324),plot(x,y,':')
hold on
plot(freq,M(:,7,1),freq,M(:,7,3),freq,M(:,7,5),freq,M(:,7,7),freq,M(:,7
,9),freq,M(:,7,11))
title('L = 30mH, vs
R'),legend('R=0.001','R=2','R=4','R=6','R=8','R=10')
hold on
plot(freq,20*log10(mag_nom),'k'),axis([0 500 -50 25]),grid,ylabel('dB')
hold off


subplot(325),plot(x,y,':')
hold on
plot(freq,M(:,9,1),freq,M(:,9,3),freq,M(:,9,5),freq,M(:,9,7),freq,M(:,9
,9),freq,M(:,9,11))
```

```
title('L = 40mH, vs
R'),legend('R=0.001','R=2','R=4','R=6','R=8','R=10')
hold on
plot(freq,20*log10(mag_nom),'k'),axis([0 500 -50
25]),grid,ylabel('dB'),xlabel('Frequency (Hz.)')
hold off


subplot(326),plot(x,y,':')
hold on
plot(freq,M(:,11,1),freq,M(:,11,3),freq,M(:,11,5),freq,M(:,11,7),freq,M
(:,11,9),freq,M(:,11,11))
title('L = 50mH, vs
R'),legend('R=0.001','R=2','R=4','R=6','R=8','R=10')
hold on
plot(freq,20*log10(mag_nom),'k'),axis([0 500 -70
20]),grid,xlabel('Frequency (Hz.)'),ylabel('dB')
hold off
```

5 Acoustic_impedance_modifications.m

```
================================================================
% this m-file demonstrates the effects of the acoustic impedance
%on the magnitude of the first resonant peak of a 1.5" loudspeaker
clear all
close all

r = (.75*2.54/100);
Lo = .0001;     %inductance of the voice coil, H
Ro = 31.3;      %resistance of the voice coil; ohms
l = 2.5;        %length of wire in the voice coil, m
B = 1;          %magnetic field, T

%make a assumption for the radiation impedance
a = 0;
b = 2*pi*2500; %f3 freq
A = pi*r^2;
c = (415.03); %acoustic impedance multiplier

Ze = tf([Lo Ro],[1]); %electrical impedance
Za = tf(c*[1 a],[1 b ]); %approximate acoustical impedance
Za2 = tf(c*[1 a],[1 2*pi*.1 ]);

%create a multimode system
poles = 2*pi*[-10+200i;-10-200i;-30+3000i;-30-3000i];
zeros = 2*pi*[0;];

[num,den]=zp2tf(zeros,poles,1e6);
Zm = tf(den,num);

u2i = -(B*l)/(Zm + (A^2)*Za);
u2i2 = -(B*l)/(Zm + (A^2)*Za2);
```

```
p2i = (1/A)*(Zm*u2i+B*l);
p2i2 = (1/A)*(Zm*u2i2+B*l);

v2i = -(Ze + ((B*l)^2)/(Zm + (A^2)*Za));
v2i2 = -(Ze + ((B*l)^2)/(Zm + (A^2)*Za2));

p2v = p2i*(1/v2i);
p2v2 = p2i2*(1/v2i2);

f = 1:1:4000;

[numpv,denpv] = tfdata(p2v);

[magpv, phasepv] = bode(numpv,denpv,2*pi*f);

magdbpv = 20*log10(abs(magpv));

[numpv2,denpv2] = tfdata(p2v2);

[magpv2, phasepv2] = bode(numpv2,denpv2,2*pi*f);

magdbpv2 = 20*log10(abs(magpv2));

omega = 2*pi*f;
[mag1,phase1] = bode(num,den,omega);

figure
subplot(211),plot(f,magdbpv+120,'r',f,magdbpv2+120,'b'),grid,title('Pre
ssure 2 Voltage')
ylabel('dB'),axis([0 4000 -70 10])
subplot(212),plot(f,phasepv,'r',f,phasepv2+90,'b'),grid
xlabel('Frequency, Hz'),ylabel('Degrees'),legend('f=2800 Hz.','f=200
Hz.')
```

6 Cb_manu_var_cont.m

```
================================================================
%this m-file simulates the closed box effect on manufacturing variation

close all
clear all

m = 4e-4;            %mass of driver, kg
r = (.75*2.54/100);  %radius of driver, m
s = 300;             %stiffness of diaphragm, N/m
Rm = .001;           %mechanical damping, N-s/m
Lo = .0001;          %inductance of the voice coil, H
Ro = 31.3;           %resistance of the voice coil; ohms
l = 2.5;             %length of wire in the voice coil, m
B = 1;               %magnetic field, T
rho = 1.21;          %density of air
c = 343;             %speed of sound in air
```

```
Sd = pi*r^2; %area of diaphragm

freq = .5:.5:1200;

%enclosure volume
Vb = 0.2e-4; %internal box volume, m^3

figure

s = [100 200 300 400 500 600 700 800 900 1000];

for j=1:10
   clear mag phase
%assuming unlined enclosures
Cab=Vb/(rho*c^2); %compliance of the air in the enclosure

Cas = (1/s(j))*Sd^2; %acoustic compliance of the driver

Cat = Cab*Cas/(Cab+Cas); %total compliance

Ras = Rm/Sd^2; %acoustic resistance of the drivers suspension

Rab = 0; %no resistance for an unlined enclosure

Ratc = Rab+Ras+((B*l)^2)/(Ro*Sd^2); %total system resistance

Mac = m/Sd^2; %acoustic mass

Cmec = (Mac*Sd^2)/((B*l)^2); %electrical equivalent compliance

Lcet = Cat*((B*l)^2)/Sd^2; %electrical equivalent inductance

Rec = ((B*l)^2)/((Rab+Ras)*Sd^2); %electrical equivalent resistance

Tc = sqrt(Cat*Mac); %inverse frequency

wc = 1/Tc; %natural frequency (primary)

f(j) = wc/(2*pi);

Qmc = wc*Cmec*Rec; %mechanical Q for closed box system

Qec = wc*Cmec*Ro; %electrical Q for closed box system

Qtco(j) = Qec*Qmc/(Qec+Qmc); %total Q;

alpha(j) = Cas/Cab; %compliance ratio

num = [Tc^2 0 0]; den = [Tc^2 Tc/Qtco(j) 1];

[mag, phase] = bode(num,den,2*pi*freq);

magdb(:,j) = 20*log10(abs(mag));
end

Qtco
```

```
natfreq = sqrt(s/m)/(2*pi)

f
Qtco = 9.74;
Tc = 2.04639e-4;
den = [Tc^2 Tc/Qtco 1]
[mag2, phase2] = bode(1,den,2*pi*freq);
magdb2= 20*log10(abs(mag2));

plot(freq,magdb2)
figure

plot(freq,magdb(:,1),freq,magdb(:,2),freq,magdb(:,3),freq,magdb(:,4),fr
eq,magdb(:,5),freq,magdb(:,6),freq,magdb(:,7),freq,magdb(:,8),freq,magd
b(:,9),freq,magdb(:,10))
axis([0 1200 -20 25]),ylabel('dB'),
xlabel('Frequency, Hz.')
title(['Resonant Variation for Vb= ',num2str(Vb*1000000),'
centimeters^3'])
hold on

%repeat calculation for open baffle case, approximated by Vb=2m^3
Vb=2;
for j=1:10
   clear mag phase
%assuming unlined enclosures
Cab=Vb/(rho*c^2); %compliance of the air in the enclosure

Cas = (1/s(j))*Sd^2; %acoustic compliance of the driver

Cat = Cab*Cas/(Cab+Cas); %total compliance

Ras = Rm/Sd^2; %acoustic resistance of the drivers suspension

Rab = 0; %no resistance for an unlined enclosure

Ratc = Rab+Ras+((B*l)^2)/(Ro*Sd^2); %total system resistance

Mac = m/Sd^2; %acoustic mass

Cmec = (Mac*Sd^2)/((B*l)^2); %electrical equivalent compliance

Lcet = Cat*((B*l)^2)/Sd^2; %electrical equivalent inductance

Rec = ((B*l)^2)/((Rab+Ras)*Sd^2); %electrical equivalent resistance

Tc = sqrt(Cat*Mac); %inverse frequency

wc = 1/Tc; %natural frequency (primary)

f(j) = wc/(2*pi);

Qmc = wc*Cmec*Rec; %mechanical Q for closed box system

Qec = wc*Cmec*Ro; %electrical Q for closed box system

Qtco(j) = Qec*Qmc/(Qec+Qmc); %total Q;
```

```
alpha(j) = Cas/Cab; %compliance ratio

num = [Tc^2 0 0]; den = [Tc^2 Tc/Qtco(j) 1];

[mag, phase] = bode(num,den,2*pi*freq);

magdb(:,j) = 20*log10(abs(mag));
end

plot(freq,magdb(:,1),freq,magdb(:,2),freq,magdb(:,3),freq,magdb(:,4),fr
eq,magdb(:,5),freq,magdb(:,6),freq,magdb(:,7),freq,magdb(:,8),freq,magd
b(:,9),freq,magdb(:,10))
```

7 Impedance_model.m

```
================================================================
%this m-file is a general impedance model simulator.  It also contains
%code to add additional inductance to the model

clear all
close all


m = .4e-3;           % mass of driver,kg
a = (.75*2.54/100);  % radius of driver, m
s = 300;             % stiffness N/m
Rm=.001;             % mechanical resistance Ns/m
Lo = .001;           % inductance of the voice coil, H
Ro = 31.3;           % resistance of the voice coil; ohms
l = 2.5;             % length of wire in the voice coil, m
B = 1;               % magnetic field, T

%make a assumption for the radiation impedance
a = 0;
b = 2*pi*2800; %f3 freq
A = pi*r^2;    %area of the diaphragm
c = (415.03);  %acoustic impedance multiplier


Zm = tf([m Rm s],[1 0]);   %mechanical impedance
Ze = tf([Lo Ro],[1]);      %electrical impedance
Za = tf(c*[1 a],[1 b ]);   %approximate acoustical impedance

%extra inductance
L1 = .0011;
R = 16.5;
ind = tf([L1 R],[1]);

Ze2 = Ze+ind;

u2i = -(B*l)/(Zm + (A^2)*Za);
```

```
p2i = (1/A)*(Zm*u2i+B*l);

v2i = -(Ze + ((B*l)^2)/(Zm + (A^2)*Za));
v2i2 = -(Ze2 + ((B*l)^2)/(Zm + (A^2)*Za));

p2v = p2i*(1/v2i);
p2v2 = .95*p2i*(1/v2i2);

f = 1:1:1600;

%calculate the system's electrical impedance
[numvi,denvi] = tfdata(v2i);
[magvi,phasevi] = bode(numvi,denvi,2*pi*f);

[numvi2,denvi2] = tfdata(v2i2);
[magvi2,phasevi2] = bode(numvi2,denvi2,2*pi*f);

figure
subplot(211),plot(f,magvi,f,magvi2),title('voltage - current
(Ze)'),grid,
subplot(212),plot(f,phasevi,f,phasevi2),grid,xlabel('frequency(hz)');

%calculate the p2v tf
[numpv,denpv] = tfdata(p2v);

[magpv, phasepv] = bode(numpv,denpv,2*pi*f);
magdbpv = 20*log10(abs(magpv));

[numpv2,denpv2] = tfdata(p2v2);

[magpv2, phasepv2] = bode(numpv2,denpv2,2*pi*f);
magdbpv2 = 20*log10(abs(magpv2));

%plot the p2v tf
figure
subplot(211),plot(freq,spkr_mag,'b',freq,spkrind_mag,'g',f,magdbpv,'r',
f,magdbpv2,'k'),grid,title('Pressure 2 Voltage')
ylabel('dB'),legend('Measured','Measured w/ind','Model','Model w/ind')

subplot(212),plot(freq,spkr_phase,'b',freq,spkrind_phase,'g',f,phasepv+
180,'r',f,phasepv2+180,'k'),grid,axis([0 1600 -90 270])
xlabel('Frequency, Hz'),ylabel('Degrees')


%divide out the inductor tf
diff = p2v2/p2v;
[numdiff,dendiff] = tfdata(diff);
[magdiff,phasediff] = bode(numdiff,dendiff,2*pi*f);

figure
subplot(211),plot(freq,ind_mag,'b',f,20*log10(abs(magdiff)),'r'),title(
'Inductor Transfer Function'),grid
legend('Measured','Model'),ylabel('dB')

subplot(212),plot(freq,ind_phase,'b',f,phasediff+360,'r'),xlabel('Frequ
ency, Hz'),ylabel('Degrees'),grid
```

Vita

Andrew David White was born in Harvey, Illinois on April 24, 1976. In 1979 his parents moved to Chanhassen, Minnesota where he attended grade school and then graduated from Chaska High School in 1994. In 1998 he graduated Magna Cum Laude from Michigan Technological University in Houghton, Michigan in Mechanical Engineering. During his senior year at Michigan Tech, Andrew was named the Departmental Scholar for the Mechanical Engineering - Engineering Mechanics department. In the summers of 1997 and 1998 he worked for Seagate Technology in Bloomington, Minnesota. During his time at Seagate, he worked on several projects involving vibration testing and modal analysis. Andrew was the principal investigator for a commercial contract from Hearing Enhancement Corporation, Roanoke, Virginia, focusing on using digital audio in personal devices for improved speech intelligibility. Upon receiving his Master of Science in Mechanical Engineering Andrew plans to join Adaptive Technologies, Inc. in Blacksburg, Virginia to serve as the principal investigator on a SBIR phase I contract for the U.S. Navy focusing on active noise control for the new AAAV vehicle.

Andrew David White